UNIVERSITY OF PATRAS
DEPARTMENT OF BIOLOGY

MOLECULAR AND BIOCHEMICAL MECHANISMS IN STREPTOZOTOCIN-INDUCED DIABETES AND ASSOCIATED BEHAVIORAL INDICES

MASTER THESIS
GRADUATE PROGRAM OF
BIOLOGICAL TECHNOLOGY

ALEXANDROS G. KOKKOSIS
BACHELOR OF SCIENCE-BIOLOGY

PATRAS, JUNE 2015

APPROVAL WITH SIGNATURES

Dr. MARIGOULA MARGARITY

Dr. KYRIAKOS KYPREOS

Dr. PAPACHRISTOU DIONYSIOS

MASTER THESIS COMMITTEE

Dr. MARIGOULA MARGARITY

(MASTER THESIS ADVISOR)

Associate Professor of Human and Animal Physiology, Department of Biology, University of Patras

Dr. KYRIAKOS KYPREOS

Professor of Pharmacology, Department of Medicine, University of Patras

Dr. PAPACHRISTOU DIONYSIOS

Associate Professor of Anatomy-Histology-Embryology, Department of Medicine, University of Patras

Ευχαριστίες

Η διπλωματική αυτή εργασία πραγματοποιήθηκε στα πλαίσια του Μεταπτυχιακού Προγράμματος Σπουδών ''Βιολογική Τεχνολογία'' του Τμήματος Βιολογίας του Πανεπιστημίου Πατρών. Εκπονήθηκε στο Εργαστήριο Φυσιολογίας Ανθρώπου και Ζώων του Τμήματος Βιολογίας, καθώς και στο Εργαστήριο Φαρμακολογίας του Τμήματος Ιατρικής.

Για την πραγματοποίηση και ολοκλήρωση αυτής της ερευνητικής εργασίας συνέβαλαν αρκετοί άνθρωποι τους οποίους θα ήθελα να ευχαριστήσω έστω και μέσα από τις λίγες αυτές γραμμές.

Οφείλω, πρωτίστως, να ευχαριστήσω θερμά την Επιβλέπουσα Καθηγήτριά μου κα. Μαριγούλα Μαργαρίτη, της οποίας η εμπνευσμένη παρότρυνση μου έδωσε την ευκαιρία ν' ασχοληθώ με τον Τομέα των Νευροεπιστημών και συγκεκριμένα μ' ένα άκρως ενδιαφέρον θέμα που συνδέει τη Νευροβιολογική έρευνα με κάποιο απ' τα πιο σημαντικά ιατρικά προβλήματα της σύγχρονης κοινωνίας, αυτό του Σακχαρώδους Διαβήτη, αποδεικνύοντας παράλληλα κι έναν αξιοθαύμαστο διεπιστημονισμό. Χωρίς την επιστημονική και υψηλού επιπέδου ακαδημαϊκή καθοδήγησή της και ερμηνεία των αποτελεσμάτων, στη συγγραφή της παρούσας Διατριβής και των επιστημονικών δημοσιεύσεων, ασφαλώς θα ήταν αδύνατη η εκπόνηση αυτής της ερευνητικής εργασίας. Την ευχαριστώ, επίσης, θερμά που πάνω από όλα εκτός από επιστημονισμό και ρεαλισμό στα ερευνητική μας πορεία, ήταν Άνθρωπος, και το οποίο πολλές φορές παίζει παραπάνω ρόλο από τα προηγούμενα. Παράλληλα την ευχαριστώ γιατί με ωθούσε να εξελίσσομαι επιστημονικά, αλλά και για το αισιόδοξο και φιλεργατικό πνεύμα της που με ενθάρρυναν να συνεχίσω τη διατριβή μου. Άλλωστε, με τη δική της στήριξη και παρώθηση συμμετείχα σε πληθώρα επιστημονικών, Ελληνικών και Διεθνών, συνεδριών, αποσπώντας αρκετά βραβεία αλλά και κερδίζοντας πολλά εφόδια, τόσο μέσω της επικοινωνίας και ανταλλαγής απόψεων με νέους ερευνητές, αλλά και έμπειρους επιστήμονες, όσο και από την παρουσίαση της ερευνητικής μου δουλειάς στην επιστημονική κοινότητα. Ο φιλικός της χαρακτήρας και η απόλυτη εμπιστοσύνη προς το πρόσωπο μου, πάντα θα με ακολουθεί και μακριά να είμαι, και πάντα θα είναι ο πρώτος και πιο σημαντικός μου μέντορας στην επιστήμη. Ό,τι παραπάνω και αν αναφέρω σε αυτές γραμμές και πάλι δεν θα αρκεί για να αντικατοπτρίσει τον σεβασμό μου προς το πρόσωπο της. Ευχαριστώ...

Θερμότατες ευχαριστίες οφείλω, επίσης, στον Καθηγητή κ. Κυριάκο Κυπραίο, για την τιμή που μου επεφύλαξε να είναι μέλος της Τριμελούς Επιτροπής και ο οποίος στάθηκε παρών, και αρωγός σε όλα τα στάδια αυτής της διατριβής, από τη διεξαγωγή των πειραμάτων και την ανάλυση των αποτελεσμάτων τους, ως και τη συγγραφή αυτού του πονήματος και των διαφόρων δημοσιεύσεων του, αφιερώνοντας πάντοτε αρκετό πολύτιμο χρόνο από το ασφυκτικό πρόγραμμά του. Ο ακαδημαϊσμός, η ευγένεια καθώς και οι προτάσεις του στα πλαίσια ενός ελεύθερου επιστημονικού διαλόγου, συνετέλεσαν στην προώθηση της έρευνάς μου. Τον ευχαριστώ, εξάλλου, διότι δεν παρέλειπε να μου δείχνει την εκτίμησή του, άλλοτε συμμεριζόμενος τις ιδέες μου και άλλοτε δίνοντας συμβουλές τις οποίες θα τις κρατήσω ως πολύ σημαντικά εφόδια φεύγοντας για τις Η.Π.Α. Ειδικότερα, οι εξειδικευμένες γνώσεις του, μεταξύ άλλων, στον Διαβήτη, Μεταβολισμό και τη Φαρμακολογία, ήταν καθοριστικά κατά τη διεξαγωγή των πειραμάτων. Άλλωστε, παρέχοντάς μου ουσιαστική υλικοτεχνική υποδομή, με περιέβαλε με εμπιστοσύνη και μου επέτρεψε να πραγματοποιήσω σημαντικό κομμάτι της διατριβής στο εργαστήριο Φαρμακολογίας, στο Τμήμα Ιατρικής του Πανεπιστημίου Πατρών, πράγμα για τον οποίο τον ευγνωμονώ.

Ευχαριστώ επίσης, τον Αναπληρωτή Καθηγητή κ. Διονύσιο Παπαχρήστου για την τιμή που μου επεφύλαξε να είναι μέλος της Τριμελούς Επιτροπής της παρούσας διατριβής. Οι υποδείξεις του για τη διαμόρφωση του κειμένου της διατριβής υπήρξαν ουσιώδεις για μένα.

Απεριόριστη ευγνωμοσύνη οφείλω στην Αναπληρώτρια Καθηγήτρια κα. Φωτεινή Λάμαρη, η οποία μπορεί να θεωρηθεί ως το ''Τέταρτο'' μέλος της επιτροπής. Στάθηκε πάντα δίπλα μου σε όλα τα στάδια αυτής της διατριβής, από τη διεξαγωγή των πειραμάτων και την αντιμετώπιση των διαφόρων προβλημάτων που προέκυπταν, την ανάλυση των αποτελεσμάτων τους, ως και τη συγγραφή αυτού του πονήματος καθώς και των διαφόρων δημοσιεύσεων, αφιερώνοντας πάντοτε αρκετό πολύτιμο χρόνο από το ασφυκτικό πρόγραμμά της. Ο αντίκτυπος που είχε καθ' όλη την διάρκεια των προπτυχιακών αλλά και των μεταπτυχιακών σπουδών μου, στην διεύρυνση του επιστημονικού μου ορίζοντα σε τομείς όπως της Βιοχημείας και την Χημεία Φυσικών Προϊόντων, ήταν πολύ μεγαλύτερος από όσο μπορεί να γνωρίζει. Οι γνώσεις της υπήρξαν φωτεινοί σηματοδότες στην πορεία συγγραφής της παρούσας διατριβής μέσω πολύτιμων συμβουλών και χρήσιμων υποδείξεων. Την ευχαριστώ επίσης για την παροχή υλικοτεχνικής υποδομής, καθώς και επειδή με περιέβαλε με εμπιστοσύνη και με βοήθησε ουσιαστικά να πραγματοποιήσω σημαντικό κομμάτι της διατριβής μου. Τέλος η ευγένεια του χαρακτήρα της, η καλοσύνη του πνεύματός της, αποτελούν παράδειγμα Ακαδημαϊκού δασκάλου και οι συμβουλές της θα κρατηθούν ως σημαντικά εφόδια για το μέλλον.

Ευχαριστώ επίσης, τον Αναπληρωτή Καθηγητή κ. Σακελλαρόπουλο Γεώργιο για την πολύτιμη βοήθεια και τον χρόνο που διέθεσε, με σκοπό την σωστή εκτίμηση και στατιστική επεξεργασία των αποτελεσμάτων της παρούσας διατριβής.

Είμαι, επιπλέον, ευγνώμων για την επι σειρά πολλών ετών αρμονική συνεργασία μου με όλα τα μέλη ΔΕΠ του Εργαστηρίου Φυσιολογίας Ανθρώπου και Ζώων, τους κκ. Παναγιώτη Γιομπρέ, Νικόλαο Ματσώκη, Νικόλαο

Παναγόπουλο και Αικατερίνη Δερμών, καθώς και για την αγάπη, εκτίμηση και εμπιστοσύνη που έδειχναν στο πρόσωπό μου. Ιδιαιτέρως δε οφείλω να ευχαριστήσω την κα Χρυσάνθη Γκαρτζώνη, μέλος ΕΤΕΠ του Εργαστηρίου Φυσιολογίας Ανθρώπου και Ζώων, για την κάθε φορά άμεση ανταπόκρισή της στην επίλυση πρακτικών και τεχνικών ζητημάτων, καθώς και για την αγάπη που έδειχνε στο πρόσωπό μου.

Θα ήθελα να αναφερθώ στη σπουδαιότητα της συνεργασίας μου με την Μεταδιδάκτορα κα. Κατερίνα Κωνσταντίνου, η οποία στάθηκε πάντα δίπλα μου στην διεξαγωγή των πειραμάτων και την αντιμετώπιση των διαφόρων προβλημάτων που προέκυπταν κατά την διάρκεια της εκπόνησης της διατριβής. Ο σχεδιασμός των πειραμάτων καθώς και η αμέριστη βοήθειά της σε ό,τι και αν χρειάστηκα, βοήθησαν κατά πολύ μεγάλο βαθμό στην αρτιότητα της παρούσας διατριβής.

Θα ήταν παράλειψη να μην αναφερθεί και η σπουδαιότητα της συνεργασίας μας με όλους εκείνους τους νέους μεταπτυχιακούς ερευνητές του Εργαστηρίου Φυσιολογίας Ανθρώπου και Ζώων, που η ζωντάνια του πνεύματός τους καλλιεργεί στον Πανεπιστημιακό χώρο συνθήκες γόνιμης δημιουργίας. Η Βάσω, ο Θέμης, η Μάρθα και ο Στέφανος ήταν πάντα εκεί για οποιαδήποτε βοήθεια, και ένα ιδιαίτερο ευχαριστώ στον Παναγιώτη με τον οποίο περάσαμε άπειρες ώρες στο εργαστήριο μαζί, συζητώντας και βοηθώντας ο ένας στον άλλον, καθώς και επειδή όποτε ήταν ανάγκη ήταν πρόθυμος να βοηθήσει.

Από την άλλη μεριά, είμαι ευγνώμων για την αμέριστη βοήθεια που είχα από τους μεταπτυχιακούς ερευνητές του εργαστηρίου Φαρμακολογίας. Ιδιαιτέρως δε θα ήθελα να ευχαριστήσω την Εύα, την Λίλια και τον Βασίλη γιατί ήταν πάντα εκεί προς παροχή οποιασδήποτε βοήθειας χρειαζόμουν, καθώς και για την εμπιστοσύνη και την φιλία που έδειξαν προς το πρόσωπό μου.

Τέλος, το μεγαλύτερο ευχαριστώ το χαρίζω στους αγαπημένους μου γονείς και την οικογένεια μου για την υποστήριξη όχι μόνο κατά τη διάρκεια της περάτωσης αυτής της εργασίας αλλά και καθ' όλη τη διάρκεια των σπουδών μου.

Πάτρα, Ιούνιος 2015

Αλέξανδρος Γ. Κοκκόσης

«Η ολοκλήρωση της διπλωματικής εργασίας συγχρηματοδοτήθηκε μέσω της Πράξης Πρόγραμμα χορήγησης υποτροφιών ΙΚΥ για Μεταπτυχιακές Σπουδές Πρώτου Κύκλου (Μάστερ) - Οριζόντια Πράξη, από πόρους του ΕΠ «Εκπαίδευση και Δια Βίου Μάθηση», του Ευρωπαϊκού Κοινωνικού Ταμείου (ΕΚΤ) του ΕΣΠΑ, 2007-2013»

«Ἓν οἶδα ὅτι οὐδὲν οἶδα»

ΣΩΚΡΑΤΗΣ

ABSTRACT

Diabetic encephalopathy, characterized by impaired cognitive function may involve neuronal dysfunction and neurochemical abnormalities. Here we investigated the effects of streptozotocin-induced type I diabetes (T1D) and its treatment by insulin on behavioral indices and the neurochemical profile in male mice. We focused on the cholinergic system and brain oxidative profile. Mice (n=32) were divided into three groups (n=10-11/group). Two groups became diabetic by intraperitoneal administration of streptozotocin (50mg/kg body weight/per day), for five consecutive days. After 21 days one diabetic group was treated intraperitoneally with glargine (6 IU/kg) for an additional six days. As control, the third group of the study remained euglycemic. All three groups underwent behavioral analysis (fear-anxiety, memory-learning and depression-like behavior) two days following insulin administration to diabetic mice. Also, plasma glucose, cholesterol and triglycerides levels, were determined. In addition, biochemical analyses including determination of acetylcholine (ACh) levels and acetylcholinesterase (AChE) activity, as well the activities of superoxide dismutase, glutathione peroxidase, catalase, glutathione levels (markers of antioxidant defense), and malondialdehyde (marker of lipid peroxidation),were performed in various brain regions (cerebral cortex, midbrain, hippocampus, striatum, diencephalon and cerebellum). Our data indicate that T1D engendered anxiogenesis, memory loss and depression-like behavior in mice that were associated with statistically significant decrease in ACh levels and a parallel increase in the AChE activity in the brain regions studied. The enzymatic anti-oxidant activity was significantly increased in diabetic mice presumably as a means of defense against the increased oxidative stress. Western blot analysis on mitochondrial lysates and cytoplasmic samples indicated neuronal apoptosis on most of the brain regions examined (cerebellum, cerebral cortex, midbrain, hippocampus, striatum and diencephalon). Insulin treatment significantly attenuated the cognitive deficits, cholinergic dysfunction, oxidative stress and neuronal apoptosis the diabetic mice in a brain region-dependent manner. Our findings support that T1D leads to cognitive dysfunction, cholinergic system aberrations, oxidative stress and neuronal apoptosis, which are reversed following insulin treatment (Fig. 1).

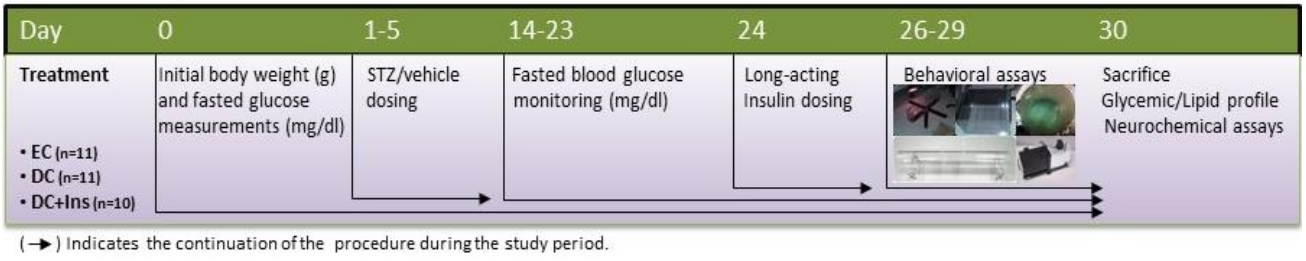

Figure 1. Graphical Abstract

ΠΕΡΙΛΗΨΗ

Η διαβητική εγκεφαλοπάθεια, χαρακτηρίζεται από μειωμένη γνωστική λειτουργία και πιθανόν περιλαμβάνει νευρωνική δυσλειτουργία και νευροχημικές ανωμαλίες. Ερευνήσαμε την επίδραση του επαγμένου με στρεπτοζοτοκίνη διαβήτη τύπου Ι (ΔΤ1), και θεραπεία του με ινσουλίνη επί συμπεριφορικών και νευροχημικών δεικτών σε αρσενικούς μυς. Εστιάσαμε στο χολινεργικό σύστημα και το οξειδωτικό προφίλ εγκεφαλικών περιοχών. Οι μύες (n=32) χωρίστηκαν σε τρεις ομάδες (n=10-11/group). Στις δύο ομάδες έγινε επαγωγή διαβήτη με ενδοπεριτοναϊκή χορήγηση στρεπτοζοτοκίνης (50mg/kg βάρους σώματος/ημέρα), επί πέντε διαδοχικές ημέρες. Έπειτα από 21 ημέρες, στη δεύτερη διαβητική ομάδα χορηγήθηκε ενδοπεριτοναϊκά glargine (6 IU/kg) επί έξι διαδοχικές ημέρες. Η τρίτη ομάδα παρέμεινε ευγλυκαιμική (μάρτυρες). Οι τρεις ομάδες υποβλήθηκαν σε ανάλυση συμπεριφοράς (φόβος-άγχος, μνήμη-μάθηση και καταθλιπτική τάση), δύο ημέρες μετά τη χορήγηση ινσουλίνης στα διαβητικά ποντίκια. Έπειτα προσδιορίσθηκαν τα επίπεδα γλυκόζης, χοληστερόλης και τριγλυκεριδίων πλάσματος. Επιπλέον, διεξήχθησαν βιοχημικές αναλύσεις: επίπεδα ακετυλοχολίνης (ACh) και ενεργότητα ακετυλοχολινεστεράσης (AChE), καθώς και ενεργότητες υπεροξειδικής δισμουτάσης, υπεροξειδάσης της γλουταθειόνης, καταλάσης, επίπεδα γλουταθειόνης (δείκτες αντιοξειδωτικής άμυνας) και της μαλονδιαλδεΰδης (δείκτης υπεροξείδωσης λιπιδίων) σε εγκεφαλικές περιοχές (εγκεφαλικός φλοιός, μεσεγκέφαλος, ιππόκαμπος, ραβδωτό σώμα, διεγκέφαλος και παρεγκεφαλίδα). Τα αποτελέσματα υποδεικνύουν ότι ο ΔΤ1 προκάλεσε αγχογένεση, απώλεια μνήμης και καταθλιπτική τάση στους μυς και συσχετίστηκε με σημαντική μείωση των επιπέδων της ACh και παράλληλη αύξηση της δραστηριότητας της AChE των εγκεφαλικών περιοχών. Η αντιοξειδωτική ενζυμική δραστικότητα των εγκεφαλικών περιοχών ήταν σημαντικά αυξημένη στους διαβητικούς μυς, πιθανώς ως μέσο άμυνας έναντι του αυξημένου οξειδωτικού στρες. Η ανάλυση κατά Western στα μιτοχονδριακά κυτταρολύματα και στα κυτταροπλασματικά δείγματα, υποδεικνύουν απόπτωση νευρικών κυττάρων στις περισσότερες εγκεφαλικές περιοχές που εξετάστηκαν (εγκεφαλικός φλοιός, μεσεγκέφαλος, ιππόκαμπος, ραβδωτό σώμα, διεγκέφαλος και παρεγκεφαλίδα).. Η χορήγηση ινσουλίνης στους διαβητικούς μυς εξασθένησε σημαντικά τις γνωστικές διαταραχές, τη χολινεργική δυσλειτουργία, το οξειδωτικό στρες και την απόπτωση στα νευρικά κύτταρα των υπό μελέτη εγκεφαλικών περιοχών κατά ιστοειδικώς εξαρτώμενο τρόπο. Τα ευρήματά μας υποστηρίζουν ότι ο ΔΤ1 οδηγεί σε γνωστικές δυσλειτουργίες, μεταβολές στο χολινεργικό σύστημα, οξειδωτικό στρες και νευροεκφύλιση τα οποία αντιστρέφονται έπειτα από θεραπεία με ινσουλίνη (Εικόνα).

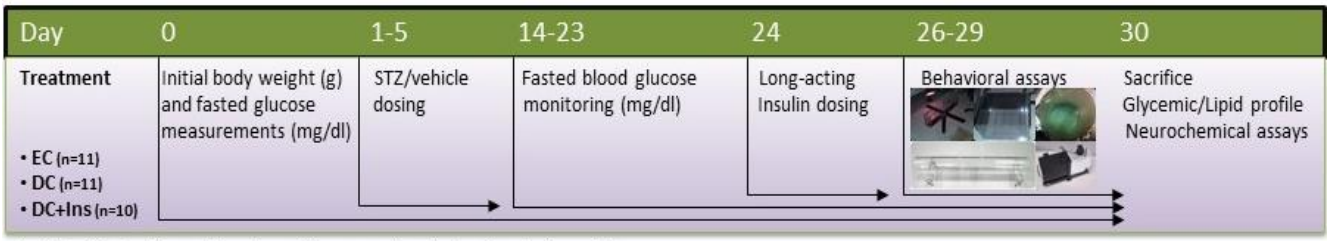

(→) Indicates the continuation of the procedure during the study period.

Table of Contents

I. INTRODUCTION

1.1. Diabetes Mellitus

Diabetes mellitus is a common metabolic disorder, characterized by hyperglycemia and associated with chronic complications such as nephropathy, angiopathy, retinopathy and peripheral neuropathy. The World Health Organization (WHO) states that in 2011 there were 366 million people diagnosed with diabetes and by 2030 this number will rise to 552 million. There are four major forms of diabetes: Type I diabetes (T1DM) is characterized by lack of insulin (Ins) secreting pancreatic *β* cells while type II diabetes (T2DM) by reduced sensitivity of peripheral tissues to Ins, gestational diabetes and diabetes due to other known causes (Figure 2) (1).

Types of Diabetes	Old nomenclature	Etiology
Type 1 Type 1A Type 1B	Juvenile-onset insulin-dependent diabetes mellitus	β-cell destruction. autoimmune unknown
Type 2	Non-insulin-dependent diabetes mellitus	insulin resistance/β-cell loss
Gestational		onset during pregnancy
Other types	secondary diabetes	specific genetic defects pancreas disease Endocrinopathies, etc.

Figure 2. Classification of diabetes mellitus (Jahromi MM, and Eisenbarth GS, 2007).

1.2. Type 1 diabetes mellitus

Type 1 diabetes, formerly known as either juvenile onset diabetes (because of the early age of onset) or insulin-dependent diabetes mellitus (because of the clinical need for insulin), is an autoimmune disease, caused by the destruction of insulin producing pancreatic β-cells (2). **There are two forms of T1DM:**

1. **Type 1A or immune based diabetes**, which results from cellular-mediated autoimmune destruction of β-cells in the pancreas; abnormal activation of T-cells leads to insulitis and production of antibodies against β-cells (humoral B cell response), which may constitute useful markers of immune destruction (3).
2. **Type 1B, or idiopathic diabetes**, which is a type of diabetes with no autoimmune markers, in which the reason for β-cell destruction is unknown. T1B mainly occurs in Asian or African people, who have varying degrees of insulin deficiency between episodes of ketoacidosis (4).

In type 1 diabetes, autoimmunity erupts early and the autoimmune process lasts for years (5). The eruption of the autoimmune process is determined by genetic polymorphism (6) and triggered by environmental factors (7) as well as infectious agents (8). Type 1A diabetes accounts for approximately 90% of childhood-onset diabetes and 5–10% of adult onset diabetes (9). About 40% of persons with type 1A diabetes develop the disease before 20 years of age, thus making it one of the most common severe chronic diseases of childhood (9).

1.3. Diabetic Neuropathy

1.3.1. Cognitive disorders in diabetic patients and experimental animal models

Clinical neuropsychology studies (10, 11) as well as epidemiological cross-sectional reports (12, 13) and reviews have shown that patients with T1DM present impaired cognitive function, associating diabetes with anxiety (14), depression (15), memory impairment (16) and other various cognitive deficits (17, 18). A study showed that early onset of diabetes was associated with lower IQ performances and lower full-scale IQ (19). It has been recognized that early onset of T1DM results in worse neuropsychological performances (20) and that males are more vulnerable than females (21).

Neurocognitive research has shown that type 1 DM is primarily associated with psychomotor slowing and reductions in mental efficiency with structural changes on MR imaging (22, 23). Using voxel-based morphometry, patients with type 1 diabetes showed lower gray matter densities (GMD) in posterior temporal, hippocampus, and parahippocampal gyri, which contribute to memory, compared to healthy controls (24). Decreased GMD was

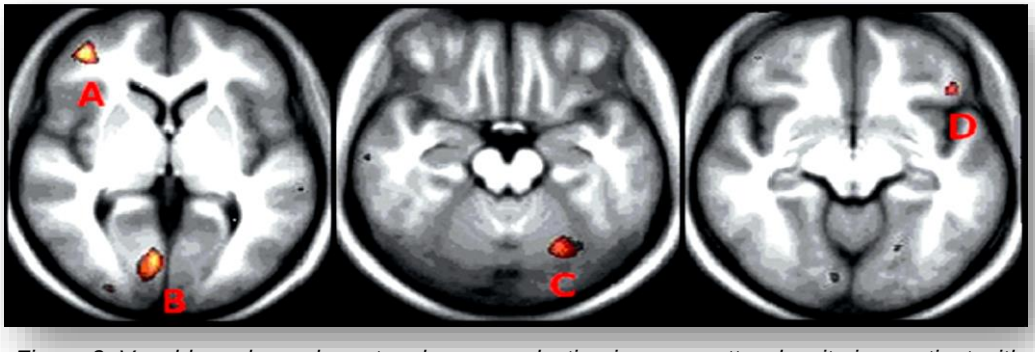

Figure 3. Voxel-based morphometry shows a reduction in gray matter density in a patient with type 1 diabetes and retinopathy. Changes in gray matter density are shown on a mean normalized structural image in axial planes. The images show areas of significantly reduced gray matter density in right frontal gyrus (A), right occipital lobe (B), left cerebellum (C), and left middle frontal gyrus (D). Left in the image is right in the brain (Wessels et al., 2006).

also seen in the superior temporal gyrus and angular gyri, which are important in language processing, in comparison to healthy controls. In conclusion, type 1 DM with end organ involvement has a tendency to involve gray matter more than white matter, correlating well with generalized cerebral atrophy and cognitive disturbances (16, 25) (Figure 3).

Over the years, studies on cognitive functioning in diabetic rodents have employed various learning tasks (26, 27).There are clear indications that the physiological responses to a novel environment, or to stressful stimuli which are often part of learning paradigms, are altered in STZ-diabetic rodents (26). In more complex learning tasks, such as an active avoidance T-maze, or a Morris water maze, performance of STZ-diabetic rodents was consistently found to be impaired (28). Similar to the observations on evoked potential latencies, the development of the deficits was dependent on the duration of diabetes (28).Insulin treatment could prevent but not completely reverse the learning deficits (28). In light of the crucial role of the hippocampus in certain types of learning and memory, behavioral studies were complemented with detailed evaluations of hippocampal function. The research focused on long-term potentiation (LTP) and depression (LTD), two forms of activity-dependent synaptic plasticity thought to be relevant to the underpinnings of learning and memory (29-31). In LTP, brief high-frequency afferent activity leads to a long-lasting increase in the strength of synaptic transmission, whereas in LTD prolonged low-frequency activity results in a persistent reduction in synaptic strength. Learning deficits in STZ-diabetic rats proved to be accompanied by distinct changes in synaptic plasticity in hippocampal slices (26, 32). A deficit in the expression of N-methyl-D-aspartate (NMDA)-dependent LTP in the CA1 field was shown to develop gradually, reaching a maximum 12 weeks after diabetes induction (33, 34). In contrast to LTP, expression of LTD was enhanced in the CA1 field following low-frequency stimulation of slices from diabetic rats (34, 35).

1.3.2. Imaging studies in Type 1 diabetes

Volumetric MRI studies in patients with diabetes for 12 years showed significant decreases in white matter volumes in parahippocampus, temporal and frontal lobes as well as decreased gray matter volumes of the thalami, hippocampi and insular cortex (19).
Voxel-based morphometric analyses of patients with T1DM for 15–25 years duration showed decreased gray matter densities in thalami, superior and middle temporal gyri and frontal gyri (24). It therefore appears that limbic temporal and frontal structures are most vulnerable.

Only few recent neuropathological reports describe structural abnormalities. Two young diabetic patients with diabetes since age four and who succumbed to ketoacidosis showed marked neuronal loss in hippocampus and frontal cortex and white matter atrophy of frontal and temporal regions (36). These findings were associated with marked down-regulation of both insulin and IGF-I receptors and activation of pro-inflammatory factors. Such structural deficits probably underlie cognitive deficits such as memory, information processing, executive function and attention and have been related to impaired functional connectivity (37). It is therefore now becoming accepted that T1DM results in various cognitive deficits related to gray matter deficits, particularly in limbic structures as well as white matter atrophy. Such deficits are more prevalent in patients with onset of diabetes at a young age.

1.3.3. Mechanisms underlying cognitive dysfunction in Type 1 diabetes and animal studies

It is generally accepted that the pathogenesis of diabetic encephalopathy is multifactorial, involving complex interactions between the degree of glycemic control, diabetes duration, age-related neuronal attrition, and other factors such as blood pressure, lipid levels, and weight (38). The main potential underlying factors are (Figure 4):

1.3.3.1. Polyol Pathway

Structural abnormalities have been accompanied by increased sorbitol and decreased taurine levels, suggesting activation of the polyol-pathway and impaired neurotrophic support (39). Taurine has many fundamental biological roles, such as conjugation of bile acids, anti-oxidation, osmoregulation, membrane stabilization, and modulation of calcium signaling. According to animal studies, taurine produces an anxiolytic effect and may act as a modulator or antianxiety agent in the central nervous system by activating the glycine receptor (40).

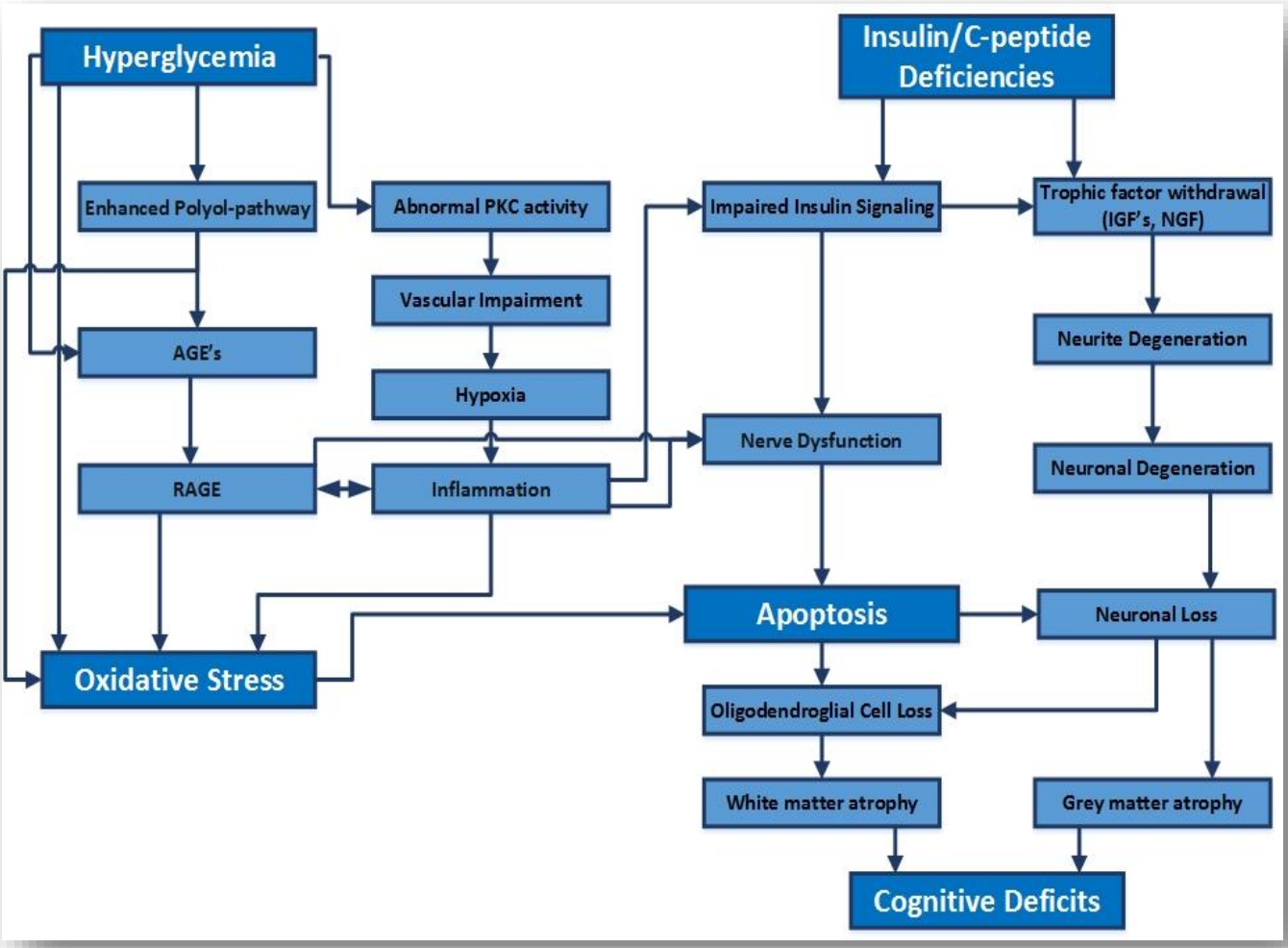

Figure 4. Proposed sequential mechanisms underlying T1DM encephalopathy. Insulin and C-peptide deficiencies result in impaired insulin signaling affecting inflammation, oxidative stress and apoptosis. It leads to suppressed expression of neurotrophic factors and their receptors impacting on neuronal integrity with neurite degeneration as well as increased apoptotic activity with neuronal loss and gray matter atrophy. Apoptotic cell loss of white matter oligodendroglial cells results in white matter atrophy. Hyperglycemia and activation of the polyol pathway lead to increased AGE's formation that contributes to increased RAGE expression, inflammation and apoptosis. The progressive deficits in gray and white matter structures of vulnerable areas result in cognitive deficits.

The polyol pathway, also called the sorbitol-aldose reductase pathway, appears to be implicated in diabetic complications. While most cells require the action of insulin for glucose to gain entry into the cell, the cells of the retina, kidney, and nervous tissues are insulin-independent, so glucose moves freely across the cell membrane, regardless of the action of insulin. These cells will use glucose for energy as normal, and any glucose not used for energy will enter the polyol pathway. When blood glucose is normal (about 100 mg/dl), this interchange causes no problems, as aldose reductase has a low affinity for glucose at normal concentrations. In a hyperglycemic state, the affinity of aldose reductase for glucose rises, causing much sorbitol to accumulate, and using much more NADPH, leaving less NADPH for other processes of cellular metabolism.

Excessive activation of the polyol pathway increases intracellular and extracellular sorbitol concentrations, Activation of the polyol pathway results in a decrease of reduced NADPH and oxidized NAD^+ (41)(Figure 5). These are necessary cofactors in redox reactions throughout the body, and under normal conditions.

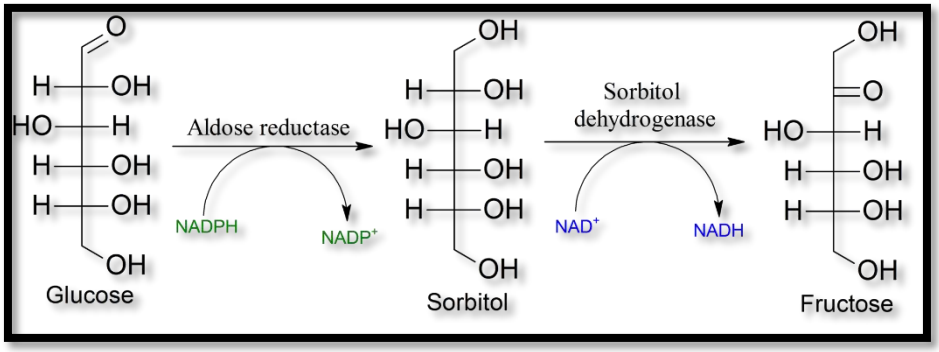

Figure 5. The polyol metabolic pathway (Wikipedia.org)

The decreased concentration of NADPH leads to decreased synthesis of reduced glutathione, nitric oxide, myo-inositol, and taurine. Myo-inositol is particularly required for the normal function of nerves. Sorbitol may also glycosylates proteins, such as collagen, and the

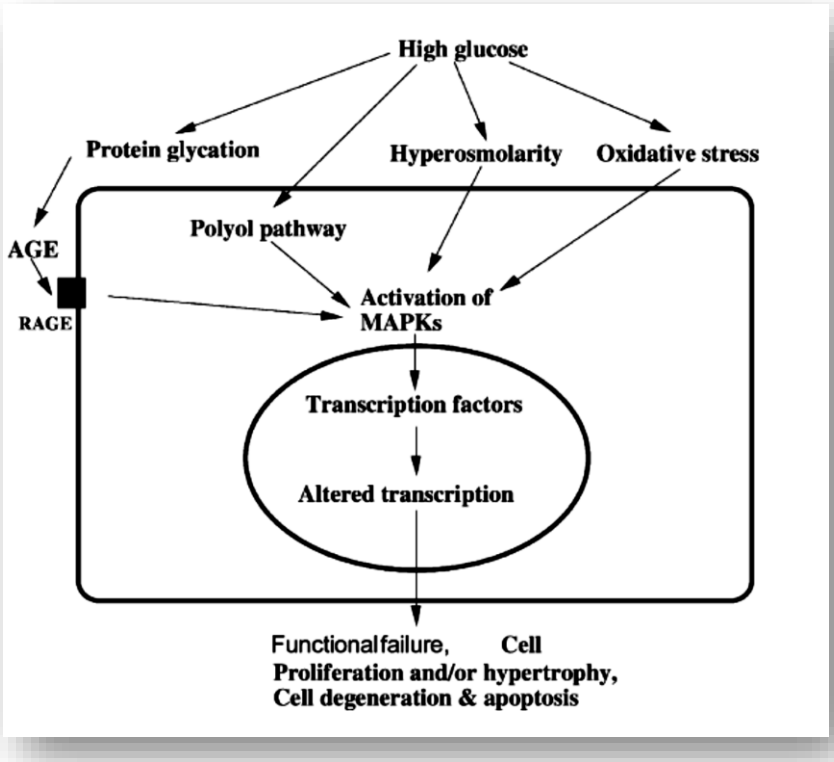

Figure 6. Hypothetical mechanism of diabetic complications suggesting the possible roles of mitogen-activated protein kinases (MAPKs) in the development of the complications including diabetic neuropathy. Hyperglycemia exerts several metabolic effects on cells, leading to activation of MAPKs, which may be involved in cell functional or degenerative changes through activation of transcription factors.(H. Yasuda et al. 2003).

products of these glycations are referred-to as AGEs (advanced glycation endproducts). AGEs are thought to cause disease in the human body, one effect of which is mediated by RAGE (receptor for advanced glycation endproducts) and the ensuing inflammatory responses induced (Figure 5). Also, the amount of sorbitol that accumulates, however, may not be sufficient to cause osmotic influx of water, hence it produces osmotic stresses on cells by drawing water into the insulin-independent tissues.

1.3.3.2. Protein kinase C (PKC)

PKC family of enzymes are activated by the diacylglycerol (DAG) or calcium ions (Ca^{2+}) resulting from receptor-mediated hydrolysis of inositol phospholipids. PKC participates in a variety of functions, including signal transduction, regulation of ion channels and neurotransmitter release, control of cell growth and differentiation, and changes in cell morphology and gene expression (42).

Reports show that PKCβ inhibition ameliorates decreases in both nerve conduction velocity and nerve blood flow in STZ-induced diabetic rats suggesting that inhibition of PKC activity of endoneurial microvasculature may be responsible for the observed changes (43). One important consideration is that each isoform may show different activity, expression and/or distribution in diabetic state; it was reported that total PKCα immunoreactivity was unchanged with its significantly reduced cytosolic fraction, whereas total and cytosolic PKCβII immunoreactivity were reduced in diabetes, and nerve crush increased only PKCα immunoreactivity (44).

Moreover, recent research regarding the role of PKC in the central diabetic neuropathy, indicates a disturbance of CaMKII/PKA/PKC phosphorylation in the hippocampus is an early change that may be associated with the development and progression of diabetes-related cognitive dysfunction (45). Also, other findings suggest that a PKC activity increase in the glio-pial tissue of diabetic rats may be due to the selective upregulation of PKC-α, and ultimately lead to the impairment of neurovascular coupling (46). Impaired cerebral blood flow was also indicated in the one single-photon emission tomography study in frontal areas and basal ganglia (47).

Mitogen-activated protein kinases (MAPKs) play an instrumental role (Figure 6) in the transmission of signals from cell surface receptors and environmental cues to the transcriptional machinery. MAPKs are involved in directing cellular responses to a diverse array of stimuli, such as mitogens, osmotic stress, heat-shock and proinflammatory cytokines.

MAPKs regulate cell functions including proliferation, gene expression, differentiation, mitosis, cell survival, and apoptosis.

Three major hypothetic pathways (Figure 6) in the pathogenesis of diabetic complications including enhanced sorbitol pathway, non-enzymatic glycation of proteins and increased oxidative stress may contribute to the activation of MAPKs, leading to tissue dysfunction through the phosphorylation of transcription factors. In addition, PKC, which has recently been shown to be a potent candidate for diabetic complications, is able to activate MAPKs (48).Thus, MAPKs may act as a signal transducer that trigger cellular events in the development of diabetic complications, including neuropathy, possibly in part by affecting nerve regenerative capacity (49) (Figure 6, 7).

1.3.3.3. Insulin- and C-peptide deficiencies

The BB/Wor rat model (breed that develops autoimmune T1DM) shows complete insulin- and C-peptide deficiencies and severe hyperglycemia which is maintained by small daily insulin doses (50, 51). Longitudinal studies in this model have revealed early neurobehavioral abnormalities using the radial arm maze occurring after 3 months of diabetes and were associated with marked down-regulation of the IR, IGF-IR, IGF-I and IGF-II as well as NGF and NGF-R-TrA expression in hippocampus (50, 51) (Figure 7). C-peptide from onset of diabetes showed full prevention of the early neurobehavioral deficits and significant prevention of neurotrophic factors expression in hippocampus (50, 51). C-peptide replacement increased the glucose metabolic rate by approximately threefold in various brain regions in diabetic rats. The findings were associated with severe compromise of the insulin signaling as measured by decreased levels of p-Akt and GSK-3β (50, 51).

Both insulin and NGF provide important functions in hippocampus with respect to acetylcholine and glutamate synthesis and protection of cholinergic neurons (52, 53).In 4-month diabetic rats, this was reflected in a severe suppression of presynaptic synaptophysin and a marked decrease in presynaptic densities. Interestingly, these deficits were fully prevented by C-peptide substitution (37).These data suggest that insulin deficiency and impaired signaling may have a greater impact on the early abnormalities than does hyperglycemia.

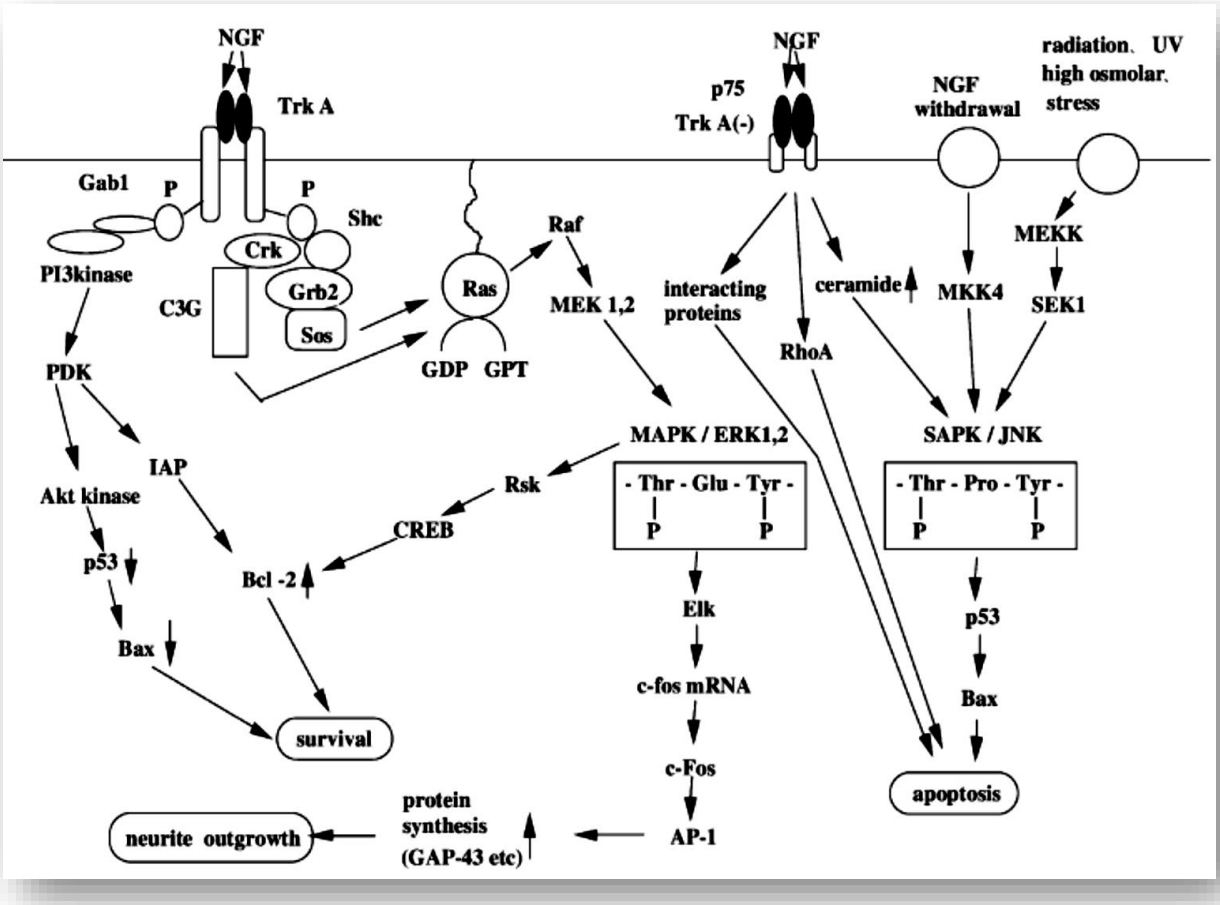

Figure 7. Schematic representation of neurotrophin signal transduction. Neurotrophins use two types of receptors, TrkA and p75NTR, to regulate the growth, development, survival and repair of the nervous system. These receptors collaborate with or inhibit each other's actions to mediate neurotrophin effects. The signaling pathways include Akt and MAPK-induced signaling via TrkA and JNK and p53 via p75NTR (H. Yasuda et al. 2003).

1.4. Plasma glucose regulating hormones

Table 1. Hormones that influence plasma glucose concentrations.

Insulin	Released by the pancreatic β-cell, when blood glucose concentrations are high; it stimulates the uptake of glucose in muscle and adipose tissue. At the same time, insulin suppresses hepatic production of glucose. Thus, when insulin sensitivity is impaired, glucose concentrations in plasma will rise due to a diminished uptake, but also due to an increased hepatic gluconeogenesis, as a consequence of the lesser suppression by insulin.
Glucagon	Released from the pancreatic α-cells, when plasma glucose concentrations drop. Glucagon acts on the liver to stimulate glucose production through glycogenolysis, but probably also reduces glucose uptake in liver and muscle.
Corticosterone (or cortisol in humans)	Released by the adrenal cortex in response to stress by the adrenocorticotropic hormone (ACTH). Corticosterone acts on the liver to increase glucose production through gluconeogenesis to ensure enough glucose within the bloodstream thus providing enough energy for the brain.
Adrenaline (epinephrine)	Released by the adrenal medulla in response to stress and by sympathetic stimulation. Adrenaline also acts on the liver to increase glucose production, but contrary to corticosterone/cortisol by a focus on glycogenolysis.
Noradrenaline (norepinephrine)	Stimulates glucose production by its release from sympathetic nerve endings, but at the same time also stimulates the release of glucagon and inhibits the release of insulin.

Plasma glucose concentrations are the net result of glucose output and glucose uptake. Several organs, hormones, and metabolites are important to keep glucose concentrations within physiological boundaries. During feeding, glucose is taken up from the gut, and in times of fasting, glucose production in the liver is stimulated resulting in an increased output of glucose from the liver to the circulation. Glucose produced by the liver is the result of glycogen breakdown (glycogenolysis) and the forming of new glucose from amino acids (gluconeogenesis). The main hormones that regulate glucose production and glucose uptake are shown in this table. In addition to their action within peripheral organs, all these hormones also have receptors in the central nervous system and thus may also affect glucose metabolism through the brain (54).

1.5. Insulin & Insulin Receptors

1.5.1. Insulin has a functional role in the brain

Insulin is a peptide hormone, normally secreted by the pancreas in response to increasing levels of metabolic fuels in the blood. Preproinsulin is a biologically inactive precursor to the biologically active endocrine hormone insulin. Preproinsulin is converted into proinsulin by signal peptidases, which remove its signal peptide from its N-terminus. Finally, proinsulin is converted into the bioactive hormone insulin by removal of two basic pairs of amino acids: the C-peptide.

The response of a tissue to insulin amounts, refers to the stimulatory effect insulin has on the uptake of monosaccharides, fatty acids, and amino acids, and their conversions to the forms of glycogen, triglycerides and protein (55). For instance, the majority of glucose uptake by peripheral tissues is under the control of insulin via the insulin-sensitive glucose transporter, GLUT-4 (56). Early studies of brain glucose metabolism suggested that uptake of glucose by CNS tissue is not dependent on insulin and, therefore, the brain was characterized as being insulin insensitive. Recently Hoyer and colleagues have demonstrated that hippocampal glucose metabolism is sensitive to application of exogenous insulin and that this sensitivity occurs via the insulin receptor (57). Therefore, insulin can promote glucose utilization in some brain areas. Furthermore, overall energy homeostasis is sensitive to CNS insulin levels (58), with CNS insulin implicated in the control of food intake (58, 59) and energy expenditure (60, 61). Additionally, firing rates of hypothalamic (62), suprachiasmatic nucleus (63) and hippocampal (64, 65) neurons are sensitive to insulin. It appears that insulin does affect activity of some neurons and, therefore, has the capacity to affect central nervous system function (66).

1.5.2. The source of CNS insulin

Insulin-like immunoreactivity has been found throughout the brain [18, 19]. There are two competing but not exclusive viewpoints on the source of central insulin: penetration of the blood-brain barrier by insulin of pancreatic origin or synthesis by neural tissue.

1.5.2.1. Peripheral insulin crosses the blood-brain barrier

Transport of insulin from the plasma into cerebrospinal fluid (CSF) in a dose-dependent manner has been documented in several species: rats, dogs, rabbits and mice and in different situations: following a meal or after peripheral administration of glucose or insulin (67, 68). Uptake of insulin into the CNS appears to occur via an active transendothelial transport across the blood-brain barrier (BBB) (68, 69). This transport process appears to be specific for insulin (70) and is saturable at blood insulin levels that are found during euglycemia (71). Thus, the uptake of insulin into the brain may be regulated independently of peripheral effects on blood glucose levels. Conditions such as obesity (72) or high glucocorticoid levels (73) decrease transport of insulin into the CNS. Both of these conditions are associated with insulin resistance in the periphery, and thus are consistent with the hypothesis that insulin uptake into the CNS is an insulin receptor-dependent process.

1.5.2.2. Synthesis of insulin in CNS

De novo insulin synthesis in brain has been proposed as an alternative source of insulin in CNS. This hypothesis has been supported by the detection of preproinsulin I and II mRNA in rat fetal brain and cultured neurons and also by insulin immunoreactivity in neuronal endoplasmic reticulum, Golgi apparatus, cytoplasm, axon, dendrites, and synapses (74). Additionally, high levels of insulin in brain extracts (75), its presence in immature nerve cell bodies (76), the rapid transport of peripherally injected insulin into the CSF (77), further support the idea that insulin can be synthesized in brain. However, the unequivocal evidence supporting this hypothesis is that insulin can be synthesized in cultured rat brain neurons and released upon K^+- and Ca^{2+}- induced membrane depolarization (78). More specifically, insulin synthesis seems to occur in pyramidal neurons (e.g., from hippocampus, prefrontal cortex, enthorhinal cortex, and olfactory bulb), but not in glial cells (79). Thus, it is not surprising that insulin is highly enriched in brain cortex, olfactory bulb, hippocampus, hypothalamus, and amygdala (75).

1.5.3. Insulin receptors in the CNS

The insulin receptor is a tetrameric, membrane spanning protein (80). Binding of insulin by the receptor induces autophosphorylation of the intracellular domain, which in turn initiates the receptor's protein tyrosine kinase activity. Tyrosine phosphorylation of intracellular substrates such as the insulin-receptor substrate family (IRS) (81) then leads to activation of multiple signals, including phosphatidyl inositol- 3 kinase and GTPase regulators (Figure 8).

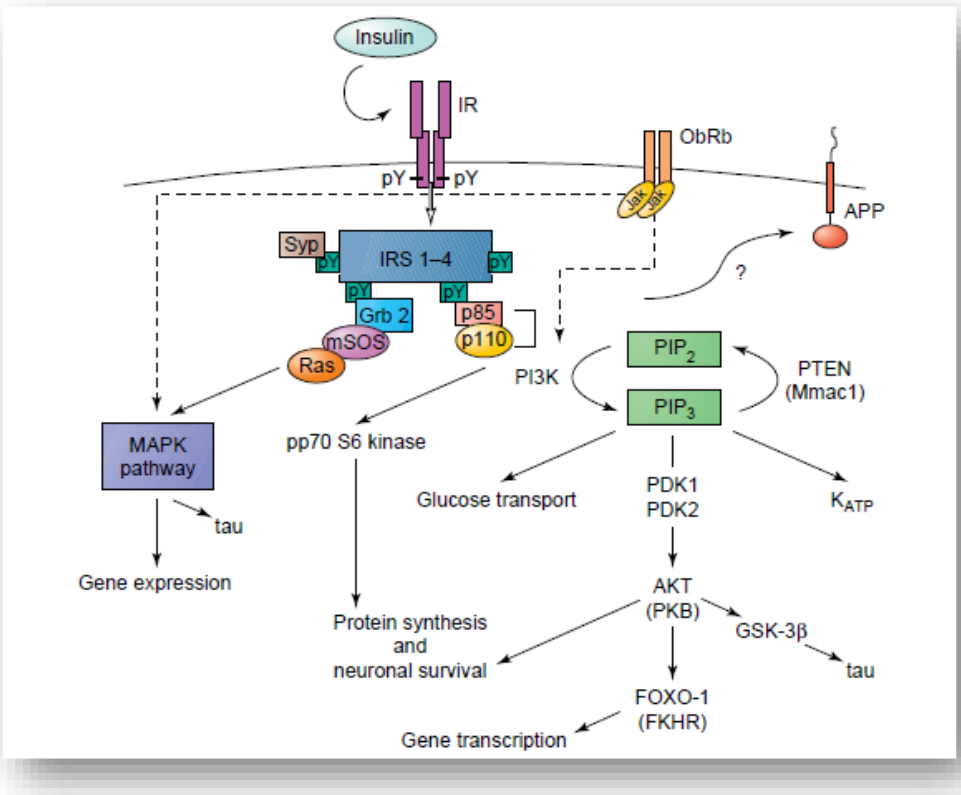

Figure 8. Insulin receptor signal transduction with respect to neuronal function. (Plum et al., 2005).

There are two types of insulin receptors found in the adult mammalian brain; peripheral types which are only found on glial cells, and a neuron-specific brain type (82). However, both types appear to be similar in insulin-signal transducing properties. Several studies have found high levels of insulin receptors in the CNS at specific locations. The 2 concentrations of insulin receptors in the brain are in olfactory bulb, cerebral cortex, hippocampus, cerebellum and hypothalamus (75, 83, 84). Furthermore, areas with high levels of insulin receptors correspond to the areas with the highest level of extractable insulin (85). Most insulin receptor immunoreactivity is on neurons, with very little seen on glial cells (84, 86). In the hippocampus, insulin binding is detected in the molecular layer of the dentate gyrus, and

in the dendritic fields of CA1 pyramidal cells (84, 87). Importantly, insulin binding in the hippocampus is associated with immunocytochemically detectable phosphotyrosine and IRS-1, one of the putative cellular intermediates in insulin action (86).

1.6. Cholinergic system

1.6.1. Acetylcholine

Acetylcholine is the only low-molecular-weight amine transmitter substance that is not an amino acid or derived directly from one. The biosynthetic pathway for ACh has only one enzymatic reaction, catalyzed by choline acetyltransferase (Figure 9). This transferase is the characteristic and limiting enzyme in ACh biosynthesis.

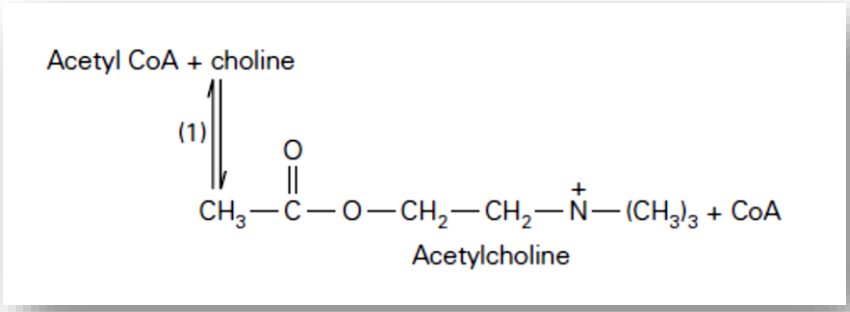

Figure 9.Biosynthesis of Acetylcholine (Principles of Neural Science, 5th Edition).

Nervous tissue cannot synthesize choline, which is derived from the diet and delivered to neurons through the blood stream. The co-substrate, acetyl coenzyme A (acetyl CoA), participates in many general metabolic pathways and is not restricted to cholinergic neurons. Acetylcholine is released at all vertebrate neuromuscular junctions by spinal motor neurons (Figure 10).

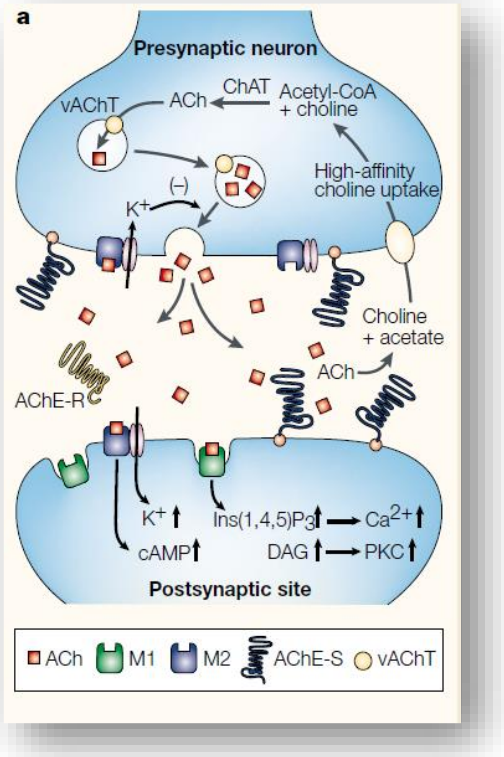

Figure 10. Cholinergic signaling is terminated by metabolism of acetylcholine (ACh) to the inactive choline and acetate by acetylcholinesterase (AChE), which is located in the synaptic cleft. Choline (Ch) is transported back into the nerve terminal (light blue arrow) by the choline transporter (CHT), where choline acetyltransferase (ChAT) subsequently catalyzes acetylation of choline to reform ACh. The ACh is transported into the vesicle by the vesicular ACh transporter (VAChT) (H. Soreq & S. Seidman, 2001).

In the autonomic nervous system it is the transmitter for all preganglionic neurons and for parasympathetic postganglionic neurons as well. Cholinergic neurons form synapses throughout the brain; those in the nucleus basalis have particularly widespread projections to the cerebral cortex. Acetylcholine (together with a noradrenergic component) is a principle neurotransmitter of the reticular activating system, which modulates arousal, sleep, wakefulness, and other critical aspects of human consciousness.

1.6.2. Acetylcholinesterase

Acetylcholinesterase (AChE) rapidly hydrolyzes the neurotransmitter acetylcholine (ACh) at brain cholinergic synapses as well as at neuromuscular junctions (88) (Figure 11).

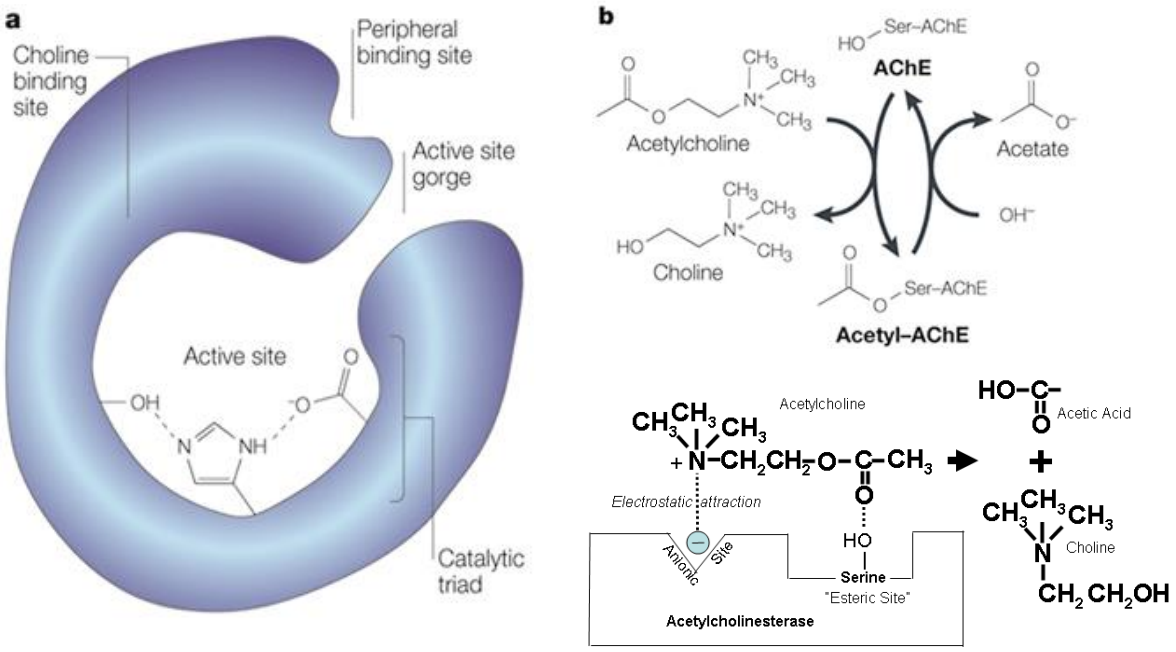

Figure 11. Acetylcholinesterase.
A | Structural features of the enzyme. X-ray crystallography has identified an active site at the bottom of a narrow gorge, lined with hydrophobic amino-acid side chains. At the time, the catalytic triad was unique among serine hydrolases in having a glutamate side chain in lieu of the familiar aspartate side chain. A choline-binding site (anionic site) featured hydrophobic tryptophan residues instead of the expected anionic groups; a peripheral binding site has also been identified by site-directed mutagenesis.
B | The acetylcholinesterase (AChE) reaction. AChE promotes acetylcholine hydrolysis by forming an acetyl-AChE intermediate with the release of choline, and the subsequent hydrolysis of the intermediate to release acetate (H. Soreq & S. Seidman, 2001).

Alternate promoter usage and alternative splicing together modify the 5′ and 3′ termini of AChE mRNA, allowing the production of six protein subunits with different N- and C-termini. Three different carboxy termini exist: the “synaptic” or S variant, which is also called “tailed” (89), the “erythrocytic” or E variant (90) and the “readthrough” or R variant (91). These join

the two different N-termini to yield variants with the common or the “extended” N-terminus. Whereas the catalytic domain of all AChE isoforms remains invariable, the characteristics of these different terminal peptides alter several key features of the protein. A prominent characteristic of AChE-S, the most abundant form in the nervous system, is a C-terminal cysteine residue located three amino acids from the end of the protein. This cysteine residue allows disulfide bonding with other AChE-S units, giving rise to amphipathic homodimers and homotetramers. Beyond its different amino-acid sequence, the AChE-R C-terminus differs from that of AChE-S in two obvious characteristics: (1) it is hydrophilic, and (2) since it lacks the C-terminal cysteine residue found in the AChE-S C-terminus, it cannot tetramerize by disulfide bonding with other subunits. This produces a soluble monomeric molecule, instead of the amphipathic tetramers composed of dimers. AChE-S tetramers associate with one of two membrane anchoring molecules, which partially determine the synaptic localization of the protein: collagen Q (ColQ) in neuromuscular junctions, and a proline-rich membrane anchor (PRiMA) in brain synapses. (Figure 12). PRiMA-associated AChE tetramers are traditionally designated as G4 (for globular), and monomers and homodimers not associated to any anchorage protein are designated as G1 and G2, respectively (Figure 12) (92).

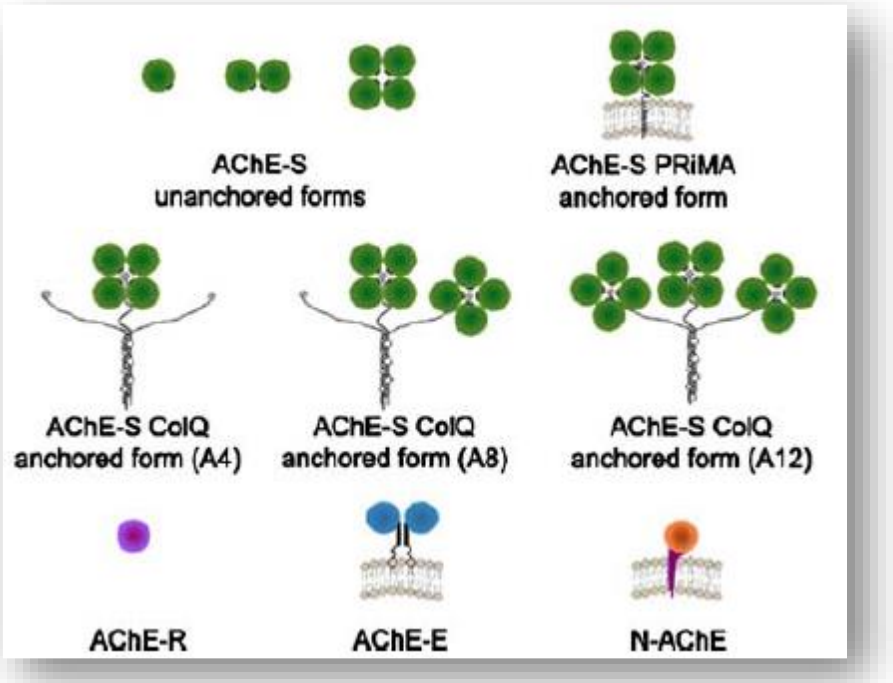

Figure 12. Alternative protein products of the ACHE gene. AChE-S units can dimerize, tetramerize, or remain as monomers. AChE-S tetramers can remain soluble or become anchored to the membrane by the molecules ColQ or PRiMA. AChE-R inherently remains as a soluble monomer. AChE-E forms glypiated dimers linked to the red blood cells membrane (G. Zimmerman & H. Soreq, 2006)

1.6.3. Acetylcholine receptors

An acetylcholine receptor (AChR) is an integral membrane protein that responds to the binding of acetylcholine, a neurotransmitter. The two main cholinergic receptors are:

- **Nicotinic acetylcholine receptors** (nAChR, also known as "ionotropic" acetylcholine receptors) are particularly responsive to nicotine. The nAChRs are ligand-gated ion channels, and, like other members of the "cys-loop" ligand-gated ion (Na^+ and K^+) channel superfamily, are composed of five protein subunits symmetrically arranged like staves around a barrel (Figure 13).

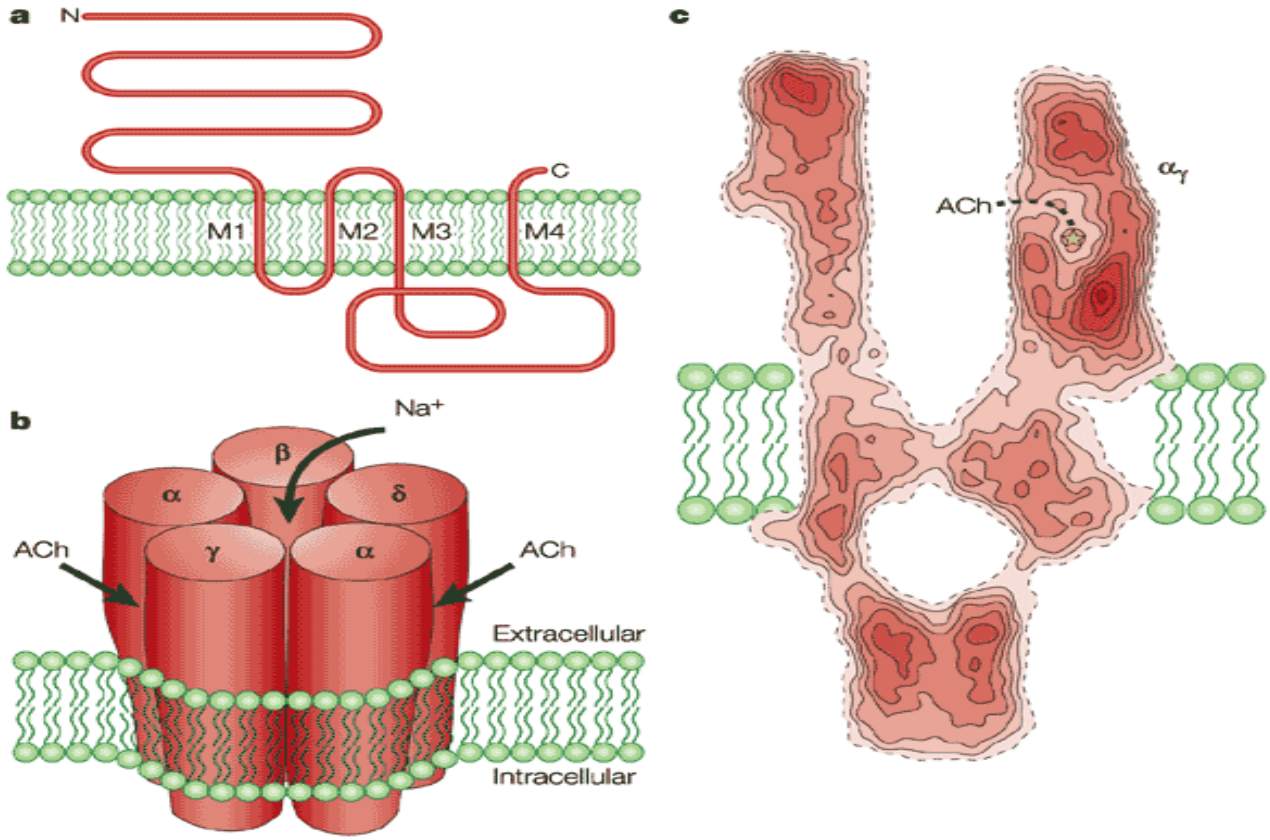

Figure 13. a | The threading pattern of receptor subunits through the membrane. b | A schematic representation of the quaternary structure, showing the arrangement of the subunits in the muscle-type receptor, the location of the two acetylcholine (ACh)-binding sites (between an alpha- and a gamma-subunit, and an alpha- and a delta-subunit), and the axial cation-conducting channel. c | A cross-section through the 4.6-Å structure of the receptor determined by electron microscopy of tubular crystals of Torpedo membrane embedded in ice. Dashed line indicates proposed path to binding site (A. Karlin, 2002).

- **Muscarinic acetylcholine receptors** (mAChR, also known as "metabotropic" acetylcholine receptors) are particularly responsive to muscarine. They belong to the superfamily of G-protein-coupled receptors that activate other ionic channels via a second messenger cascade. The muscarinic cholinergic receptor activates a G-protein when bound to extracellular ACh (Figure 14).

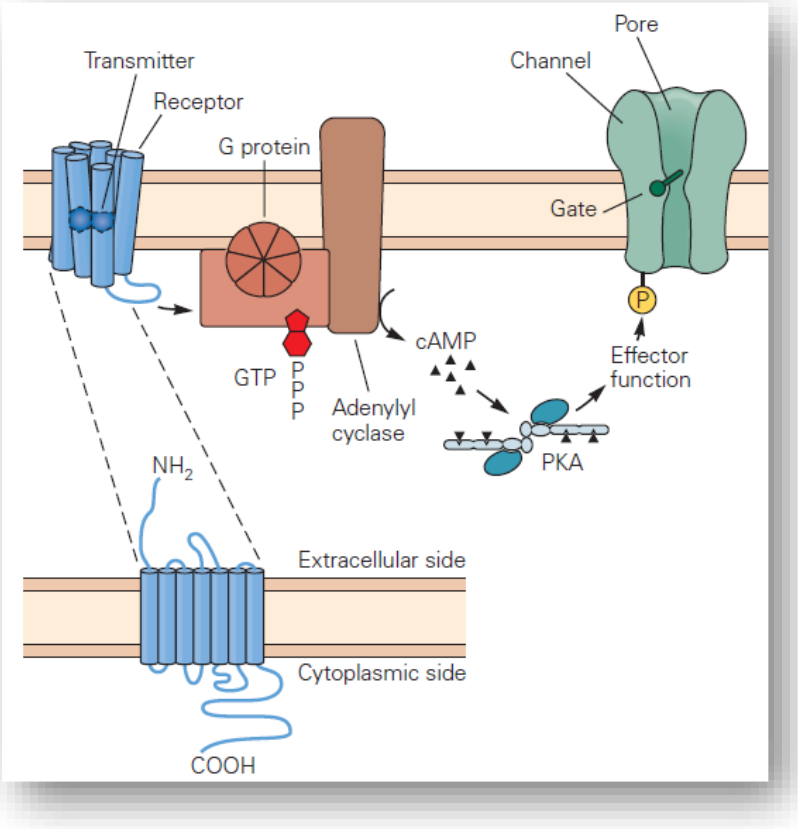

Figure 14. A receptor that indirectly opens an ion channel is a distinct macromolecule separate from the channel it regulates. In one large family of such receptors, the receptors are composed of a single subunit with seven membrane-spanning helical regions that bind the ligand within the plane of the membrane. These receptors activate a guanosine triphosphate (GTP)–binding protein (G protein), which in turn activates a second-messenger cascade that modulates channel activity. In the cascade illustrated here the G protein stimulates adenylyl cyclase, which converts adenosine triphosphate (ATP) to cAMP. The cAMP activates the cAMP-dependent protein kinase (PKA), which phosphorylates the channel (P), leading to a change in function (Principles of Neural Science, 5th edition).

1.6.4. Cholinergic system and glucose levels regulation

There is evidence to be an inverted-U dose effect curve for glucose effect on cognition and the ACh release in euglycemic mice. On the one hand, acetylcholine (ACh) output increases in the hippocampus of rats performing a spatial alternation task and peripheral and hippocampal injections of glucose enhance that release along with increasing scores on the behavioral task (93, 94). However, there appears to be an inverted-U dose effect curve for glucose effect on memory (95) and ACh release (93), indicating the negative effects that high glucose levels have, even if it is a single quickly absorbable injection of glucose.

1.6.5. Cholinergic system and insulin

Peripheral administration of insulin in euglycemic mice, also acts to increase ACh levels in the amygdala (96) while intracerebroventricular administration increases ACh levels in the mid-brain, caudate nucleus and pons medulla (97). Additionally, Messier has reported that peripheral insulin administration in euglycemic mice attenuates scopolamine-induced deficits in an operant task (98) suggesting an increase in cholinergic activity.

1.7. Oxidative Stress

1.7.1. Oxidative Stress and antioxidant defense mechanisms

Radicals derived from oxygen (ROS) and nitrogen (RNS: derived from nitric oxide: NO) are the largest class of radical species generated in living systems. ROS and RNS are products of normal cell metabolism and have either beneficial or deleterious effects, depending on the concentration reached in the tissues (99, 100). Free radicals can be defined as molecules or molecular fragments containing one or more unpaired electrons in molecular orbits. These unpaired electrons give a considerable degree of reactivity to the free radical. ROS are produced as intermediates in reduction–oxidation (redox) reactions leading from O_2 to H_2O (101).

The neuronal cell oxidative stress (OS) response has an intense interest for neuroscientists because it is a hotspot on neurodegeneration. The generation of reactive oxygen species (ROS) and oxidative damage is believed to be involved in the pathogenesis of neurodegenerative disorders. Biological systems that require oxygen for life are always under various levels of OS. The main ROS involved in neurodegeneration are superoxide anion (O_2^-), hydrogen peroxide (H_2O_2), and the highly reactive hydroxyl radical ($HO^\bullet$). Furthermore, reactive nitrogen species (RNS) such as nitric oxide (NO) can also damage neurons. The free radical NO can react with O_2^- to produce peroxynitrite ($ONOO^-$), a powerful oxidant, which may decompose to form $HO^\bullet$. Oxidative stress results from an imbalance between ROS generation and antioxidant defenses (102), combined with a disruption of thiol-redox circuits, which leads to aberrant cell signaling and dysfunctional redox control (103). In the blood, oxidative stress results from an imbalance between pro-oxidants and antioxidants, which can be quantified as the redox state of plasma glutathione/glutathione disulphide: GSH/GSSG. As details become available concerning subcellular redox organization, a new generation of targeted antioxidants may become available which restore redox signaling and facilitate disease prevention (Figure 15) (104, 105).

Superoxide dismutases in the mitochondria (Mn-SOD) and cytoplasm (Cu/Zn-SOD) convert O_2^- to oxygen (O_2) and H_2O_2 (Figure 15).In turn, catalase and glutathione peroxidases convert H_2O_2 to water (Figure 15). CAT is responsible for the high concentrations of H_2O_2, usually undertakes H_2O_2 located in the peroxisome. GPx is responsible for the low concentrations of H_2O_2, and usually undertakes the H_2O_2 located in the cytosol and the mitochondrial matrix. It takes usually H_2O_2 produced by the action of SOD. These antioxidant enzymes are critical for preventing oxidative damages to cells (101) (Figure 15).

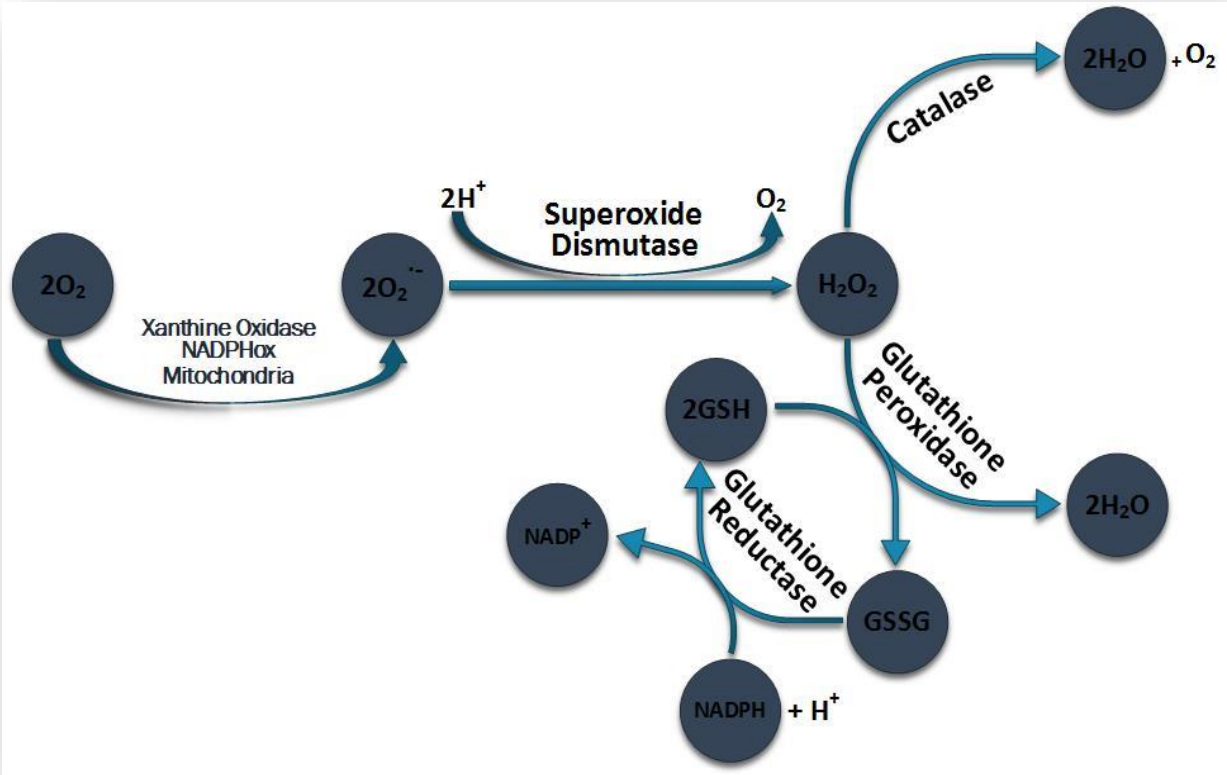

Figure 15. Schematic representation of the main antioxidant activity. $O_2^{\bullet-}$, superoxide; CAT, catalase; Cu-SOD, copper SOD; Mn-SOD, manganese SOD; GPx, glutathione peroxidase; GSH, glutathione; GSSG, glutathione disulfide; H_2O_2, hydrogen peroxide; NAD(P)H, nicotinamide adenine dinucleotide phosphate

Lipids are particularly vulnerable to oxidation because membranes of some cells are rich in polyunsaturated fatty acids and because of the presence of oxygen at millimolar levels in the lipid bilayer. Unsaturated phospholipids, glycolipids, and cholesterol in cell membranes and other organized systems are prominent targets of oxidant attack. This can result in lipid peroxidation, a degenerative process that disturbs structure/ function of the target system. Lipid hydroperoxides (LOOHs) derived from unsaturated phospholipids, glycolipids, and cholesterol are prominent intermediates of peroxidative reactions induced by activated species such as hydroxyl radical, peroxyl radicals, singlet oxygen, and peroxynitrite. If lipid peroxides are not neutralized by endogenous antioxidants, they will fragment unsaturated and diffusible aldehydes (acrolein; 4-hydroxynonenal (HNE); and 4-hydroxyhexenal (HHE), 4-ONE: 4-oxononenal; MDA: malondialdehyde). These are highly reactive electrophiles (106), and like ROS/RNS, they are capable of covalently modifying proteins, DNA and other macromolecules (Figure 16).

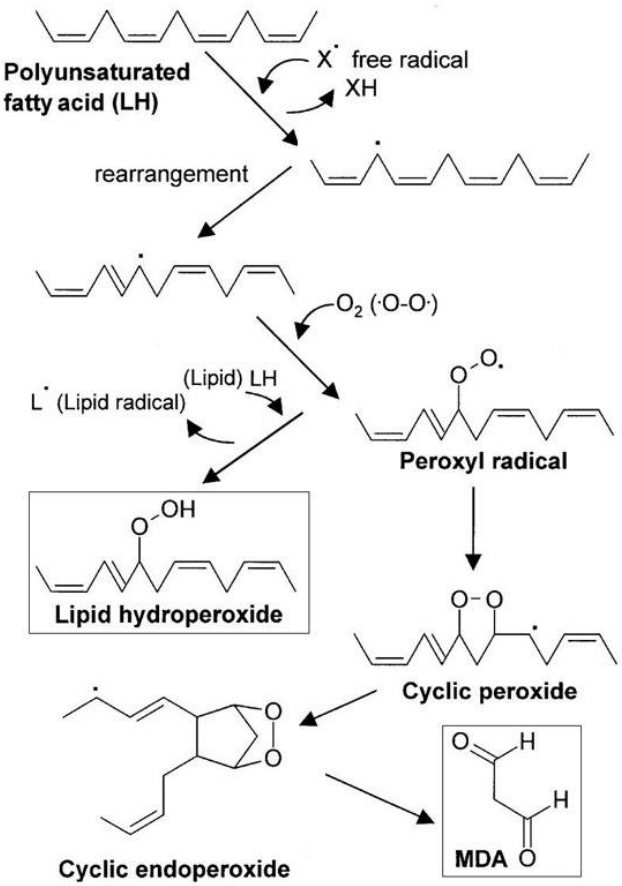

Figure 16. Steps in lipid peroxidation process (N.M. Dukic et al., 2012).

1.7.2. Oxidative stress in diabetic neuropathy

It is commonly thought that oxidative stress is the critical pathologic process in a number of diabetes-related complications including nerve degeneration (107, 108). The persistent hyperglycemia appears to have a major role in the onset of cognitive and affective disorders associated with diabetes (109). It has been suggested that hyperglycemia causes tissue dam-age through several mechanisms, such as an increase in glucose flux and other sugars through the polyol pathway, increase of advanced glycation end-products (AGEs) synthesis, increase of AGEs receptor expression, activation of protein kinase C isoforms and overactivity of the hexosamine pathway (110). Furthermore, evidence indicates that these mechanisms are activated by increased oxidative stress (111), which results from increasing

of reactive species of oxygen or nitrogen (ROS/RNS) production and/or impairment of antioxidant defenses (112). In fact, the oxidative stress can lead to damage of the main components of the cellular structure, including nucleic acids, proteins, amino acids and lipids (113), affecting several cell functions, such as metabolism and gene expression, which in turn can precipitate or impair other pathological conditions (114). The persistence of oxidative stress also leads to a cascade of events resulting in neurodegenerative apoptotic injury (115). Diabetes-induced oxidative stress in sensory neurons and peripheral nerve is demonstrated by increased production of reactive oxygen species (ROS), lipid peroxidation (107, 116, 117), and protein nitrosylation (118), and diminished levels of reduced glutathione (107) and ascorbate (95).

1.7.3. Aberrant mitochondrial function and generation of oxidative stress in diabetes

It has been hypothesized that high glucose concentration drives excessive electron donation to the respiratory chain in mitochondria resulting in mitochondrial hyperpolarization and elevated production of ROS (116). Brownlee et al. have proposed that this mitochondrial-dependent process is a critical modulator of oxidative stress at sites of complications in diabetes (116, 119). The proposal implies that high glucose concentration in tissue targets for diabetic complications leads to increased supply of NADH in the mitochondria, and that this increased electron availability and/or saturation may induce partial reduction of oxygen to superoxide radicals in the proximal part of the electron transport chain (116, 119). Subsequent large elevations in ROS then induce degeneration of tissue. Studies in cultured embryonic sensory neurons have shown that high glucose concentration induces toxicity through an apoptotic route involving a mitochondrial-dependent pathway (108).

1.8. Experimental model of Streptozotocin

Streptozotocin (STZ) is a β-cytotoxic agent that can be injected intravenously, subcutaneously or intraperitoneally. The nitrosure amoiety of STZ is responsible for its cellular toxicity, which is mediated through a decrease in NAD levels and the formation of intracellular free radicals (120, 121). The deoxyglucose moiety of STZ facilitates its transport across the cell membrane, in which the GLUT-2 glucose- transporter appears to play an essential role (120). The insulin-producing β-cells of the islets of Langerhans combine a high expression of GLUT-2 transporters with a relatively low NAD content, making them particularly vulnerable to STZ toxicity (120). The absence of GLUT-2 glucose-transporters at the blood-brain barrier (122) limits STZ access to the brain after systemic injection. STZ-diabetic rodents are hypoinsulinemic, but do not require insulin treatment to survive. Blood glucose levels are 20–25 mmol/l (normal 5 mmol/l).These high blood glucose levels lead to marked polydipsia and polyuria and weight loss. Like diabetic patients, STZ-diabetic rats develop end-organ damage affecting the eyes, kidneys, heart, blood vessels, and nerves(123).

1.9. Aim of the study

The aim of the study was to investigate of the effects of streptozotocin-induced Type I diabetes. For this reason, STZ-treated C57BL/6 mice were either administered insulin or placebo for 6 days, and examined:

Glycemic profile: plasma glucose, total cholesterol and triglycerides levels.

Behavioral indices: fear-anxiety, learning-memory and depressive-like behavior.

Cholinergic system: acetylcholine levels (ACh), SS and DS acetylcholinesterase activity (AChE) of brain regions.

Oxidant markers:

- Antioxidant defense markers: Activities of superoxide dismutase (SOD), catalase (CAT), glutathione peroxidase (GPx) and the ratio of oxidized/reduced glutathione (GSSG/GSH ratio) of brain regions.
- Lipid peroxidation marker: Malondialdehyde levels (MDA) of brain regions.

Neuronal apoptosis: Ratio of the cytoplasmic cytochrome c content to the mitochondrial cytochrome c content by using western blot analysis on mitochondrial lysates and cytoplasmic samples of brain regions.

Brain areas examined

Cerebellum (Ce), hippocampus (Hip), striatum (Str), cerebral cortex (Cx), midbrain (Mb) and diencephalon (Die)

Overall, this work sought to correlate diabetic state in mice with cognitive function.

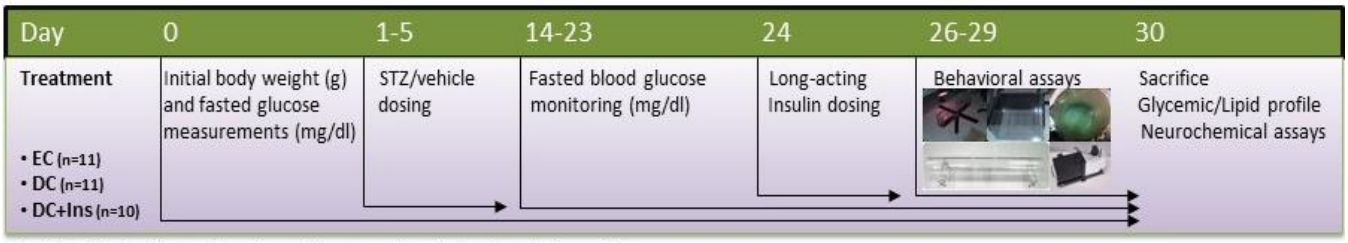

(→) Indicates the continuation of the procedure during the study period.

II. MATERIAL & METHODS

2.1. Animal studies

Male adult C57BL/6 mice at 2-4 months-old (The Jackson Laboratories, Bar Harbor, ME, USA), weighing 25-32 g were maintained at the animal house of the Medical School of the University of Patras, under standard conditions (24 °C; humidity from 23% to 42%; 12-h light/dark cycle, lights on at 8:00 am) and received food and water ad libitum. The protocol for the experiment is presented in Figure 1. All experimentation was carried out in accordance to the European Communities Council Directive of the *Protocol for the Protection and Welfare of Animals* (86/609/EEC) and the Greek National Laws (Animal Act, PD 56/13). In the present study, we took into consideration the 3Rs (reduce, refine, replace).

2.2. Experimental induction of diabetes

Mice (n=32) were randomly divided into 3 groups (n=10-11/group). Streptozotocin induced diabetic group (DC): The mice of this group (n=11) became diabetic after intraperitoneal (IP) administration of Streptozotocin (STZ) (7.5 mg/ml; Sigma-Aldrich, St. Louis, MO) diluted in 0.1M sodium-citrate buffer (pH 4.5), at the dosage of 50 mg/kg body weight/per day, for 5 consecutive days. Streptozotocin induced diabetic group + insulin treatment (DC+Ins): The mice of this group (n=10) became diabetic after intraperitoneal (IP) administration of Streptozotocin (7.5 mg/ml; Sigma-Aldrich) diluted in 0.1M sodium-citrate buffer (pH 4.5), at the dosage of 50mg/kg body weight/per day, for 5 consecutive days. Subsequently, the mice of this group were treated with the long-acting insulin glargine. Euglycemic Control group (EC): A euglycemic control animal group (n=11) was also included in the study and received an equivalent amount of the sodium-citrate buffer. Fasted blood glucose levels were measured periodically, from the 14th day after the last STZ injection, using a portable Freestyle glucometer (Precision Xtra meter, Abbott Laboratories Hellas, Greece). Blood was obtained via tail snip. Mice with fasting blood glucose values of 200 mg/dL or above were included in the diabetic groups. Body weight, daily food and water consumption were measured regularly during the experiment.

2.2.1. Insulin treatment

At the 24th day the DC+Ins group was given long-acting insulin glargine (0.5 Ui/ml) diluted in saline, at the dosage of 6 IU/kg/day, for 6 consecutive days (Lantus® SoloSTAR®

Pen, Sanofi-Aventis, Greece). The EC and DC groups received an equivalent amount of saline respectively.

2.3. Plasma lipid determination

Following a 16 h fasting period (starting at 6:30 PM on the first day and ending at 10:30 AM the next day), plasma samples were isolated from the experimental mice. Plasma triglycerides and total cholesterol were assessed spectrophotometrically using the Triglycerides FS 10' kit (Diagnostic Systems GmbH, catalog no. 1 5710 99 10 021) and the Cholesterol FS 10' kit (Diagnostic Systems GmbH, catalog no. 1 1300 99 10 021) according to the manufacturer's instructions. Five μL of serum sample were diluted with 20 μL of phosphate-buffered saline (PBS), and 7.5 μL of the diluted sample were analyzed for triglycerides. Five μL of serum sample were diluted with 45 μL of phosphate-buffered saline (PBS), and 7.5 μL of the diluted sample were analyzed for total cholesterol. Triglyceride and cholesterol concentrations were determined spectrophotometrically at 490 nm.

2.4. Behavioral studies

Towards ascertaining the correct evaluation of the behavioral effects of diabetes and insulin treatment, mice participated to a maximum of two behavioral tests in order to not be exposed to excessive stress. Specifically, 15 mice (5 per group) performed the elevated-plus maze test and the forced swim test, while 17 mice (5-6 per group) performed the open-field test and the step-through passive avoidance test.

2.4.1. Anxiety-like behavior

In order to assess the effects of diabetes on anxiety-like behavior, we used two behavioral tests, based on the animals' fear/anxiety for the unknown environment (open field and height), despite its tendency to explore it. The application used for the recording rodents' behavior during the open-field and the elevated plus-maze tests was the software Phobos.

2.4.1.1. Open field test

On day 26, we assessed the anxiety-like behavior of thigmotactism using the open-field test (OFT). Thigmotactism refers to the preference of mice to walk near the walls of an

open field device. The experimental device was first described by Simon et al. (124). The apparatus, made of transparent PVC, had a white floor of 50 cm×50 cm and transparent walls (divided by black lines into squares of 10 cm×10 cm), 40-cm high. On day 26, mice were kept for 1 h in a both slightly illuminated and sound-isolated room to habituate. Then, each mouse was gently placed into the center of the device and recorded for 10 min. Thigmotaxis time, which is the time spent close to the walls of the apparatus (<5 cm) were recorded and used as an index of anxiety (125), while the entries to the center were used as an index of anxiolysis.

2.4.1.2. Elevated plus-maze test

On day 26, we assessed the anxiety-like behavior using the elevated plus-maze test (EPM) (126, 127). Mice were kept for 1 h in a both slightly illuminated and sound-isolated room to habituate. The duration of the test was 10 min. The device used for this test is cross-shaped, with two open arms (30 cm x 5 cm) and two closed arms (30 cm x 5 cm x15 cm) that extended from a central platform (5 cm x 5 cm). The entire maze was elevated 40 cm above the floor. On the one hand, the enclosed arms offer safety; on the other hand, the open arms give to the rodent the motive of exploration.

In a slightly illuminated room, each animal was placed in the central square of the apparatus, facing an enclosed arm; an arm entry was defined when all four paws entered an arm. The time spent in open arms was recorded. The % ratio of open/total time spent on open and enclosed arms of the plus maze, as well as the entries to the open arms were used as an index of anxiolysis (125).

2.4.3. Step-through passive avoidance test

The step-through passive avoidance test is based on negative reinforcement to examine long-term memory (128). A two-compartment passive avoidance apparatus (white/dark, separated by a guillotine door) was used. The floor of non-illuminated compartment was composed of 2 mm stainless steel rods. Mice were subjected to single trial of passive avoidance task according to previously described procedures with minor modifications (128, 129). Briefly, on day 27 each mouse was placed in the illuminated compartment and left for 100 s to habituate the apparatus (habituation trial). One hour after the habituation trial, in the acquisition trial, each mouse was placed in the illuminated chamber and the guillotine door was opened. Once the animal crossed all four paws in the dark

chamber an electric foot shock (25 V, 3 mA, 5 s) was applied. The initial latency (IL) required to enter the dark compartment was measured (max time allowed 180 s). Twenty four hours later, the retention trial was performed. Each mouse was placed in the illuminated compartment of the apparatus, the door was opened and the step-through latency time (STL) until the mouse enters the dark chamber was recorded (maximum time allowed 300 s). During these sessions, no electric shock was applied.

2.4.4. Forced swimming test

Forced swimming test (FST) was carried out as described elsewhere with slight modifications (130, 131). On day 28, mice after 1 hour of habituation at the experimental room, were placed individually into an inescapable Plexiglas cylindrical tank (height: 30 cm, diameter: 22.5 cm) filled with tap water to a depth of 15 cm and maintained at 25 °C. In this test, after an initial vigorous activity of 2 min, mice acquired an immobile posture which was characterized by motionless floating in the water and making only those movements necessary to keep the head above the water. The duration of immobility (s), was recorded during the last 4 min of the 6 min test.

2.5. Tissue preparation

On day 30, mice were euthanized by cervical dislocation and plasma and tissue samples were collected. Brain was excised immediately, and the main brain structures isolated: cerebellum (Ce), hippocampus (Hip), striatum (St), cerebral cortex (Cx), midbrain (Mb) and diencephalon (Die). All tissues were rinsed with saline immediately, frozen in liquid nitrogen, and stored at -80 °C until performing the experiments. The brain tissues from 15 mice, intended for the biochemical assays, were weighed and homogenized with a glass-Teflon homogenizer (Thomas Philadelphia, USA, No B 13957) in ice-cold in 30 mM Na_2HPO_4 buffer (pH 7.6; Sigma-Aldrich). The 150 μl of the volume of each homogenate was separated and stored -75°C for the acetylcholine (ACh) assay. The rest of the volume of the homogenate was used for the acetylcholinesterase (AChE) assay and the oxidative assays. The homogenates were centrifuged at 12,600 *g*, for 20 min at 4°C. Supernatants constituted the salt-soluble (SS) fractions and were stored at -75°C, for both the evaluation of the activity of SS-AChE and the oxidative assays. The pellets were re-suspended in an equal volume of 1% (w/v) Triton X-100 (in 30 mM Na_2HPO_4, pH 7.6; Sigma-Aldrich) and then once again

centrifuged at 12,600 *g* for 20 min at 4 °C. Supernatants, the detergent-soluble (DS) fractions, were collected and stored at -75°C. This double-extraction method was performed in order to recover the cytosolic (SS fraction) and membrane-bound (DS fraction) isoforms of achetylcholinesterases (132). The protein concentrations were determined by the Bradford assay (133) with bovine serum albumin as a standard (0.05–1.00 mg/mL; Sigma-Aldrich).

2.6. Colorimetric determination of AChE activity

AChE activity was determined using Ellman's colorimetric method (134) in which, as it has been presented by others (135) and our group (136) the term AChE is actually referred to the total ChE activity since no specific inhibitors for butyryl-ChE (BuChE) were used. It is important to point out that the Bu-ChE holds only a small fraction of the total ChE activity in the brain (136). The AChE activity was expressed as μmol/min/g tissue. Briefly, in the 96 well plates, 25 μL of 15 mM ATCI (Sigma-Aldrich), 75 μL of 3 mM DTNB (Sigma-Aldrich) and 75 μL of 50 mM Tris–HCl (Sigma-Aldrich), pH 8.0, containing 0.1% BSA, were added and the absorbance was read at 405 nm after 5 min incubation at RT. Any increase in absorbance due to the spontaneous hydrolysis of the substrate was corrected by subtracting the rate of the reaction before adding the enzyme. Then, 25 μL of sample (SS and DS fraction of brain homogenates) were added and the absorbance was read again after 5 min of incubation at RT. All determinations were carried out in triplicate. The AChE activity was expressed as μmol/min/g tissue.

2.7. Colorimetric determination of ACh

ACh was determined by using the method of Hestrin (137), with minor modifications in order to determine ACh in small volumes with a rapid and sensitive procedure. In brief, brain homogenate aliquots (133 μL) were mixed with 233 μL of distilled water, 33 μL of eserine 1.5 mM (Sigma-Aldrich), and 133 μL of trichloroacetic acid 1.84 M (Sigma-Aldrich) and blended adequately. After centrifugation (10,000 *g*, 15 sec at 4 ^{o}C), supernatant was collected and 83 μL of each tissue was added to the plate. Then, 83 μL of basic hydroxylamine (by mixing equal volumes of hydroxylamine hydrochloride 2 M and NaOH 3.5 M; Sigma-Aldrich) was added and the mixture was incubated for 20 minutes at 25 ^{o}C. Finally, 41.5 μL of HCl 3.75 M and 41.5 μL of $FeCl_3$ 0.75 M were added. Absorbance was determined at 540nm. Standard

concentrations of acetylcholine chloride (0.078–10 mM; Sigma-Aldrich) were used for the construction of a calibration curve. All determinations were performed in triplicate. The results are expressed as μmol/mg protein.

2.8. Assessment of oxidative stress

2.8.1. Determination of superoxide dismutase activity

The superoxide dismutase (SOD) activity was determined according to the Superoxide Dismutase Assay Kit (Item No. 706002), Cayman Chemical Company, which is based on the formation of a tetrazolium salt for the detection of superoxide radicals generated by xanthine oxidase and hypoxanthine. The SOD assay provides measures all three types of SOD (Cu/Zn, Mn, FeSOD). The absorbance was read at 450 nm. The results are expressed as units/mg of protein, where one unit of SOD is defined as the amount of enzyme needed to exhibit 50% dismutation of the superoxide anion.

2.8.2. Determination of catalase activity

The peroxidative activity of catalase (CAT) was determined according to the modified method of Sinha (138). The method is based on the reaction of the enzyme with methanol in the presence of an optimal concentration of H_2O_2. The formaldehyde produced is measured colorimetrically at 540 nm with reaction with Purpald (4-amino-3-hydrozino-5-mercapto-1,2,4-triazole; Sigma-Aldrich) as the chromogen. Purpald specifically forms a bicyclic heterocycle with aldehydes, which upon oxidation with KIO_4 (Sigma-Aldrich), changes from colorless to a purple color. Standard concentrations of formaldehyde (0–75 μM; Sigma-Aldrich) were used for the construction of a calibration curve. All determinations were performed in triplicate. The results are expressed as μM/min/mg of protein.

2.8.3. Determination of glutathione peroxidase activity

Glutathione peroxidase (GPx) activity was determined colorimetrically following Rotruck et al. (139) to estimate the rate of the glutathione oxidation by H_2O_2. Reduced glutathione was used as substrate and 5,5′-dithiobis(2-nitrobenzoic acid) as a chromogen. Suitable aliquots of standard concentrations of GPx (0.0125–1 U/ml; Sigma-Aldrich) were also used for the construction of the calibration curve. The color that was developed was read

against a reagent blank at 412 nm. Results were expressed as Ui/mg of protein/min (one unit was the amount of enzyme that converted 1 μmol of reduced to the oxidized form of glutathione in the presence of H_2O_2; Sigma-Aldrich). All determinations were performed in triplicate.

2.8.4. Determination of reduced and oxidized glutathione content

A modification of Hissin and Hilf's method was used for the determination of the ratio of the oxidized (GSSG) glutathione content to the reduced glutathione (GSH) content in the brain regions (140). The two forms of glutathione were estimated fluorometrically after reaction with o-phthalaldehyde (OPT). The samples were treated with 50% trichloroacetic acid (TCA) and centrifuged to eliminate the protein content. The supernatant was extracted three times with diethyl ether. The aqueous fraction was used to determine the GSH and GSSG content; GSH selectively reacted with OPT (10 mg/ml in pure methanol; Sigma-Aldrich) at pH 8.0 (500 mM Na_2HPO_4 buffer), whereas after the addition of 5 mM N-ethyl maleimide (NEM; Sigma-Aldrich) in the samples, only GSSG reacted with OPT at pH 12.0 (0.2 N NaOH). Standard concentrations of GSH and GSSG (0.75–30 μM; Sigma-Aldrich) were used. The excitation wavelength was at 340 nm and the fluorescence intensity was determined at 420 nm. The respective concentrations in μmol/gr of protein were calculated from the respective calibration curves. All determinations were performed in triplicate.

2.8.5. Determination of lipid peroxidation content

Lipid peroxidation was determined by the evaluation of malondialdehyde (MDA) levels in the brain regions. Due to the small volume of tissue sample, the fluorimetric method of Grotto et al. (141) and Jentzsch et al. (142) was used with slight modifications to measure MDA levels using a 96-well microplate. MDA was determined after the reaction with thiobarbituric acid (Sigma-Aldrich) and extraction with n-butanol (Sigma-Aldrich). The excitation wavelength was at 515 nm and the fluorescence intensity was determined at 553 nm. The results were expressed as μmol MDA/gr of protein against a standard curve (0.05–10 μM MDA; Sigma-Aldrich).

2.9. Isolation of mitochondria

Tissue samples were collected as above. Brain was excised immediately, and the main brain structures isolated: hippocampus (Hip), striatum (St), cerebral cortex (Cx), midbrain (Mb) and diencephalon (Die). All tissues were rinsed with saline immediately, frozen in liquid nitrogen and stored at -80 °C until performing the experiments. The brain tissues from 9 mice, intended for western blot analysis, were weighed and homogenized as described previously (143) with minor modifications. Tissues were homogenized in sucrose buffer (0.32 M sucrose, 1mM EDTA, 10 mM Tris-HCl, pH 7.4; Sigma-Aldrich); diluted to 25% (w/v), with a glass-Teflon homogenizer (Thomas Philadelphia, USA, No B 13957). The brain homogenization was performed with 15-20 strokes at 700 rpm. Homogenates were then centrifuged at 1,000 *g* for 5 min at 4 °C, to pellet nucleus. The supernatants (cytoplasm + mitochondria) are collected to a fresh line of tubes and centrifuged at 12,000 g for 10 min at 4 °C, to pellet mitochondria. The supernatants (cytoplasm) were collected to a fresh line of tubes; protease inhibitors (#BWR1018, Chongqing Biospes Co., Ltd) were added at a 1:100 ratio, and stored immediately at -80 ºC. The pellets (crude mitochondria) were washed by resuspension in 500 µl sucrose buffer and recentrifuged at 12,000 *g*, for 10 min at 4 ºC. The supernatants were discarded and the wash was repeated two more times. The pellets were resuspended in 50 µl RIPA buffer [150 mM NaCl, 50 mM Tris-HCl pH 7.4, 0.1% SDS, (1% Triton X-100 for midbrain and diencephalon/0.1% Triton X-100 for the rest regions), 0.5% Sodium deoxycholate, 1 mM EDTA pH 8.0, and protease inhibitors at a 1:100 ratio], incubated on ice for 30 min, vortexed, incubated on ice for another 30 min and stored at -80 ºC. The protein concentration of each cytoplasmic and mitochondrial sample was determined using the detergent-compatible protein assay (Bio-Rad Protein Assay Kit II - 500-0002).

2.10. Western blot analysis

Western blot analysis for murine cytochrome c, cytochrome c oxidase subunit 4 (Cox4) was performed as described previously (144), using IgG primary rabbit anti-mouse antibodies (cat# 4272, Cell Signaling, Danvers, MA; cat# 4844, Cell Signaling, Danvers, MA, respectively). Western blotting for murine a-tubulin (Tubulin) was performed using IgG primary mouse anti-mouse antibody. Briefly, cytoplasmic (20 µg/lane) and mitochondrial samples (10 µg/lane) were resolved by SDS-PAGE (12.5% acrylamide and 0.51% *N,N'*-diallyltartardiamide), transferred to polyvinylidene difluoride membranes (Porablot PVDF

membrane, REF 741260, Macherey-Nagel, Germany), and probed with the corresponding primary antibodies. Semiquantitative determination of the relative protein amounts was performed by Image J free software.

2.11. Statistical analysis

Initially, we examined whether our exam scores were normally distributed. Hence we performed a Shapiro-Wilk's test ($p>0.05$) (145), and a visual inspection of their histograms, normal Q-Q plots and box plots. Also, skewness & kurtosis z-values were in the span of -1.96 and 1.96 (146, 147). As a result, comparison of all the data from the three groups of mice (EC, DC, DC+Ins) was performed using a parametric one-way analysis of variance (ANOVA), followed by Tukey's multiple comparison HSD post-hoc tests. The data are reported as means ± estimated SEM (* represent $P < 0.05$ and ** represent $P < 0.01$; n indicates the number of animals tested in each experiment).

Analysis of effect of both glucose and body weight upon the behavioral indices was performed by univariate analysis of covariance (ANCOVA), a statistical test that in our case evaluates whether multivariate population means of our behavioral data (our dependent variables) differ between the three groups of mice (our independent variable), while statistically controlling for the effects of fasted plasma glucose levels or the body weight (our covariates) on the behavioral indices. The *F* value is the ratio of variability between groups (which in our case relates to treatment differences), divided by the variability within group (which in our case relates to glucose levels or body weight differences), and is a measure of the difference in the behavioral indices between groups. The higher the *F* value is, the higher is the difference between groups, while *P* value indicates the statistical significance of the observed differences. The *Observed power* (Op) is the statistical power of the test performed, based on the effect size of data. The higher the *Observed power* is (1 is the highest), the higher is the effect of our covariates upon our dependent variables.

Finally, we conducted the mediation process by Hayes (148), in order to examine whether we had any mediation effect upon our behavioral indices. Specifically, mediation implies a situation where the effect of the independent variable (different glucose levels between the groups) on the dependent variable (each behavioral indice) can best be explained using a third mediator variable (body weight), which is caused by the independent variable and is itself a cause for the dependent variable (Figure 17). The higher the effect is,

the higher is the indirect effect of M (body weight) upon the direct relationship of X (glucose levels) and Y (behavioral indices), while *P* value indicates the statistical significance of the observed effect.

All statistical tests were performed using the IBM Corp. Released 2013. IBM SPSS Statistics for Windows, Version 22.0. Armonk, NY: IBM Corp.

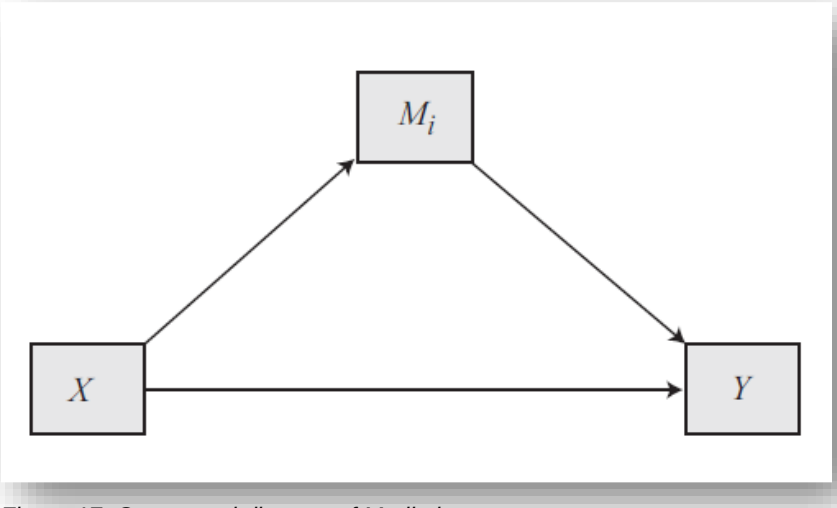

Figure 17. Conceptual diagram of Mediation

III. RESULTS

3.1. Effect of diabetes and insulin treatment on daily food and water consumption

The effect of STZ-induced diabetes and insulin treatment on daily food and water consumption in mice is presented in Table 2 and Figures 18, 19. Following a chow diet, both DC and DC+Ins were significantly higher (86.97% and 86.99%, respectively; P<0.01) in their food consumption per day compared to the EC group on day 23 (Tab.2; Fig. 18). Specifically, the DC mice increased their food consumption from 2.58±0.08 g/mouse/day on day 0 to 5.88±.0.22 g/mouse/day ($P < 0.01$) on day 23, showing a 127.66% increase. The same pattern was followed by the DC+Ins mice, which increased their food consumption from 2.54±0.01 g/mouse/day on day 0 to 5.88±.0.01 g/mouse/day ($P < 0.01$) on day 23, showing a 131.17% increase. After the insulin treatment, the DC+Ins group showed a significant decrease (32.42%, $P < 0.01$) in the food consumption per day from 5.88±0.01 g/mouse/day on day 23 to 3.98±0.16 g/mouse/day on day 30, while the food consumption in the DC group was further increased (14.68%, $P < 0.05$) from 5.88±.0.22 g/mouse/day on day 23 to 6.75±0.20 g/mouse/day on day 30. The EC group remained on the same levels throughout the time points of days 0, 23 and 30.

Regarding the water consumption, both DC and DC+Ins were significantly higher (532.41% and 568.44%, respectively; P<0.01) compared to the EC group on day 23 (Tab.2; Fig. 19). Specifically, the DC mice increased their water consumption from 5.42±0.05 ml/mouse/day on day 0 to 26.54±0.29 ml/mouse/day ($P < 0.01$) on day 23, showing a 388.80% increase. The same pattern was followed by the DC+Ins mice, which increased their water consumption from 5.66±0.25 ml/mouse/day on day 0 to 28.05±1.05 ml/mouse/day ($P < 0.01$) on day 23, showing a 395.15% increase. After the insulin treatment, the DC+Ins group showed a significant decrease (58.10%, $P < 0.01$) in the water consumption per day from 28.05±1.05 ml/mouse/day on day 23 to 11.75±0.22 ml/mouse/day on day 30, while the water consumption in the DC group was further increased (22.77%, $P < 0.01$) from 26.54±0.29 ml/mouse/day on day 23 to 32.58±0.31 ml/mouse/day on day 30. The EC group remained on the same levels throughout the time points of days 0, 23 and 30.

Table 2. Effect of diabetes and insulin treatment on the daily food (g/mouse/day) and water consumption (mL/mouse/day), across the days 0, 23 and 30.

	Food consumption (g/mouse/day)			Water consumption (mL/mouse/day)		
↓Group/Day→	**0**	**23**	**30**	**0**	**23**	**30**
EC (n=11)	3.05±0.16	3.14±0.06	3.20±0.11	4.02±0.03	4.19±0.06	4.39±0.01
DC (n=11)	2.58±0.08	5.88±.0.22 (↑86.97%) **	6.75±0.20 (↑110.81%) **	5.42±0.05	26.54±0.29 (↑532.41%) **	32.58±0.31 (↑640.66%) **
DC+Ins (n=10)	2.54±0.01	5.88±0.01 (↑86.99%) **	3.98±0.16 (↑24.24%) * [↓41.06%] **	5.66±0.25	28.05±1.05 (↑568.44%) **	11.75±0.22 (↑167.13%) ** [↓63.93%] **

Values are expressed as mean ± estimated SEM. The rate in the parenthesis ( ) is the % change compared to the levels of the EC. The rate on the hook [ ] is the % change compared to the levels of DC. * P<0.05 and **P<0.01 denote the significant differences.

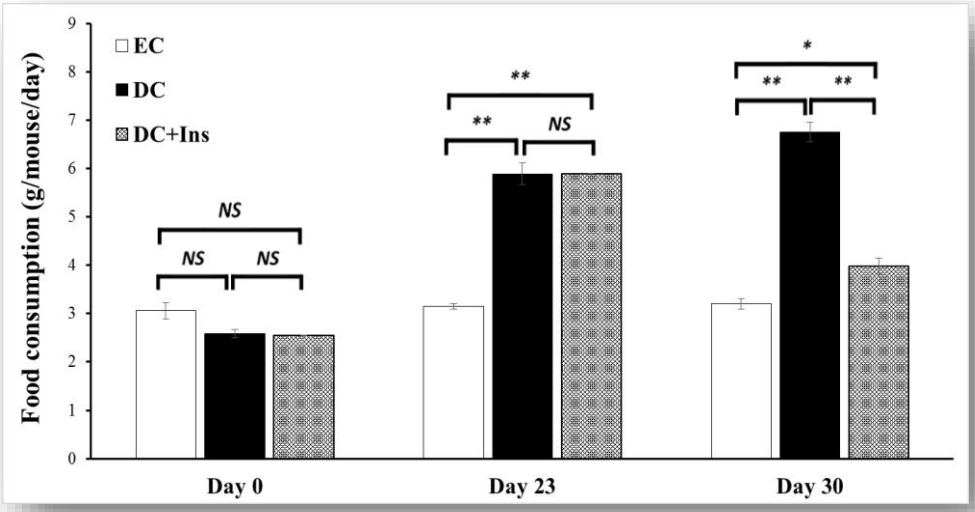

*Figure 18. Food consumption (g/mouse/day) on days 0, 23 and 30. Columns represent the mean and error bars represent estimated SEM (n=10-11 mice/group). ** indicates P < 0.01 between the compared groups. * indicates P < 0.05 between the compared groups.*

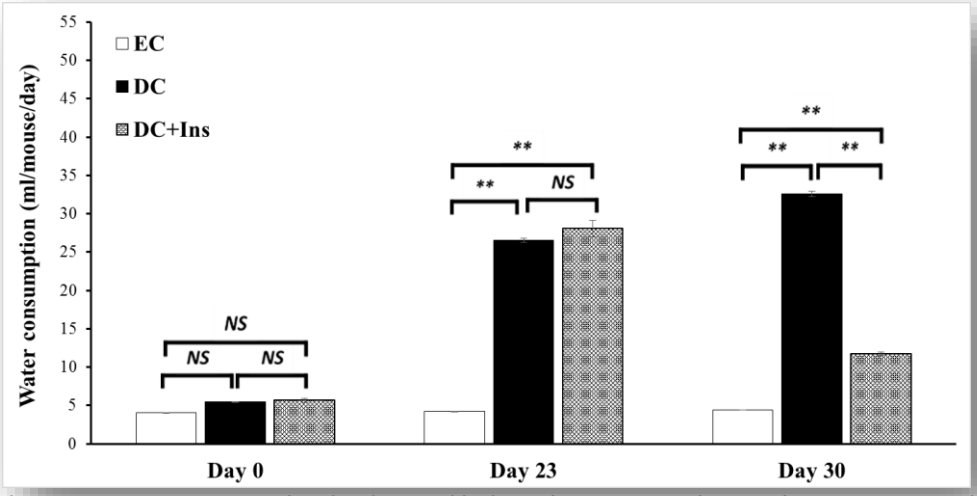

*Figure 19. Water consumption (mL/mouse/day) on days 0, 23 and 30. Columns represent the mean and error bars represent estimated SEM (n=10-11 mice/group). ** indicates P < 0.01 between the compared groups.*

3.2. Effects of diabetes and insulin treatment on plasma glucose levels and body weight

The effect of STZ-induced diabetes and insulin treatment on fasted plasma glucose levels and body weight in mice is presented in Table 3 and Figures 20, 21. The fasted plasma glucose levels were significantly higher (305.95% and 328.72%, respectively; P<0.01) in both DC and DC+Ins groups as compared to EC mice on day 23 (Tab.3; Fig. 20). Specifically, the DC mice had their glucose levels increased from 78.18±2.74 mg/dL on day 0 to 309.63±23.39 mg/dL ($P < 0.01$) on day 23, showing a 296.04% increase. The same pattern was followed by the DC+Ins mice, which had their glucose levels increased from 74.10±4.29 mg/dL on day 0 to 327.00±19.46 mg/dL ($P < 0.01$) on day 23, showing a 341.29% increase. After the insulin treatment, the DC+Ins group showed a significant decrease (65.67%, $P < 0.01$) in their glucose levels from 327.00±19.46 mg/dL on day 23 to 112.23±17.39 mg/dL on day 30, while the glucose levels of the DC group were further increased (17.80%) from 309.63±23.39 mg/dL on day 23 to 364.76±45.53 mg/dL on day 30. The EC group remained on the same glucose levels throughout the time points of days 0, 23 and 30.

Regarding the body weight, both DC and DC+Ins were significantly lower (26.33% and 24.48%, respectively; P<0.01) compared to the EC group on day 23 (Tab.3; Fig. 21). Specifically, the DC mice had their body weight decreased from 25.36±0.30 g on day 0 to 21.36±0.38 g ($P < 0.01$) on day 23, showing a 15.77% decrease. The same pattern was followed by the DC+Ins mice, which had their body weight decreased from 27.30±0.65 g on day 0 to 21.90±0.56g ($P < 0.01$) on day 23, showing a 19.78% decrease. After the insulin treatment, the DC+Ins group showed an increase (5.93%) in their body weight from 21.90±0.56 g on day 23 to 23.20±0.59 g on day 30, while at the same time the % difference the DC+Ins group had, compared to the DC group on day 23 (2.12%; No significance), was increased (10.95%; P<0.01). The DC group had their body weight further decreased (2.17%) from 21.36±0.38 g on day 23 to 20.90±0.31 g on day 30. The EC group remained on the same body weight levels throughout the time points of days 0, 23 and 30.

Table 3. Effect of diabetes and insulin treatment on the fasted plasma glucose levels (mg/dL) and body weight progress (g), across the days 0, 23 and 30.

	Fasted Plasma Glucose Levels (mg/dL)			Body Weight (g)		
↓Group/Day→	**0**	**23**	**30**	**0**	**23**	**30**
EC (n=11)	83.36±3.14	76.27±3.48	64.06±4.29	26.81±0.64	29.00±0.52	29.00±0.34
DC (n=11)	78.18±2.74	309.63±23.39 (↑305.95%) **	364.76±45.53 (↑469.37%) **	25.36±0.30	21.36±0.38 (↓26.33%) **	20.90±0.31 (↓27.89%) **
DC+Ins (n=10)	74.10±4.29	327.00±19.46 (↑328.72%) **	112.23±17.39 [↓69.23%] **	27.30±0.65	21.90±0.56 (↓24.48%) **	23.20±0.59 (↓20.00%) ** [↑10.95%] **

Values are expressed as mean ± estimated SEM. The rate in the parenthesis ( ) is the % change compared to the levels of the EC. The rate on the hook [ ] is the % change compared to the levels of DC. **P<0.01 denotes the significant differences.

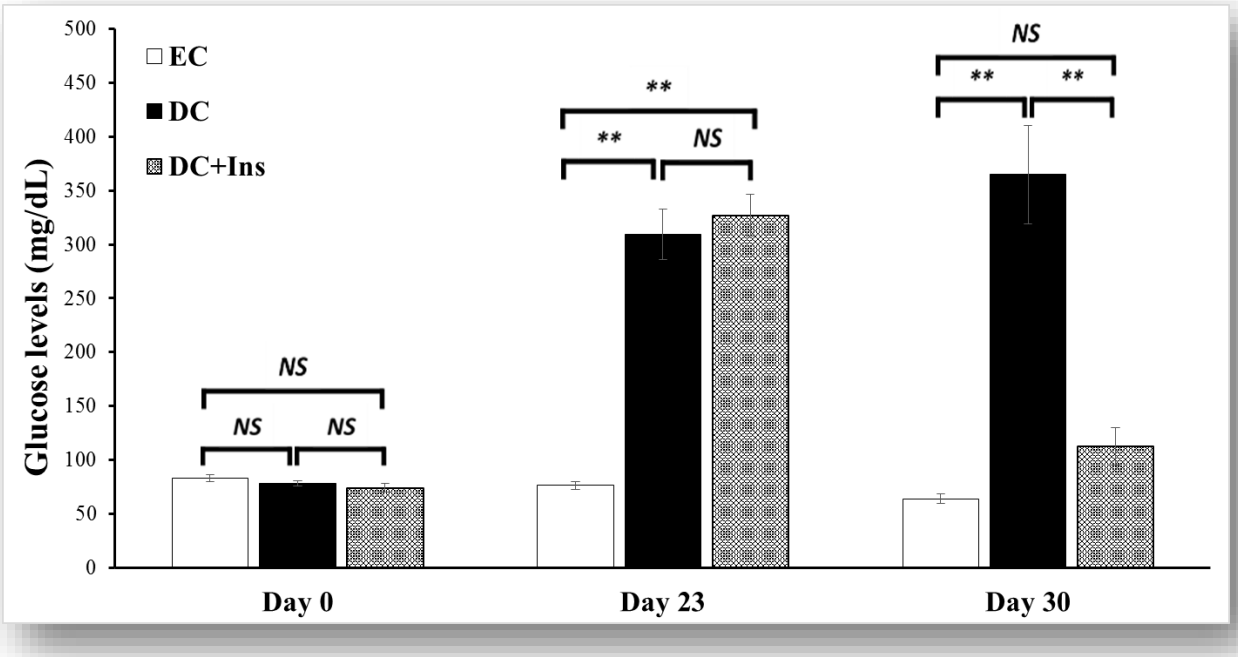

*Figure 20. Fasted plasma glucose levels (mg/dL) on days 0, 23 and 30. Columns represent the mean and error bars represent estimated SEM (n=10-11 mice/group). ** indicates* P < *0.01 between the compared groups.*

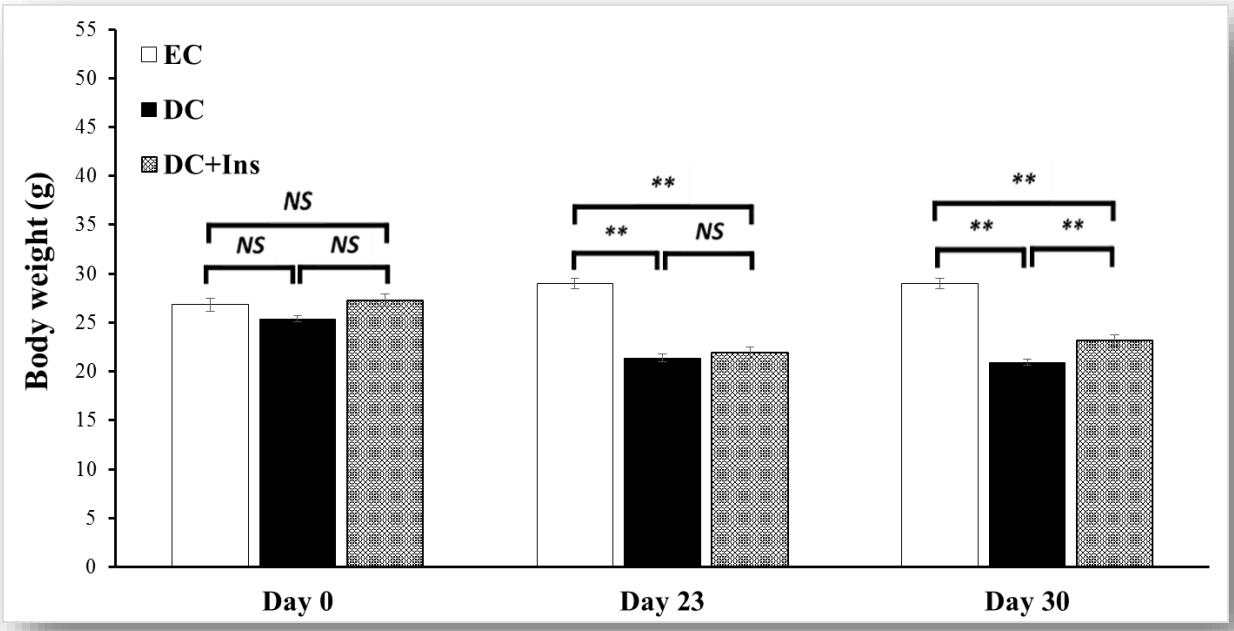

*Figure 21. Body weight progress (gr) on days 0, 23 and 30. Columns represent the mean and error bars represent estimated SEM (n=10-11 mice/group). ** indicates P < 0.01 between the compared groups.*

3.3. Effect of diabetes and insulin treatment on plasma triglycerides and total cholesterol levels

The effect of STZ-induced diabetes and insulin treatment on fasted plasma triglycerides and total cholesterol levels in mice is presented in Table 4 and Figures 22, 23. Measurements of fasted plasma triglycerides levels were significantly increased (207.13%; P<0.01) in the DC group (109.46±7.25) as compared to the EC mice (35.64±2.50) (Tab 4; Fig. 22). Moreover, the DC+Ins mice after the insulin treatment had their triglycerides levels (48.28±3.51) decreased (55.89%; P<0.01) compared to the DC group (109.46±7.25). The same pattern was followed by the fasted plasma total cholesterol levels which were significantly increased (76.46%; P<0.01) in the DC group (136.93±4.72) as compared to the EC mice (77.60±3.31) (Tab.4; Fig. 23). Moreover, the DC+Ins mice after the insulin treatment had their triglycerides levels (87.26±4.56) decreased (36.27%; P<0.01) compared to the DC group (136.93±4.72).

Table 4. Effect of diabetes and insulin treatment on the fasted plasma triglycerides and total cholesterol levels (mg/dL) on day 30.

	Triglycerides Levels (mg/dL)	Total Cholesterol Levels (mg/dL))
EC (n=11)	35.64±2.50	77.60±3.31
DC (n=11)	109.46±7.25 (↑207.13%) **	136.93±4.72 (↑76.46%) **
DC+Ins (n=10)	48.28±3.51 [↓55.89%] **	87.26±4.56 [↓36.27%] **

Values are expressed as mean ± estimated SEM. The rate in the parenthesis ( ) is the % change compared to the levels of the EC. The rate on the hook [ ] is the % change compared to the levels of DC. **P<0.01 denotes the significant differences.

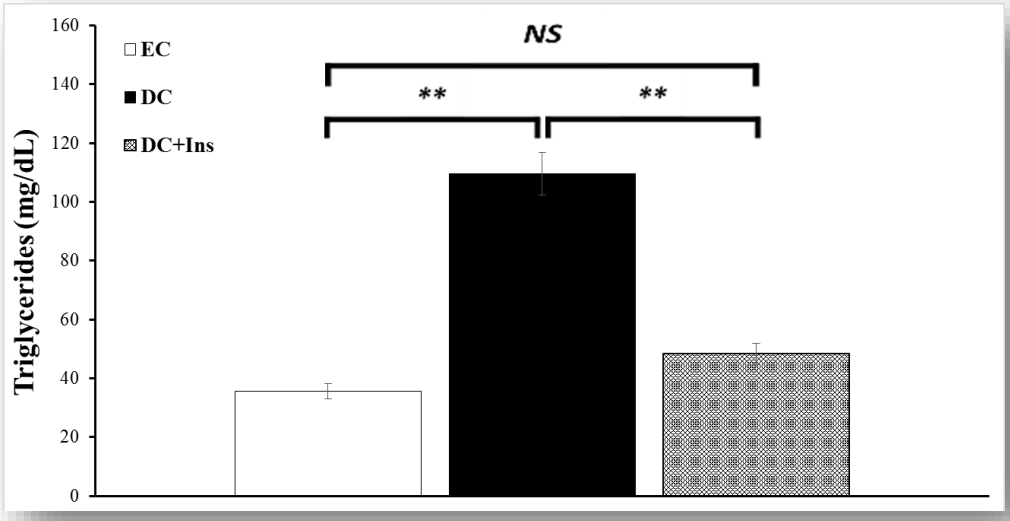

*Figure 22. Triglycerides levels (mg/dL)) on day 30. Columns represent the mean and error bars represent estimated SEM (n=10-11 mice/group). ** indicates P < 0.01 between the compared groups.*

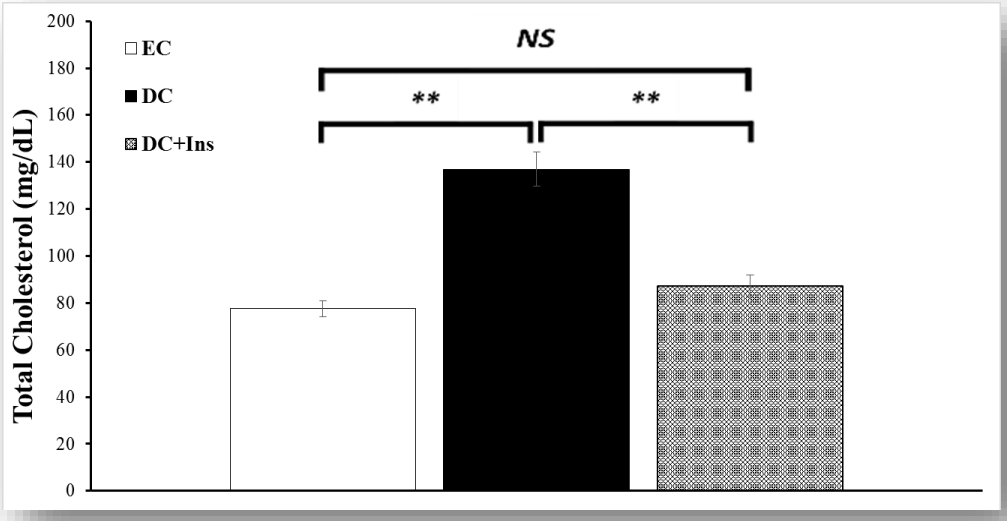

*Figure 23. Total cholesterol levels (mg/dL)) on day 30. Columns represent the mean and error bars represent estimated SEM (n=10-11 mice/group). ** indicates P < 0.01 between the compared groups.*

3.4. Effect of diabetes and insulin treatment on behavioral indices

3.4.1. Effect of diabetes and insulin treatment on anxiety-like behavior

Open-field (OFT) and elevated plus-maze (EPM) tests were used for the study of fear/anxiety of the animals after the induction of the diabetes and its treatment with insulin. As far as OFT, the DC mice showed a significant increase (66.50%; P<0.01) in their thigmotaxis time (TT) (504.50±12.86) compared to the EC (303.00±10.40), while at the same time the DC+Ins group showed a significant decrease (35.50%; P<0.01) in their TT (325.40±5.66) compared to the DC group 504.50±12.86). Moreover, the DC mice showed a significant decrease (55.72%; P<0.01) in their entries to the central square of the apparatus (19.33±1.28) compared to the EC (43.66±2.47), while the DC+Ins group showed a significant increase (95.51%; P<0.01) in their number of entries to the center (37.80±1.65) compared to the DC group (19.33±1.28) (Table 5 and Figures 24-25).

Table 5. Effect of diabetes and insulin treatment on anxiety-like behavior (Open-Field Test).

	Thigmotaxis time (s)	**Number of entries to the center**
EC (n=6)	303.00±10.40	43.66±2.47
DC (n=6)	504.50±12.86 (↑66.50%) **	19.33±1.28 (↓55.72%) **
DC+Ins (n=5)	325.40±5.66 [↓35.50%] **	37.80±1.65 [↑95.51%] **

Values are expressed as mean ± estimated SEM. The rate in the parenthesis ( ) is the % change compared to the levels of the EC. The rate on the hook [ ] is the % change compared to the levels of DC. **P<0.01 denotes the significant differences.

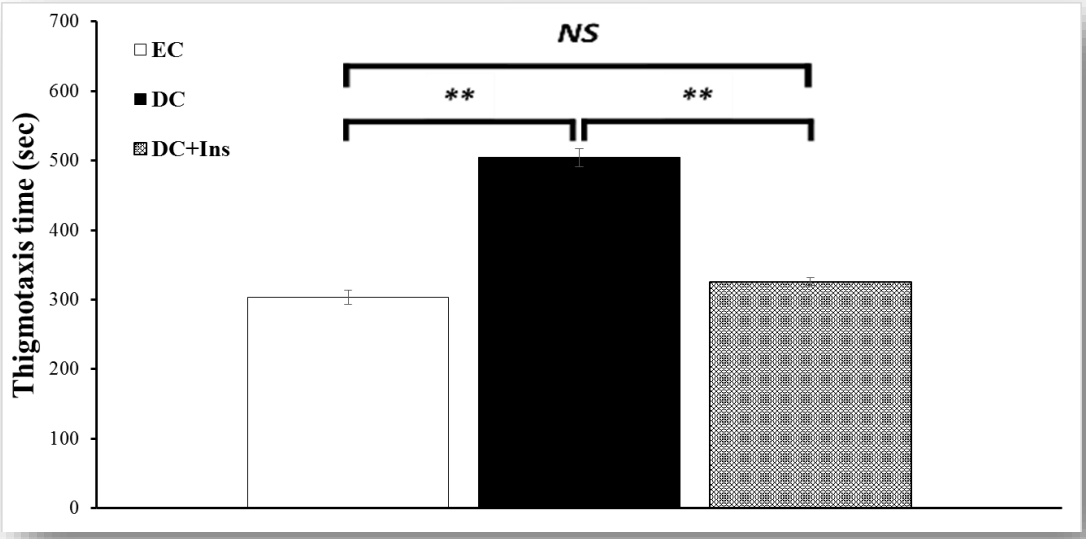

*Figure 24.Thigmotaxis time (sec). Columns represent the mean and error bars represent estimated SEM (n=5-6 mice/group). ** indicates P < 0.01 between the compared groups.*

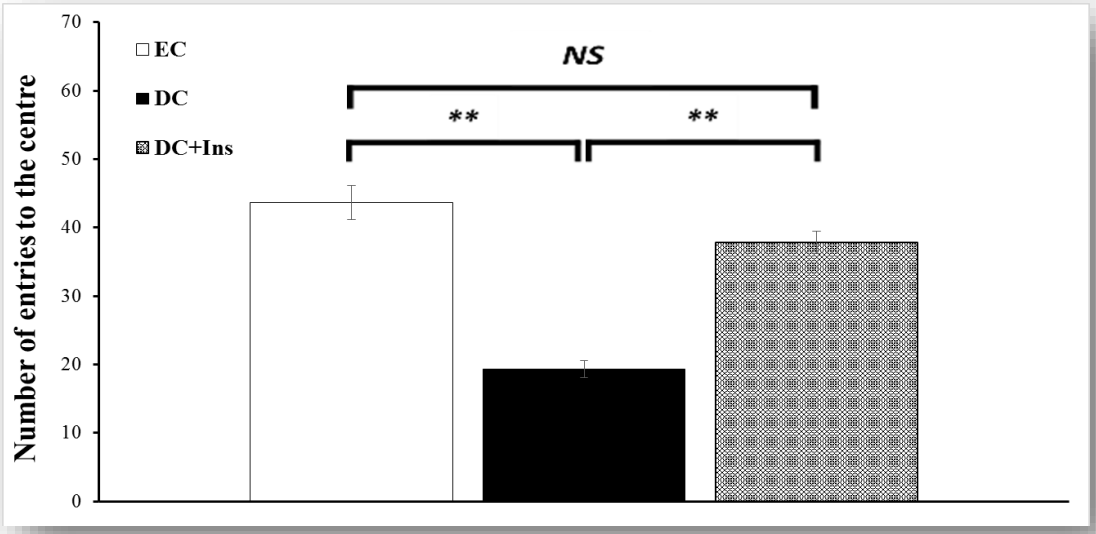

*Figure 25. Number of entries to the central square. Columns represent the mean and error bars represent estimated SEM (n=5-6 mice/group). ** indicates P < 0.01 between the compared groups.*

Concerning the EPM the DC mice showed a significant decrease (69.95%; P<0.01) in their % ratio of open/total time spent on open and enclosed arms of the plus maze apparatus (0.14±0.05), compared to the EC (0.48±0.04), while at the same time the DC+Ins group showed a significant increase (168.64%; P<0.01) in their % ratio (0.39±0.01) compared to the DC group (0.14±0.05). Moreover, the DC mice showed a significant decrease (58.42%; P<0.01) in their entries to the open arms (7.40±1.46) compared to the EC (17.80±0.96), while the DC+Ins group showed a significant increase (86.48%; P<0.05) in their number of entries to the open arms (13.80±1.46) compared to the DC group (7.40±1.46) (Table 6, Fig. 26-27).

Table 6. Effect of diabetes and insulin treatment on anxiety-like behavior (Elevated Plus-Maze Test).

	% ratio of open/total time spent on open and closed arms	Number of entries to the open arms
EC (n=5)	0.48±0.04	17.80±0.96
DC (n=5)	0.14±0.05 (↓69.95%) **	7.40±1.46 (↓58.42%) **
DC+Ins (n=5)	0.39±0.01 [↑168.64%] **	13.80±1.46 [↑86.48%] *

Values are expressed as mean ± estimated SEM. The rate in the parenthesis ( ) is the % change compared to the levels of the EC. The rate on the hook [ ] is the % change compared to the levels of DC. * P<0.05 and **P<0.01 denote the significant differences.

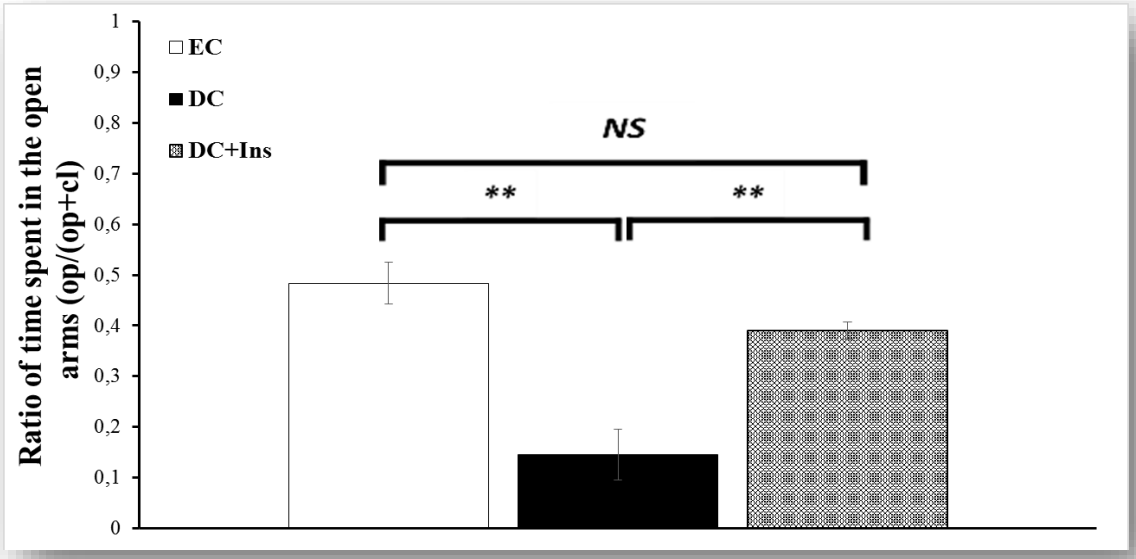

*Figure 26. % ratio of open/total time spent on open and closed arms. Columns represent the mean and error bars represent estimated SEM (n=5 mice/group). ** indicates P < 0.01 between the compared groups.*

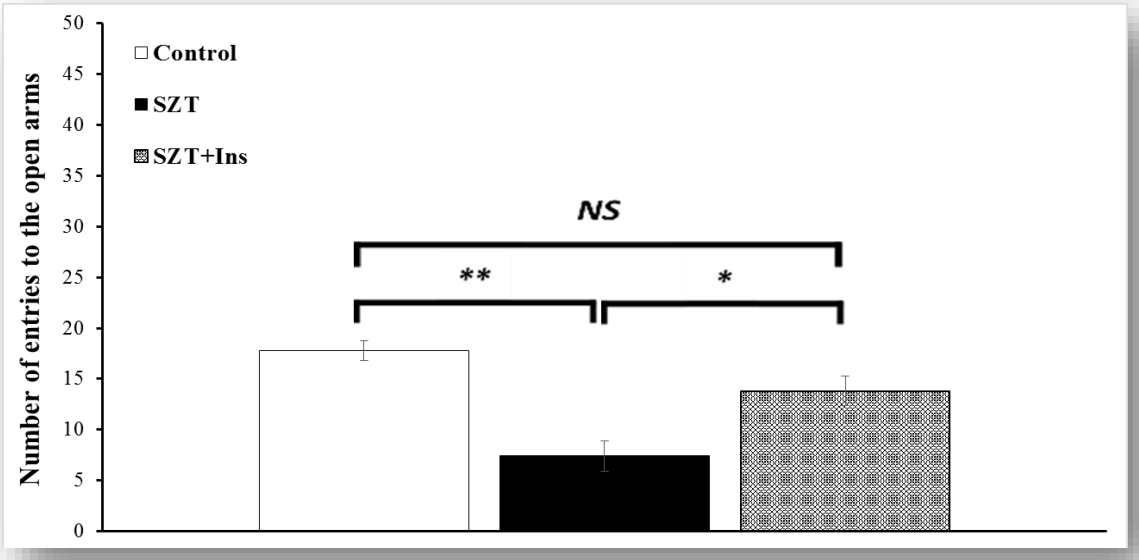

*Figure 27. Number of entries to the closed arms. Columns represent the mean and error bars represent estimated SEM (n=5 mice/group). ** indicates P < 0.01 between the compared groups. * indicates P < 0.05 between the compared groups.*

3.4.2. Effect of diabetes and insulin treatment on learning/memory

Step-through passive avoidance test was used in order to determine the learning/memory performance of the rodents after the induction of the diabetes and its treatment with insulin. Specifically, the Initial Latency time (IL) of mice, showed no statistically significant differences among groups (Table 7 and Figure 28), demonstrating that EC, DC and DC+Ins mice behave the same during the acquisition trial. Step-through Latency time (STL), which was recorded during the retention trial, indicates the consolidation of the reinforced stimuli in the memory of rodents, showing the effects of the treatments on their cognitive performance. In our study, the DC mice showed a significant decrease (77.77%; P<0.01) in their STL time (38.66±7.76) compared to the EC (174.00±13.75), while at the same time the DC+Ins group showed a significant increase (288.44%; P<0.01) in their STL time (150.20±6.49) compared to the DC group (38.66±7.76) (Table 7 and Figure 28).

Table 7. Effect of diabetes and insulin treatment on learning/memory (Step-Through Passive Avoidance Test).

	Initial Latency (s)	Step-Through Latency (s)
EC (n=6)	29.16±3.99	174.00±13.75
DC (n=6)	25.83±3.13	38.66±7.76 (↓77.77%) **
DC+Ins (n=5)	31.60±5.22	150.20±6.49 [↑288.44%] **

Values are expressed as mean ± estimated SEM. The rate in the parenthesis ( ) is the % change compared to the levels of the EC. The rate on the hook [ ] is the % change compared to the levels of DC. **P<0.01 denote the significant differences.

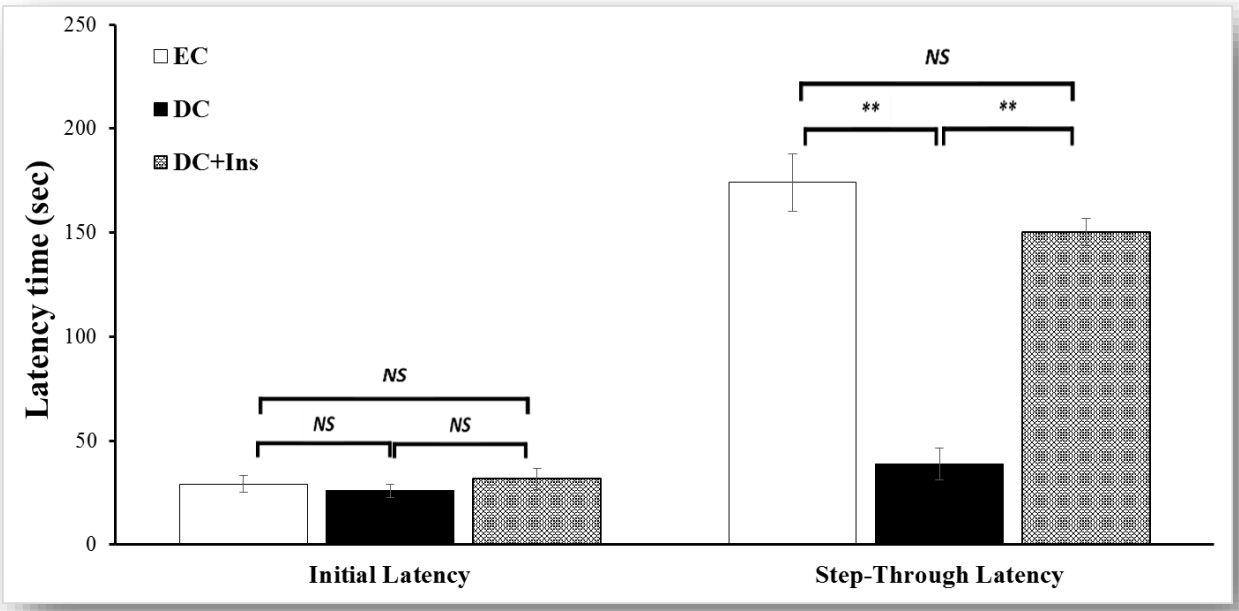

*Figure 28. Initial latency and Step-through latency. Columns represent the mean and error bars represent estimated SEM (n=5-6 mice/group). ** indicates P < 0.01 between the compared groups.*

3.4.3. Effect of diabetes and insulin treatment on depression-like behavior

The Forced-swimming test (FST) was used to assess vulnerability to STZ-diabetes induced depressive behavior after the induction of the diabetes and its treatment with insulin (Table 8 and Figure 29). Specifically, the DC mice showed a significant increase (63.36%; P<0.01) in their immobility time (161.40±3.37) compared to the EC (98.80±3.99), while at the same time the DC+Ins group showed a significant decrease (30.85%; P<0.01) in their immobility time (111.60±6.13) compared to the DC group (161.40±3.37).

Table 8. Effect of diabetes and insulin treatment on depression-like behavior (Forced-Swimming Test)

	Immobility time (s)
EC (n=5)	98.80±3.99
DC (n=5)	161.40±3.37 (↑63.36%) **
DC+Ins (n=5)	111.60±6.13 [↓30.85%] **

Values are expressed as mean ± estimated SEM. The rate in the parenthesis ( ) is the % change compared to the levels of the EC. The rate on the hook [ ] is the % change compared to the levels of DC. **P<0.01 denote the significant differences.

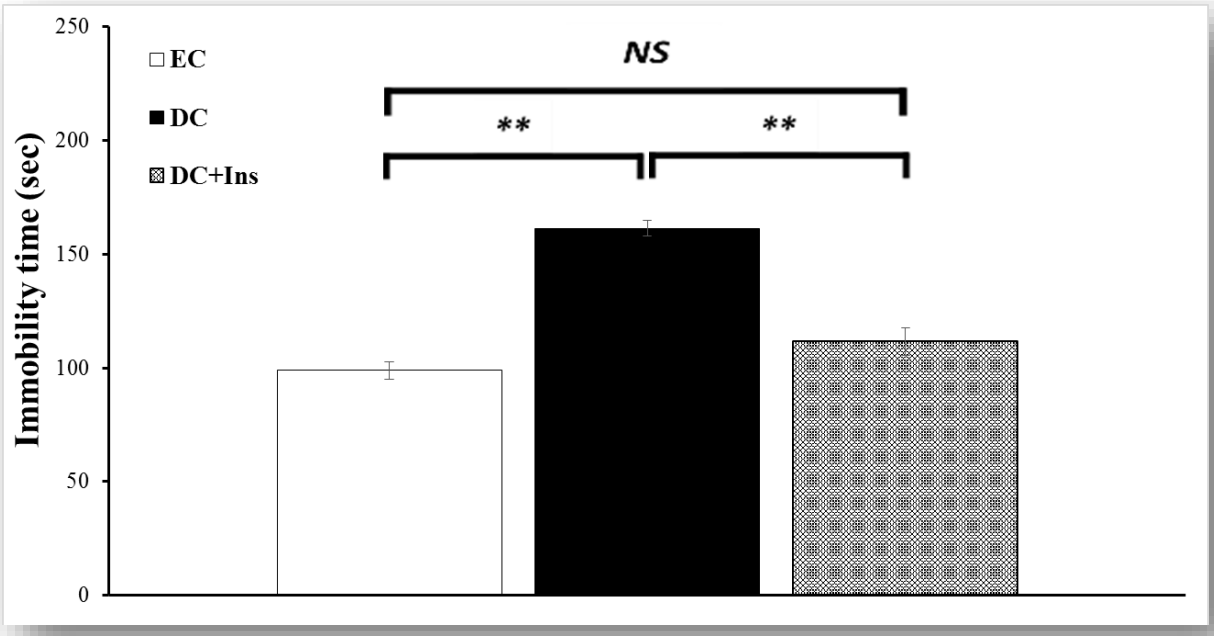

*Figure 29. Immobility time. Columns represent the mean and error bars represent estimated SEM (n=5 mice/group). ** indicates P < 0.01 between the compared groups.*

3.5. Correlation of diabetes with the behavioral indices

In an effort to determine whether the differences observed in the behavior of the DC and DC+Ins mice correlate with differences in the glucose levels of these three groups, we performed ANCOVA analysis, as described in Materials and Methods (Figures 30-A, 30-C, 30-E, 30-G, 30-I, 30-K). Respectively, the same analysis was performed to determine whether the differences observed in the behavior of the DC and DC+Ins mice correlate with the differences in the body weight of these three groups (Figures 30-B, 30-D, 30-F, 30-H, 30-J, 30-L). ANCOVA analysis showed that the covariate of glucose levels had a higher observed power (Op) than the covariate of body weight. This indicates that the effect the glucose levels have, is higher than the effect the body weight has upon the behavior. Moreover, ANCOVA analysis showed that the covariate of glucose levels had a higher *F*-value and smaller *P*-value than the covariate of body weight, which indicates that the correlation with glucose levels show higher and more significant differences between the groups than the correlation with the body weight.

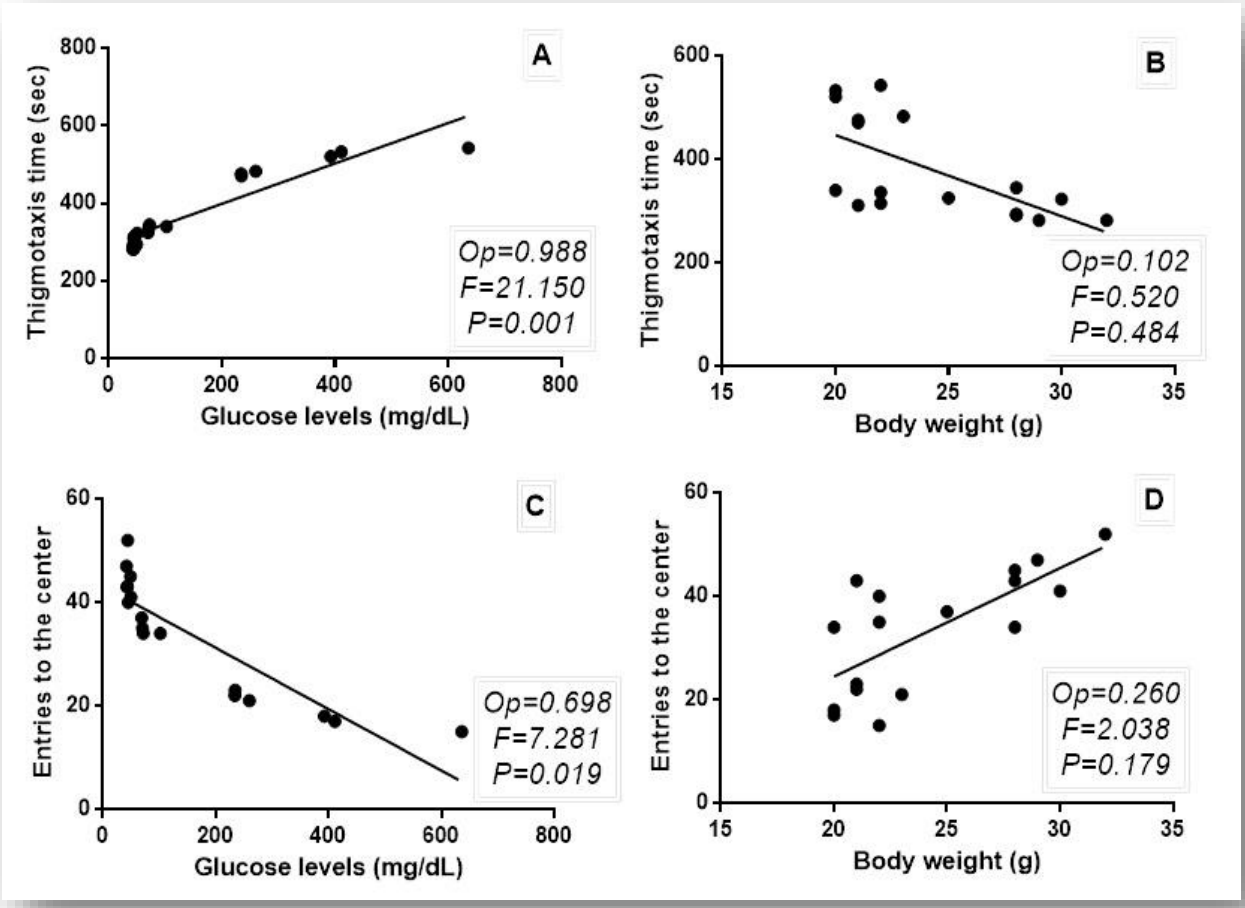

Figure 30. Linear regressions for thigmotaxis time (A-B) and entries to the central square (C-D). For each panel, ANCOVA analysis was performed, and the Observed power (Op), F- value and P-value are indicated.

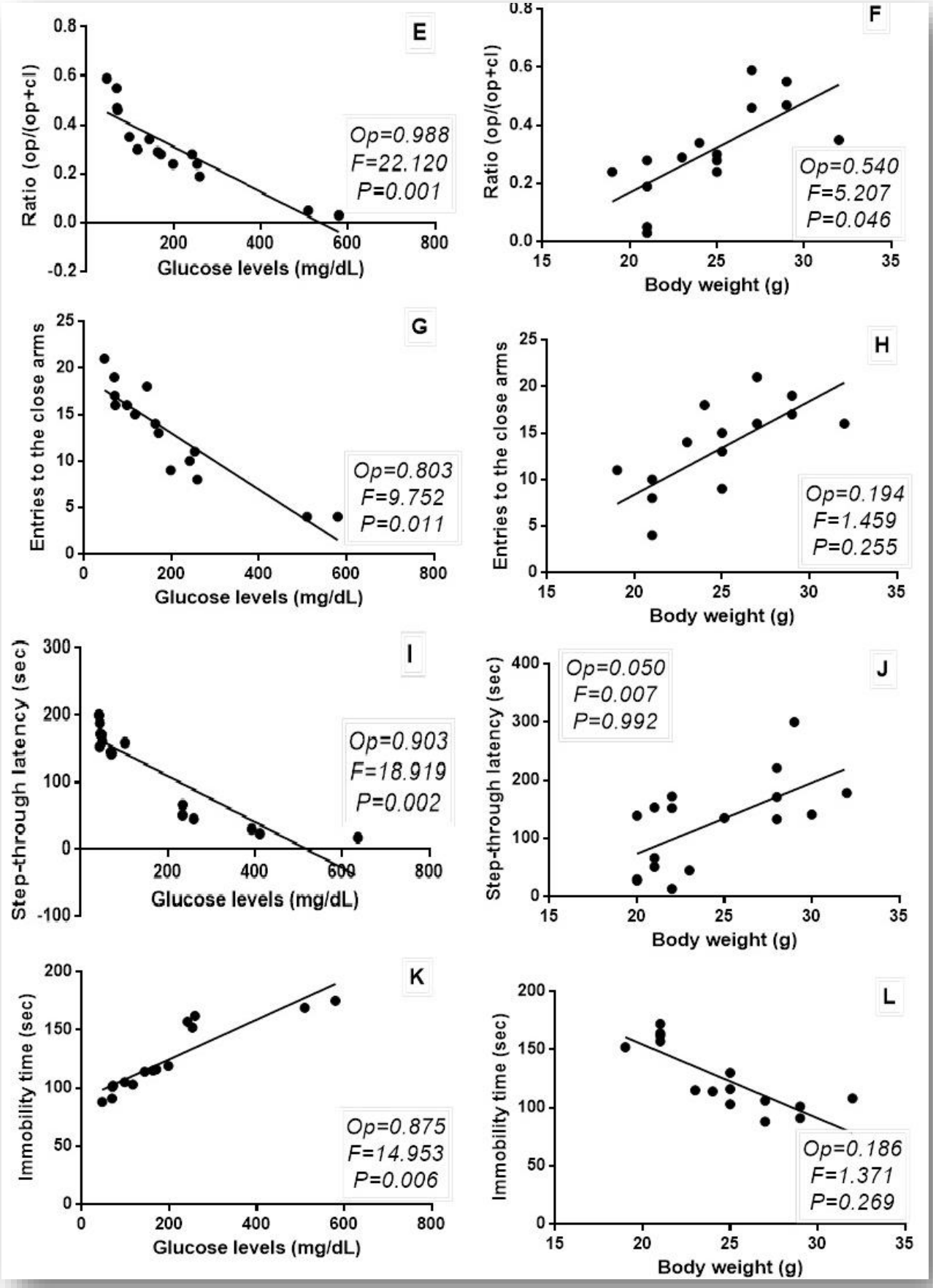

Figure 31. Linear regressions for ratio (op/(op+cl) (E-F), entries to the closed arms (G-H), latency time (I-J) and immobility time (K-L). For each panel, ANCOVA analysis was performed, and the Observed power (Op), F- value and P-value are indicated.

3.5. Mediation effect on behavioral indices

In order to examine the mediation effect upon the behavioral indices we performed the mediation process (Table 9) by Hayes as described in Materials and Methods (Figure 17). Specifically, the test showed that the covariate of body weight (mediator) had very low and insignificant (P>0.05) indirect effect (mediation) upon the direct relationship of the independent variable of glucose levels and the dependent variable of behavioral indices. On the contrary, the direct effect of the independent variable of glucose levels had a lot higher effect size upon the behavioral indices which at the same time was strongly significant (P<0.01) (Table 9).

Table 9.

	Direct effect of glucose levels (X→Y)	**P-significance of the direct effect P (X→Y)**	**Indirect effect of body weight (M→Y)**	**P-significance of the indirect effect P (M→Y)**
Thigmotaxis time	0.4529	0.0000	0.0657	0.1202
Entries to the center	0.463	0.0000	0.0127	0.0660
Ratio op/(op+cl)	0.3157	0.0011	0.0784	0.1793
Entries to the open arms	0.278	0.0001	0.0029	0.4455
Latency time	0.2879	0.0000	0.0430	0.1673
Immobility time	0.1168	0.0045	0.0462	0.0952

3.6. Effect of diabetes and insulin treatment on the cholinergic system

3.6.1. Effect of diabetes and insulin treatment on acetylcholinesterase activity

The effect of STZ-induced diabetes and insulin treatment on acetylcholinesterase (AChE) SS and DS fraction (G1 and G4 isoforms respectively) activities in mice are presented in Table 10 and Figures 32-33. As expected, the activity of the enzyme in the DS fraction (G4) is much higher than that of the SS fraction (G1) in all brain tissues. Moreover, it was observed that the DS fraction of the striatum displayed the greatest AChE activity of all tissues tested.

As presented in Table 10 and Figure 32, the SS fraction activity was significantly increased in all brain regions of the DC mice compared to the EC group. The largest AChE G1 enhancements were observed in hippocampus (36.47%; $P<0.01$), cerebral cortex (35.53%; $P<0.01$) and striatum (31.62%; $P<0.01$). The cerebellum follows (25.89%; $P<0.05$), while midbrain and diencephalon had the smallest enhancements (15.23%; $P<0.01$ and 15.71%; $P<0.05$, respectively) compared to the rest brain regions. Moreover, the DC+Ins group presented significant decrease at the SS fraction activity, in most of the brain regions examined compared to the DC group. More particularly, the largest AChE G1 inhibitions were observed in hippocampus (26.50%; $P<0.01$), striatum (20.84%; $P<0.01$) and cerebellum (20.35%; $P<0.05$). Midbrain and diencephalon follow with lower inhibitions (12.37%; $P<0.05$ and 9.66%; $P<0.05$, respectively). The only region that had no significant decrease was cerebral cortex (13.43%).

Respectively in Table 10 and Figure 33, the DS fraction activity was significantly increased in all brain regions of the DC mice compared to the EC group. The largest AChE G4 enhancements were observed in hippocampus (29.06%; $P<0.01$) and striatum (25.15%; $P<0.01$). Midbrain (24.94%; $P<0.05$) and diencephalon (23.82%; $P<0.01$) were very close, while the smallest enhancements were observed in cerebral cortex (18.93%; $P<0.05$) and cerebellum (18.12%; $P<0.05$). On the other hand, the DC+Ins group presented significant decrease at the DS fraction activity, in most of the brain regions examined compared to the DC group. More particularly, the largest AChE G4 inhibitions were observed in hippocampus (19.61%; $P<0.01$) and striatum (18.25%; $P<0.01$). Cerebellum (15.24%; $P<0.05$), midbrain (14.46%; $P<0.05$) and diencephalon (12.65%; $P<0.05$), follow with lower inhibitions.

Characteristically, the only region that had no significant decrease was cerebral cortex (6.61%).

Table 10. Effect of diabetes and insulin treatment on acetylcholinesterase activity.

		AChE Activity (µmoles/min/g tissue)		
		EC *(n=5)*	**DC** *(n=5)*	**DC+Ins** *(n=5)*
Cerebellum	**SS**	3.44±0.18	4.34±0.20 (↑25.89%) *	3.45±0.27 [↓20.35%] *
	DS	11.28±0.74	13.32±0.63 (↑18.12%) *	11.29±0.44 [↓15.24%] *
Cerebral Cortex	**SS**	10.29±0.93	13.94±0.88 (↑35.53%) *	12.07±0.97 [↓13.43%]
	DS	48.46±2.61	57.64±2.95 (↑18.93%) *	53.83±2.57 [↓6.61%]
Midbrain	**SS**	14.78±0.51	17.03±0.75 (↑15.23%) **	14.92±0.69 [↓12.37%] *
	DS	42.52±3.41	53.12±2.87 (↑24.94%) *	45.44±3.22 [↓14.46%] *
Hippocampus	**SS**	7.69±0.62	10.50±0.50 (↑36.47%) **	7.72±0.73 [↓26.50%] **
	DS	33.66±1.21	43.44±1.11 (↑29.06%) **	34.92±1.42 [↓19.61%] **
Striatum	**SS**	22.46±0.46	29.57±0.77 (↑31.62%) **	23.40±0.57 [↓20.84%] **
	DS	115.28±1.38	144.28±1.45 (↑25.15%) **	117.55±1.40 [↓18.25%] **
Diencephalon	**SS**	11.03±0.44	12.76±0.16 (↑15.71%) *	11.53±0.58 [↓9.66%] *
	DS	40.72±2.20	50.42±1.16 (↑23.82%) **	44.04±2.29 [↓12.65%] *

Values are expressed as mean ± estimated SEM. The rate in the parenthesis ( ) is the % change compared to the levels of the EC. The rate on the hook [ ] is the % change compared to the levels of DC. * P<0.05 and **P<0.01 denote the significant differences.

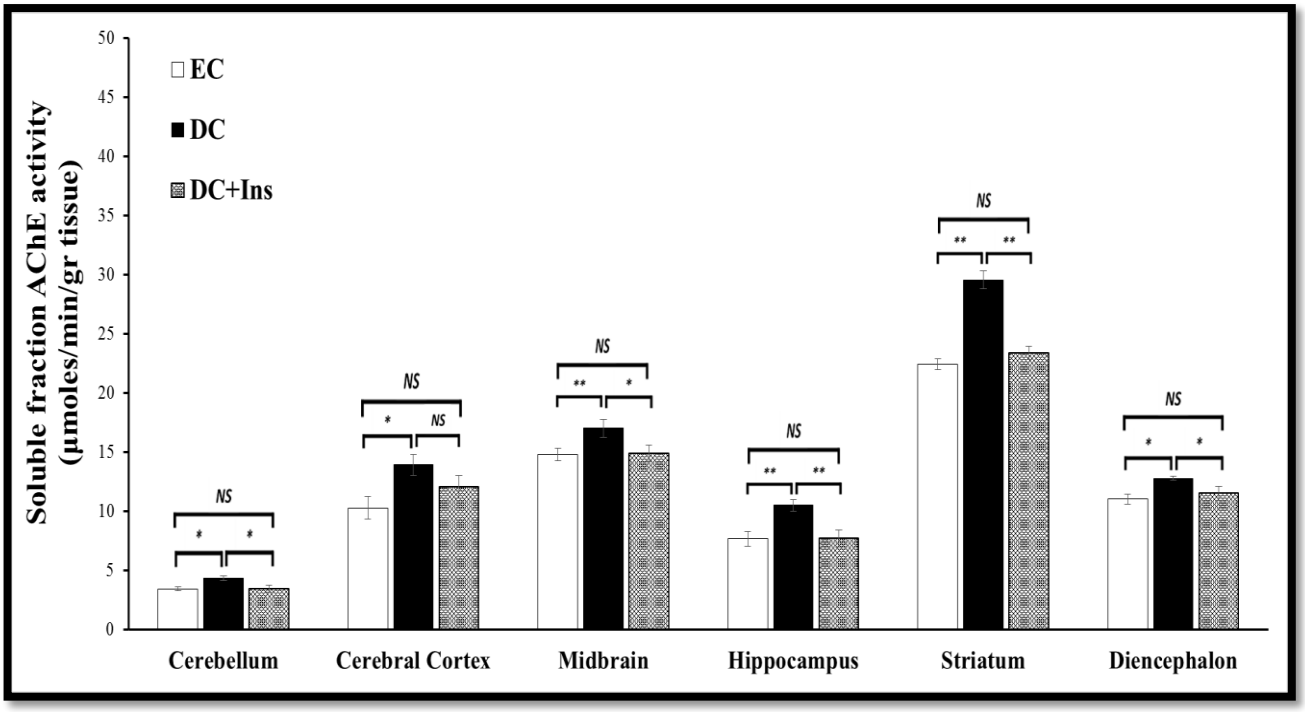

*Figure 32. Soluble fraction AChE activity. Columns represent the mean and error bars represent estimated SEM (n=5 mice/group). ** indicates P < 0.01 between the compared groups. * indicates P < 0.05 between the compared groups.*

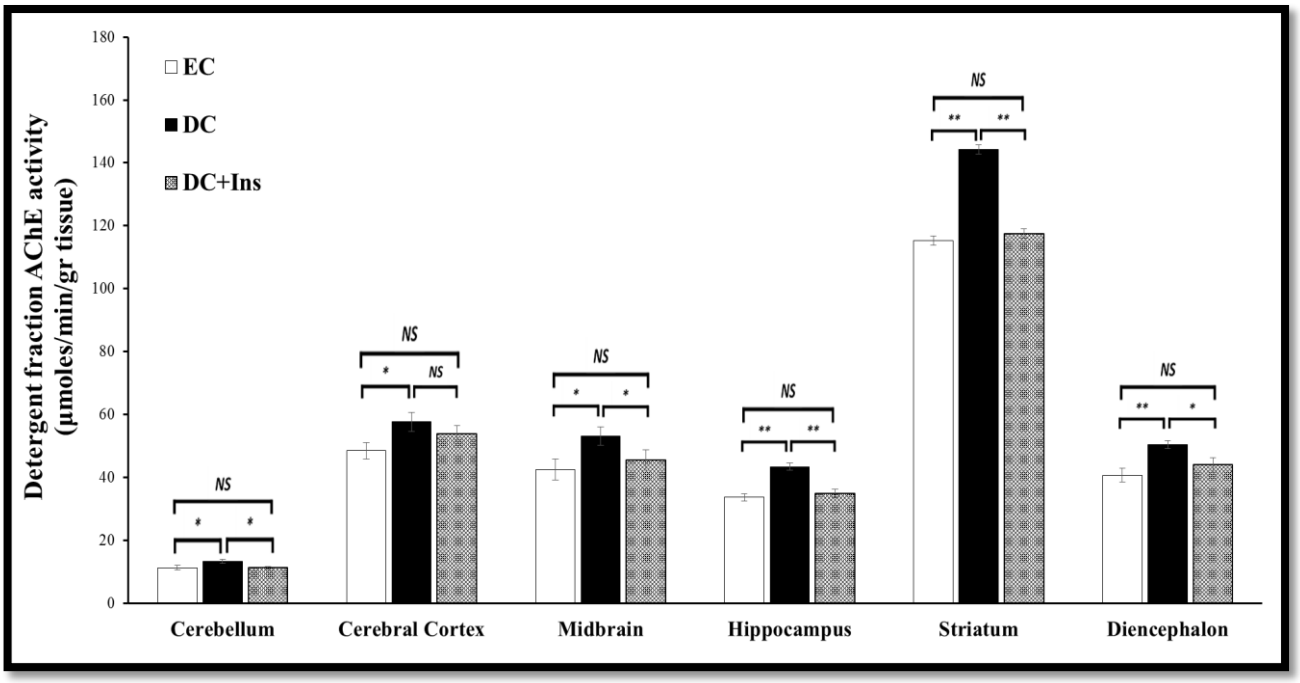

*Figure 33. Detergent fraction AChE activity. Columns represent the mean and error bars represent estimated SEM (n=5 mice/group). ** indicates P < 0.01 between the compared groups. * indicates P < 0.05 between the compared groups.*

3.6.2. Effect of diabetes and insulin treatment on Acetylcholine levels

The effect of STZ-induced diabetes and insulin treatment on acetylcholine (ACh) levels in mice are presented in Table 11 and Figure 34. As expected, the % changes upon the ACh levels are inversely proportional to the % changes of AChE activity. Moreover, it was observed that the ACh levels of the striatum were the largest between all regions.

More specifically the ACh levels were significantly decreased in all brain regions of the DC mice compared to the EC group. The largest declines of ACh levels were observed in striatum (29.60%; P<0.01) and hippocampus (22.79%; P<0.01). Midbrain (22.59%; P<0.05) and diencephalon (22.39%; P<0.05) were very close, while the smallest declines were observed in cerebellum (19.17%; P<0.05) and cerebral cortex (17.19%; P<0.05). On the other hand, the DC+Ins group presented significant increase at ACh levels, in most of the brain regions examined compared to the DC group. More particularly, the largest augmentations were observed in striatum (28.92%; P<0.01) and hippocampus (23.40%; P<0.01). Midbrain (21.65%; P<0.05) and diencephalon (21.98%; P<0.05), follow with lower augmentations. Characteristically, the only regions that had no significant increase of ACh levels were cerebellum and cerebral cortex, with the last one having a significant difference compared to the EC group (12.63%; P<0.05) indicating the incomplete recovery of this region regarding the ACh levels (Table 11 and Figure 34).

Table 11. Effect of diabetes and insulin treatment on Acetylcholine levels.

	ACh levels (μmol/mg protein)		
	EC *(n=5)*	**DC** *(n=5)*	**DC+Ins** *(n=5)*
Cerebellum	0.275±0.019	0.222±0.017 (↓19.17%) *	0.252±0.016
Cerebral Cortex	0.786±0.033	0.651±0.024 (↓17.19%) *	0.687±0.051 (↓12.63%) *
Midbrain	1.212±0.092	0.938±0.044 (↓22.59%) *	1.141±0.032 [↑21.65%] *
Hippocampus	0.596±0.030	0.460±0.024 (↓22.79%) **	0.568±0.018 [↑23.40%] **
Striatum	1.933±0.078	1.361±0.076 (↓29.60%) **	1.754±0.099 [↑28.92%] **

Diencephalon	1.279±0.083	0.992±0.096 (↓22.39%) *	1.211±0.064 [↑21.98%] *

Values are expressed as mean ± estimated SEM. The rate in the parenthesis ( ) is the % change compared to the levels of the EC. The rate on the hook [ ] is the % change compared to the levels of DC. * P<0.05 and **P<0.01 denote the significant differences.

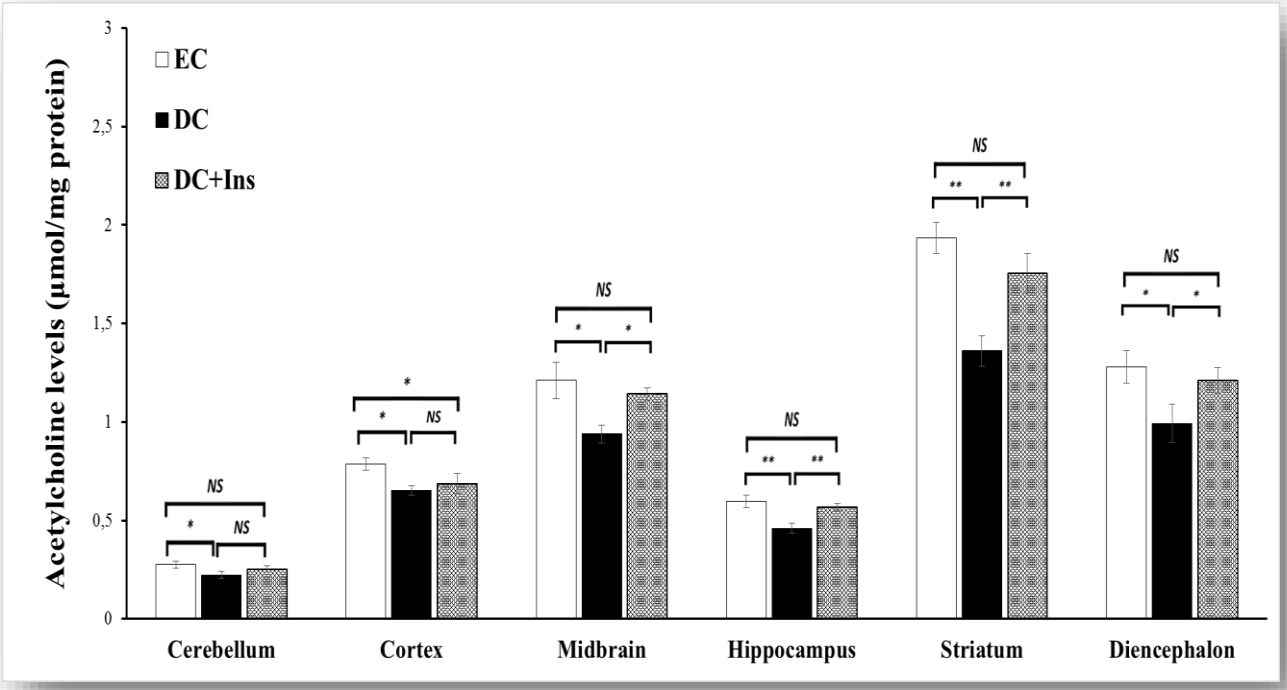

*Figure 34. Acetylcholine levels. Columns represent the mean and error bars represent estimated SEM (n=5 mice/group). ** indicates P < 0.01 between the compared groups. * indicates P < 0.05 between the compared groups.*

3.7. Effect of diabetes and insulin treatment on the antioxidant enzymatic activity

In an effort to determine whether we had any effect of STZ-induced diabetes and insulin treatment on antioxidant defense we measured the activity of three major antioxidant enzymes: superoxide dismutase, catalase and glutathione peroxidase.

3.7.1. Effect of diabetes and insulin treatment on superoxide dismutase activity

The effect of STZ-induced diabetes and insulin treatment on superoxide dismutase (SOD) activity in mice is presented in Table 12 and Figure 35. More specifically the SOD activity was significantly increased in all brain regions of the DC mice compared to the EC group. The largest increase of SOD activity was observed in hippocampus (127.86%; P<0.01) and striatum (121.52%; P<0.01). Diencephalon (118.34%; P<0.01) and midbrain (117.41%; P<0.01) follow, while the smallest augmentations were observed in cerebral cortex (89.68%; P<0.01) and cerebellum (32.66%; P<0.01). On the other hand, the DC+Ins group presented significant decrease of SOD activity, in most of the brain regions examined compared to the DC group. More particularly, the largest decrease was observed in hippocampus (47.16%; P<0.01) and striatum (43.48%; P<0.01). Diencephalon (36.63%; P<0.01), midbrain (26.06%; P<0.05) and cerebellum (17.33%; P<0.05) follow with lower decrease. Characteristically, the only region that had no significant decrease of SOD activity was cerebral cortex. The regions that were observed having significant differences compared to the EC group, were cerebral cortex (67.57%; P<0.01), midbrain (60.73%; P<0.05) and diencephalon (38.35%; P<0.05), indicating the incomplete recovery of these regions regarding the SOD activity.

Table 12. Effect of diabetes and insulin treatment on superoxide dismutase activity.

	SOD activity (units/mg protein)		
	EC *(n=5)*	**DC** *(n=5)*	**DC+Ins** *(n=5)*
Cerebellum	36.72±1.99	48.71±2.36 (↑32.66%) **	40.27±2.30 [↓17.33%] *
Cerebral Cortex	49.37±2.93	93.66±9.91 (↑89.68%) **	82.74±2.40 (↑67.57%) **
Midbrain	127.27±8.92	276.71±9.24	204.57±25.71

		(↑117.41%) **	[↓26.06%] * (↑60.73%) *
Hippocampus	39.69±2.18	90.45±7.15 (↑127.86%) **	47.78±5.04 [↓47.16%] **
Striatum	49.00±5.41	108.56±10.00 (↑121.52%) **	61.35±5.69 [↓43.48%] **
Diencephalon	113.17±6.12	247.10±12.83 (↑118.34%) **	156.57±10.61 [↓36.63%] ** (↑38.35%) *

Values are expressed as mean ± estimated SEM. The rate in the parenthesis ( ) is the % change compared to the levels of the EC. The rate on the hook [ ] is the % change compared to the levels of DC. * P<0.05 and **P<0.01 denote the significant differences.

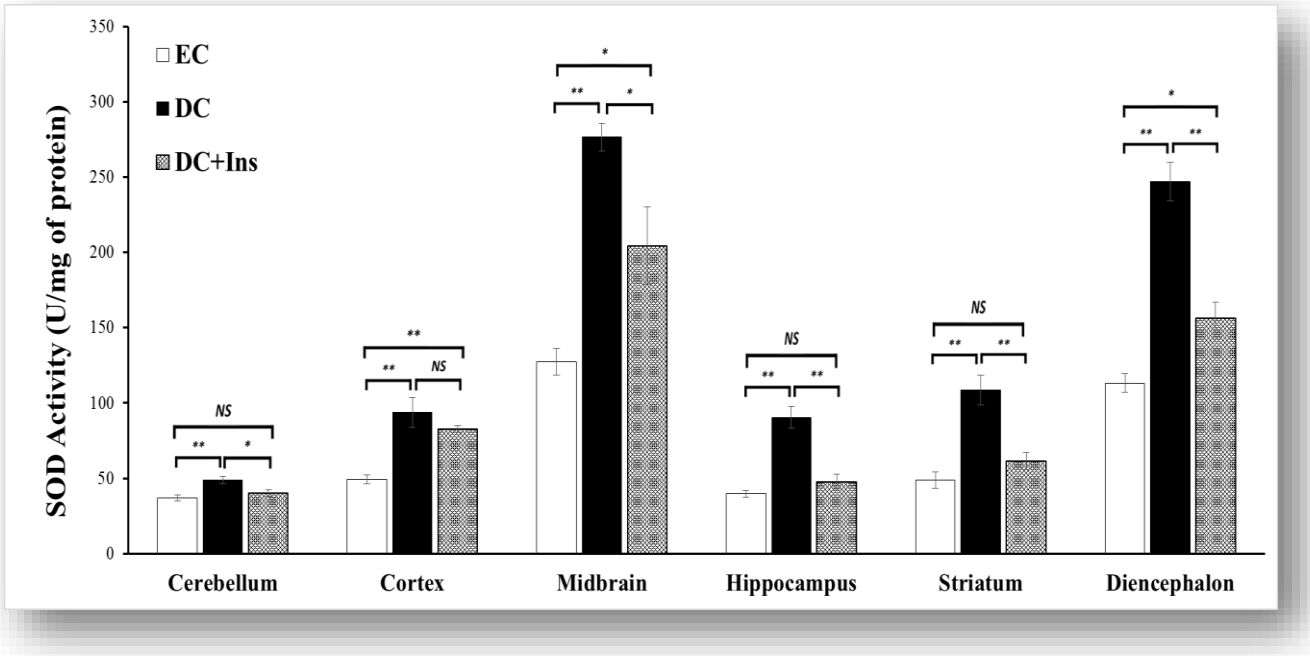

*Figure 35. SOD activity. Columns represent the mean and error bars represent estimated SEM (n=5 mice/group). ** indicates P < 0.01 between the compared groups. * indicates P < 0.05 between the compared groups.*

3.7.2. Effect of diabetes and insulin treatment on catalase activity

The effect of STZ-induced diabetes and insulin treatment on catalase (CAT) activity in mice is presented in Table 13 and Figure 36. More specifically the CAT activity was significantly increased in all brain regions of the DC mice compared to the EC group. The largest increase of CAT activity was observed in cerebral cortex (111.08%; P<0.01) and striatum (101.26%; P<0.01). Midbrain (89.89%; P<0.01) and hippocampus (80.13%; P<0.01) follow, while the smallest augmentations were observed in diencephalon (60.36%; P<0.01)

and cerebellum (44.07%; P<0.01). On the other hand, the DC+Ins group presented significant decrease of CAT activity, in all the brain regions examined compared to the DC group. More particularly, the largest decrease was observed in striatum (40.01%; P<0.01) and hippocampus (39.72%; P<0.01). Midbrain (36.23%; P<0.05) and diencephalon (33.18%; P<0.01) follow with lower decrease, while the smallest decrease was observed in cerebellum (22.49%; P<0.05) and cerebral cortex (16.05%; P<0.05). Cerebral cortex was observed having significant difference compared to the EC group (77.18%; P<0.01) indicating the incomplete recovery of this region regarding the CAT activity.

Table 13. Effect of diabetes and insulin treatment on catalase activity.

	CAT activity (μM/min/mg of protein)		
	EC *(n=5)*	**DC** *(n=5)*	**DC+Ins** *(n=5)*
Cerebellum	2.85±0.22	4.11±0.19 (↑44.07%) **	3.19±0.22 [↓22.49%] *
Cerebral Cortex	2.89±0.21	6.10±0.27 (↑111.08%) **	5.12±0.13 [↓16.05%] * (↑77.18%) **
Midbrain	4.59±0.53	8.73±0.89 (↑89.89%) **	5.57±0.61 [↓36.23%] *
Hippocampus	2.97±0.18	5.35±0.33 (↑80.13%) **	3.23±0.49 [↓39.72%] **
Striatum	2.99±0.30	6.03±0.54 (↑101.26%) **	3.62±0.47 [↓40.01%] **
Diencephalon	4.22±0.21	6.77±0.46 (↑60.36%) **	4.52±0.17 [↓33.18%] **

Values are expressed as mean ± estimated SEM. The rate in the parenthesis ( ) is the % change compared to the levels of the EC. The rate on the hook [ ] is the % change compared to the levels of DC. * P<0.05 and **P<0.01 denote the significant differences.

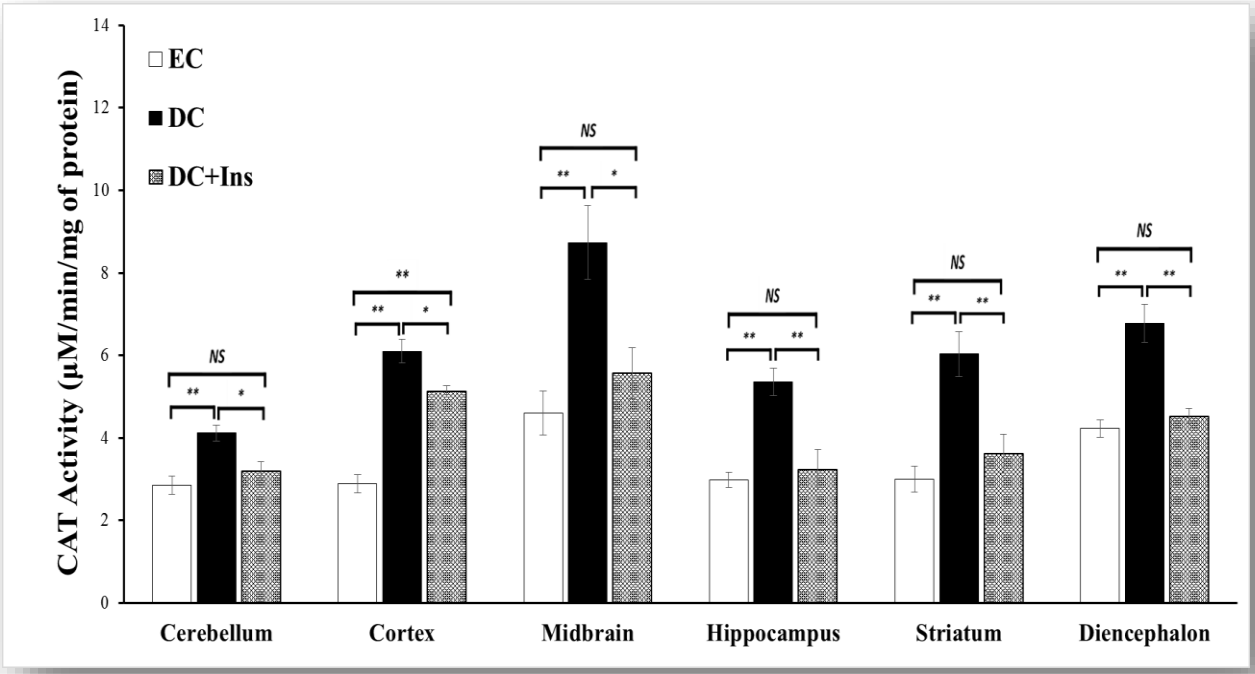

*Figure 36. CAT activity. Columns represent the mean and error bars represent estimated SEM (n=5 mice/group). ** indicates P < 0.01 between the compared groups. * indicates P < 0.05 between the compared groups.*

3.7.3. Effect of diabetes and insulin treatment on glutathione peroxidase activity

The effect of STZ-induced diabetes and insulin treatment on glutathione peroxidase (GPx) activity in mice is presented in Table 14 and Figure 37. More specifically the GPx activity was significantly increased in all brain regions of the DC mice compared to the EC group. The largest increase of GPx activity was observed in cerebral cortex (56.51%; P<0.01) and diencephalon (49.96%; P<0.01). Midbrain (43.58%; P<0.01) and cerebellum (42.93%; P<0.01) follow, while the lowest augmentations were observed in hippocampus (30.25%; P<0.01) and striatum (20.06%; P<0.01). On the other hand, the DC+Ins group presented significant decrease of GPx activity, in all the brain regions examined compared to the DC group. More particularly, the largest decrease was observed in cerebellum (22.60%; P<0.01) and diencephalon (20.44%; P<0.01). Hippocampus (19.16%; P<0.01) and midbrain (16.06%; P<0.05) follow with lower decrease, while the smallest decline was observed in striatum (15.77%; P<0.01) and cerebral cortex (14.96%; P<0.05). Cerebral cortex and midbrain were observed having significant difference compared to the EC group (33.10%; P<0.01 and 20.51%; P<0.05, respectively) indicating the incomplete recovery of these regions regarding the GPx activity.

Table 14. Effect of diabetes and insulin treatment on glutathione peroxidase activity.

	GPx activity (Units/mg of protein/min)		
	EC *(n=5)*	**DC** *(n=5)*	**DC+Ins** *(n=5)*
Cerebellum	3.37±0.13	4.82±0.11 (↑42.93%) **	3.73±0.24 [↓22.60%] **
Cerebral Cortex	3.66±0.15	5.73±0.22 (↑56.51%) **	4.87±0.19 [↓14.96%] * (↑33.10%) **
Midbrain	3.74±0.12	5.37±0.22 (↑43.58%) **	4.50±0.24 [↓16.06%] * (↑20.51%) *
Hippocampus	5.88±0.23	7.66±0.32 (↑30.25%) **	6.19±0.19 [↓19.16%] **
Striatum	6.26±0.18	7.52±0.17 (↑20.06%) **	6.33±0.20 [↓15.77%] **
Diencephalon	3.72±0.13	5.58±0.19 (↑49.96%) **	4.44±0.27 [↓20.44%] **

Values are expressed as mean ± estimated SEM. The rate in the parenthesis ( ) is the % change compared to the levels of the EC. The rate on the hook [ ] is the % change compared to the levels of DC. * P<0.05 and **P<0.01 denote the significant differences.

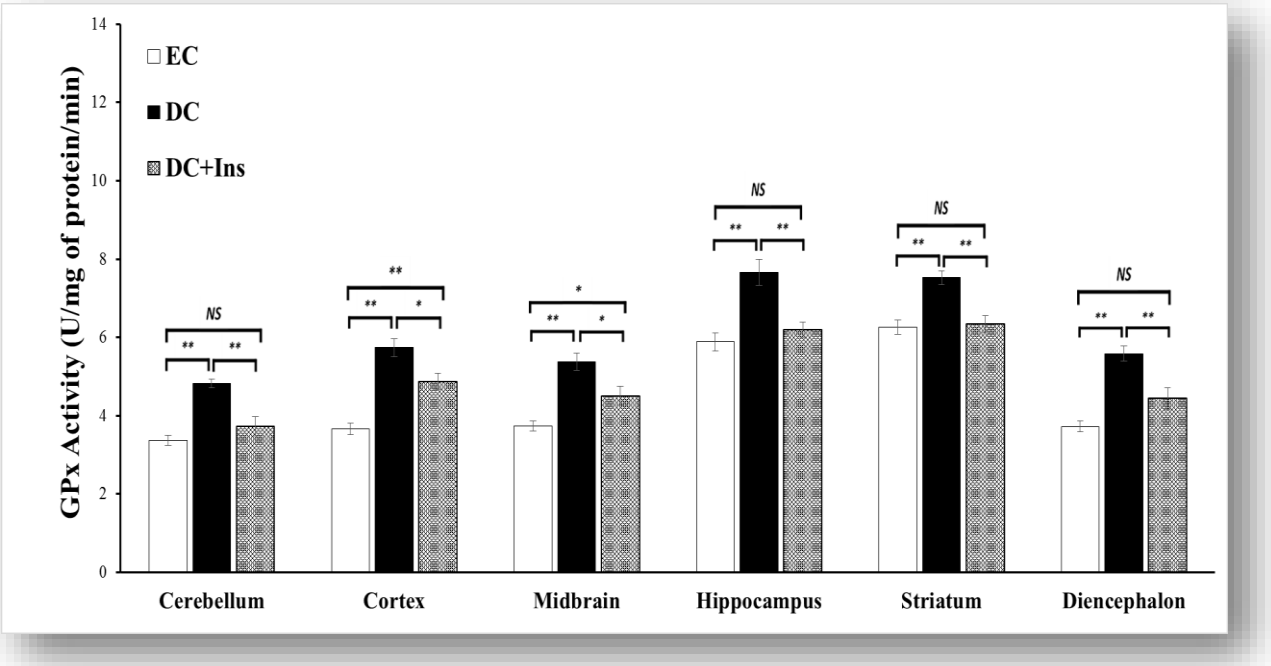

*Figure 37. GPx activity. Columns represent the mean and error bars represent estimated SEM (n=5 mice/group). ** indicates P < 0.01 between the compared groups. * indicates P < 0.05 between the compared groups.*

3.8. Effect of diabetes and insulin treatment on oxidized and reduced glutathione content

In an effort to determine the effect of STZ-induced diabetes and insulin treatment on the free radical scavenger, glutathione, we determined the ratio of the oxidized (GSSG) glutathione levels to the reduced glutathione (GSH) levels and is presented in Table 15 and Figure 38. More specifically the GSSG/GSH ratio was significantly increased in all brain regions of the DC mice compared to the EC group. The largest increase of GSSG/GSH ratio was observed in hippocampus (116.81%; P<0.01) and striatum (93.49%; P<0.01). Cerebral cortex (69.48%; P<0.01) and cerebellum (60.80%; P<0.01) follow, while the smallest augmentations were observed in diencephalon (36.58%; P<0.01) and midbrain (35.46%; P<0.01). On the other hand, the DC+Ins group presented significant decrease of GSSG/GSH ratio, in all the brain regions examined compared to the DC group. More particularly, the largest decrease was observed in hippocampus (47.04%; P<0.01) and striatum (43.28%; P<0.01). Cerebellum (27.52%; P<0.01) and cerebral cortex (19.59%; P<0.05) follow with lower decrease, while the smallest decline was observed in midbrain (17.11%; P<0.01) and diencephalon (14.00%; P<0.01). Cerebral cortex, diencephalon and midbrain were observed having significant difference compared to the EC group (36.28%; P<0.05, 17.45%; P<0.01 and 12.28%; P<0.05, respectively) indicating the incomplete recovery of these regions regarding the GSSG/GSH ratio.

Table 15. Effect of diabetes and insulin treatment on oxidized and reduced glutathione content.

	GSSG/GSH ratio		
	EC *(n=5)*	**DC** *(n=5)*	**DC+Ins** *(n=5)*
Cerebellum	0.079±0.004	0.127±0.008 (↑60.80%) **	0.092±0.001 [↓27.52%] **
Cerebral Cortex	0.086±0.004	0.147±0.007 (↑69.48%) **	0.118±0.007 [↓19.59%] * (↑36.28%) *
Midbrain	0.118±0.002	0.159±0.003 (↑35.46%) **	0.132±0.002 [↓17.11%] ** (↑12.28%) *

Hippocampus	0.078±0.002	0.170±0.006 (↑116.81%) **	0.090±0.003 [↓47.04%] **
Striatum	0.128±0.002	0.248±0.013 (↑93.49%) **	0.140±0.002 [↓43.28%] **
Diencephalon	0.126±0.002	0.172±0.002 (↑36.58%) **	0.148±0.004 [↓14.00%] ** (↑17.45%) **

Values are expressed as mean ± estimated SEM. The rate in the parenthesis ( ) is the % change compared to the levels of the EC. The rate on the hook [ ] is the % change compared to the levels of DC. * P<0.05 and **P<0.01 denote the significant differences.

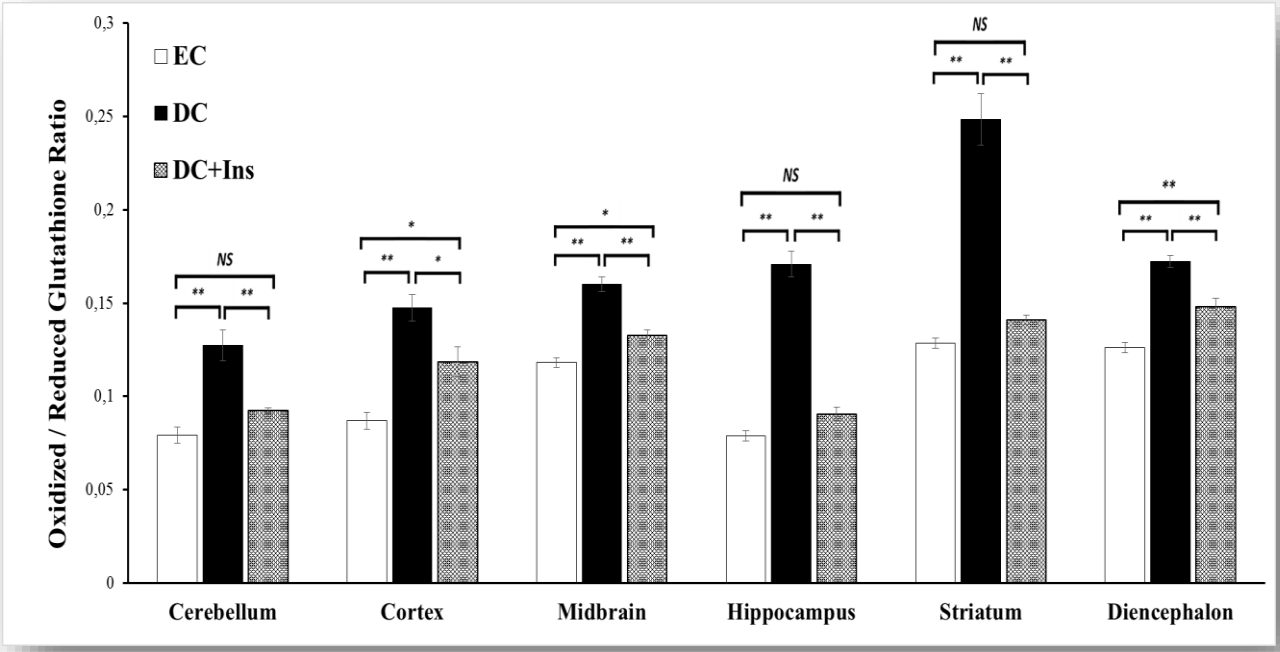

*Figure 38. GSSG/GSH ratio. Columns represent the mean and error bars represent estimated SEM (n=5 mice/group). ** indicates P < 0.01 between the compared groups. * indicates P < 0.05 between the compared groups.*

3.9. Effect of diabetes and insulin treatment on lipid peroxidation content

In an effort to determine the effect of STZ-induced diabetes and insulin treatment on lipid peroxidation, we used the reaction with thiobarbituric acid and expressed the results as malondialdehyde (MDA) equivalent levels in the brain regions (Table 16 and Figure 39). More specifically the MDA levels were significantly increased in all brain regions of the DC mice compared to the EC group. The largest increase of MDA levels was observed in hippocampus (54.14%; P<0.01) and diencephalon (47.67%; P<0.01). Midbrain (44.37%; P<0.01) and

striatum (42.42%; P<0.01) follow, while the smallest augmentations were observed in cerebral cortex (40.62%; P<0.01) and cerebellum (35.67%; P<0.05). On the other hand, the DC+Ins group presented significant decrease of MDA levels, in most of the brain regions examined compared to the DC group. More particularly, the largest decrease was observed in striatum (28.01%; P<0.01) and hippocampus (26.21%; P<0.01). Diencephalon (24.56%; P<0.01) and cerebellum (23.50%; P<0.05) follow with lower decrease, while the smallest decline was observed in midbrain (21.32%; P<0.05). Characteristically, the only region that had no significant decrease of MDA levels compared to the DC group was cerebral cortex, while at the same time it was observed having significant difference compared to the EC group (27.06%; P<0.05) indicating the incomplete recovery of this region regarding the MDA levels.

Table 16. Effect of diabetes and insulin treatment on lipid peroxidation content.

	MDA levels (μmol/g of protein)		
	EC *(n=5)*	**DC** *(n=5)*	**DC+Ins** *(n=5)*
Cerebellum	6.60±0.53	8.96±0.51 (↑35.67%) *	6.85±0.46 [↓23.50%] *
Cerebral Cortex	10.43±0.64	14.66±0.84 (↑40.62%) **	13.25±0.44 (↑27.06%) *
Midbrain	8.01±0.50	11.57±0.67 (↑44.37%) **	9.10±0.36 [↓21.32%] *
Hippocampus	7.32±0.35	11.29±0.11 (↑54.14%) **	8.33±0.29 [↓26.21%] **
Striatum	8.37±0.60	11.93±0.76 (↑42.42%) **	8.59±0.25 [↓28.01%] **
Diencephalon	7.66±0.42	11.32±0.76 (↑47.67%) **	8.53±0.28 [↓24.56%] **

Values are expressed as mean ± estimated SEM. The rate in the parenthesis ( ) is the % change compared to the levels of the EC. The rate on the hook [ ] is the % change compared to the levels of DC. * P<0.05 and **P<0.01 denote the significant differences.

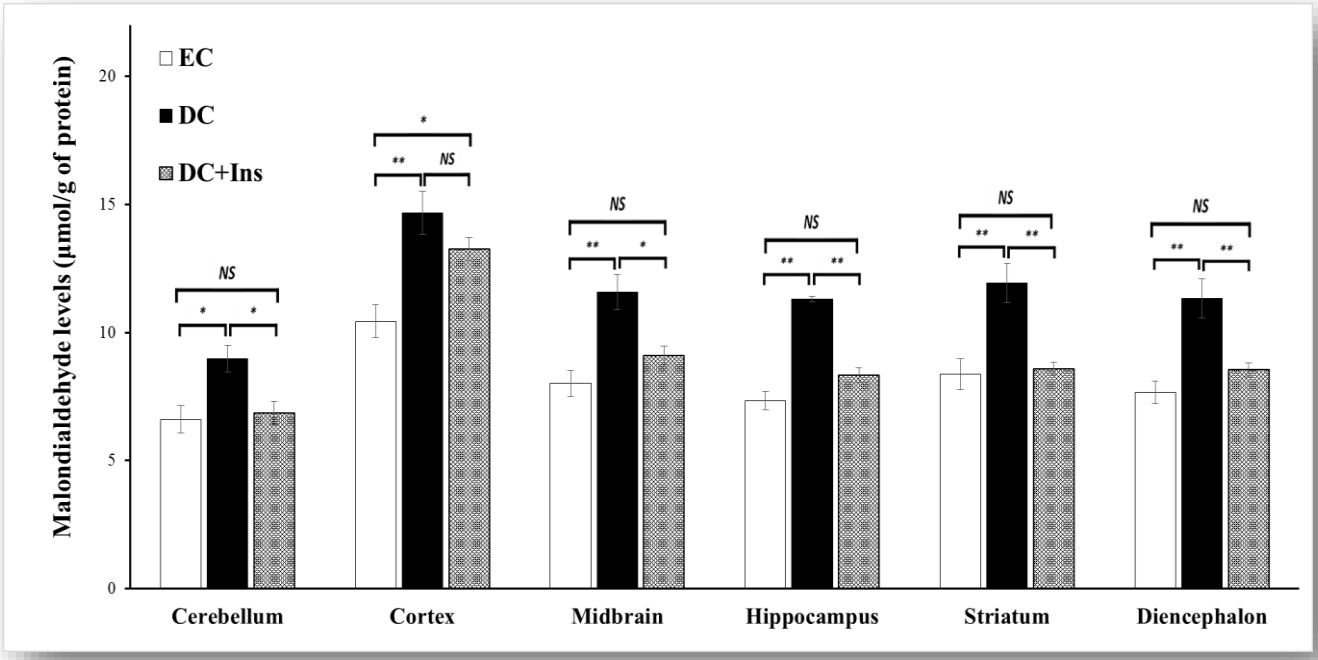

*Figure 39. MDA levels. Columns represent the mean and error bars represent estimated SEM (n=5 mice/group). ** indicates P < 0.01 between the compared groups. * indicates P < 0.05 between the compared groups.*

3.10. Effect of diabetes and insulin treatment on cytochrome c localization

In an effort to determine the effect of STZ-induced diabetes and insulin treatment on the induction of neuronal apoptosis, we performed Western blot analysis on mitochondrial lysates and cytoplasmic samples. The purpose was to determine the localization of cytochrome c in each brain region by measuring the ratio of the cytoplasmic cytochrome c content to the mitochondrial cytochrome c content (Tables 16-20 and Figures 25-39). As a cytoplasmic loading control it was used a-tubulin (Tubulin), while for mitochondrial loading control it was used cytochrome c oxidase subunit 4 (Cox4).

3.10.1. Effect of diabetes and insulin treatment on cerebral cortex cytochrome c levels ratio

Western blot analysis on mitochondrial lysates and cytoplasmic samples of cerebral cortex, determined the ratio of the cytoplasmic cytochrome c content to the mitochondrial cytochrome c content. More specifically, the cytochrome c levels ratio of the DC mice had no significant increase (10.12%) compared to the EC group. At the same pattern, the cytochrome c levels ratio of the DC+Ins mice had no significant increase (28.93%) compared to the EC group (Table 17; Figures 40-42).

Table 17. Effect of diabetes and insulin treatment on cerebral cortex cytochrome c levels ratio.

	Cytochrome c ratio levels (cytoplasm/mitochondria)		
	EC *(n=3)*	**DC** *(n=3)*	**DC+Ins** *(n=3)*
Cerebral Cortex	0.51±0.082	0.56±0.040 (↑10.12%)	0.66±0.071 (↑28.93%)

Values are expressed as mean ± estimated SEM. The rate in the parenthesis ( ) is the % change compared to the levels of the EC. The rate on the hook [ ] is the % change compared to the levels of DC.

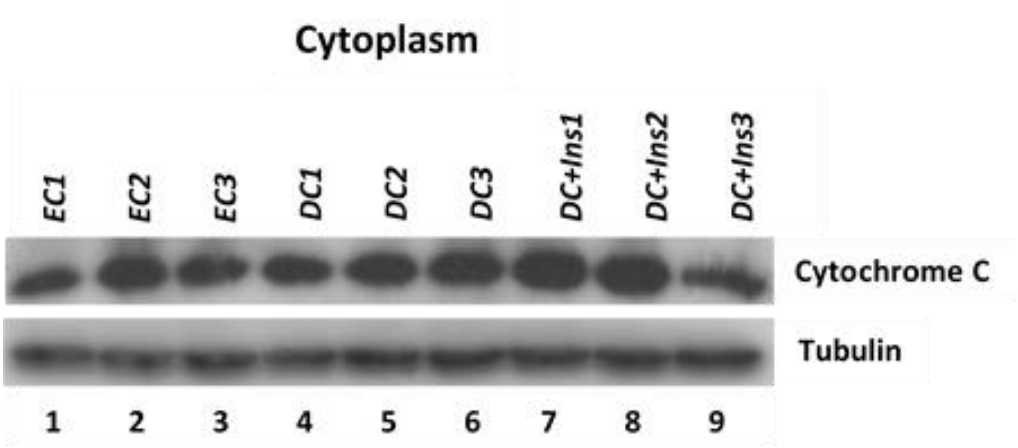

Figure 40. Cerebral Cortex-Western blot analysis for cytoplasmic cytochrome c levels with its cytoplasmic internal control Tubulin. Data were produced from the same blot probed with the indicated antibodies.

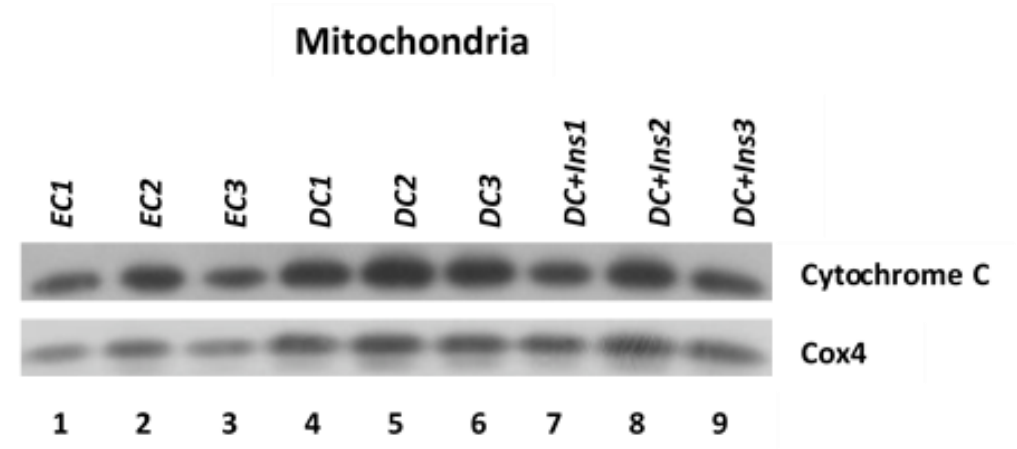

Figure 41. Cerebral Cortex-Western blot analysis for mitochondrial cytochrome c levels with its mitochondrial internal control Cox4. Data were produced from the same blot probed with the indicated antibodies.

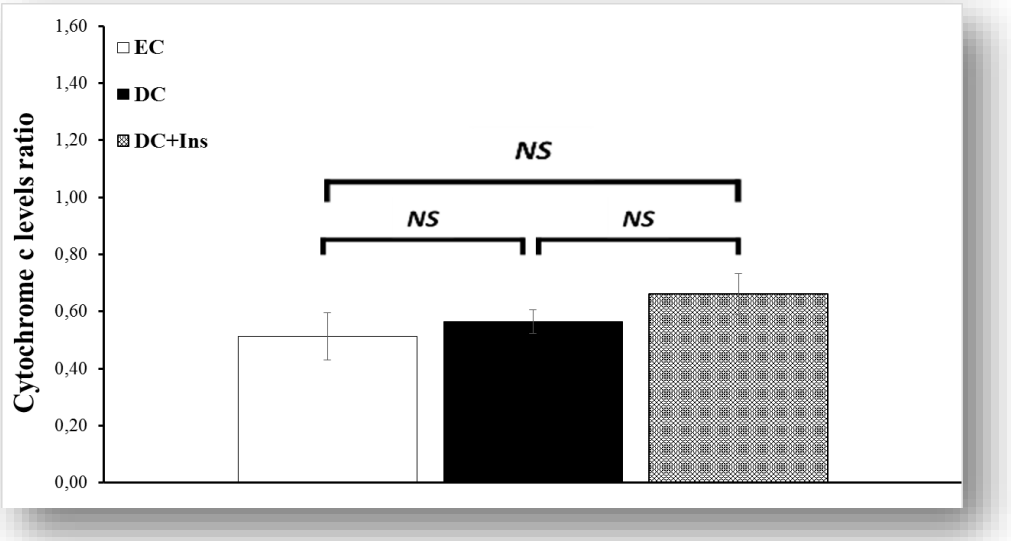

Figure 42. Cerebral Cortex-Cytochrome c levels ratio. Columns represent the mean and error bars represent estimated SEM (n=3 mice/group).

3.10.2. Effect of diabetes and insulin treatment on midbrain cytochrome c levels ratio

Western blot analysis on mitochondrial lysates and cytoplasmic samples of midbrain, determined the ratio of the cytoplasmic cytochrome c content to the mitochondrial cytochrome c content. More specifically the cytochrome c levels ratio of the DC mice was significantly increased (59.79%; P<0.01) compared to the EC group. On the other hand, the cytochrome c levels ratio of the DC+Ins mice showed no significant decrease compared to the DC group, while at the same time it was significantly increased (42.38%; P<0.05) compared to the EC group indicating the incomplete recovery of this region (Table 18; Figures 43-45).

Table 18. Effect of diabetes and insulin treatment on midbrain cytochrome c levels ratio.

	Cytochrome c ratio levels (cytoplasm/mitochondria)		
	EC *(n=3)*	**DC** *(n=3)*	**DC+Ins** *(n=3)*
Midbrain	0.14±0.018	0.22±0.012 (↑59.79%) **	0.20±0.010 (↑42.38%) *

Values are expressed as mean ± estimated SEM. The rate in the parenthesis ( ) is the % change compared to the levels of the EC. The rate on the hook [ ] is the % change compared to the levels of DC. * P<0.05 and **P<0.01 denote the significant differences.

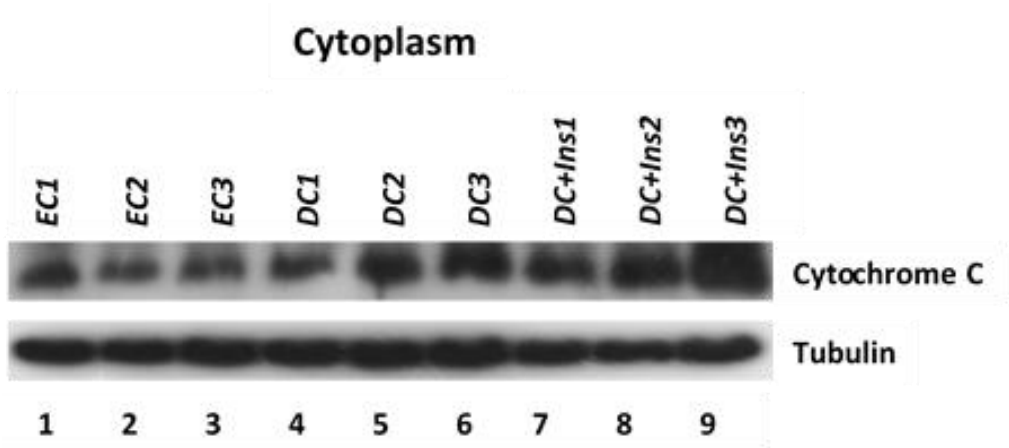

Figure 43. Midbrain-Western blot analysis for cytoplasmic cytochrome c levels with its cytoplasmic internal control Tubulin. Data were produced from the same blot probed with the indicated antibodies.

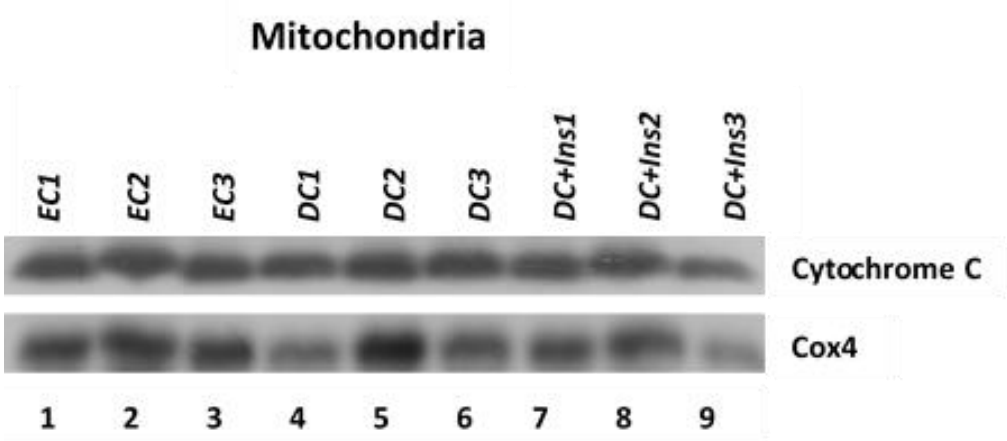

Figure 44. Midbrain-Western blot analysis for mitochondrial cytochrome c levels with its mitochondrial internal control Cox4. Data were produced from the same blot probed with the indicated antibodies.

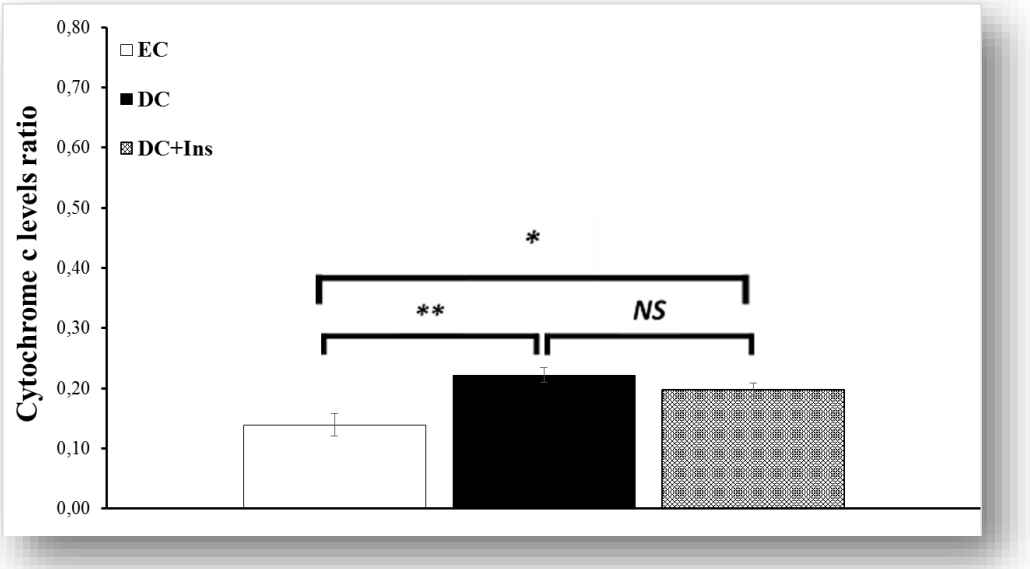

*Figure 45. Midbrain-Cytochrome c levels ratio. Columns represent the mean and error bars represent estimated SEM (n=3 mice/group). ** indicates P < 0.01 between the compared groups. * indicates P < 0.05 between the compared groups.*

3.10.3. Effect of diabetes and insulin treatment on hippocampus cytochrome c levels ratio

Western blot analysis on mitochondrial lysates and cytoplasmic samples of hippocampus, determined the ratio of the cytoplasmic cytochrome c content to the mitochondrial cytochrome c content. More specifically the cytochrome c levels ratio of the DC mice was significantly increased (36.76%; P<0.01) compared to the EC group. On the other hand, the cytochrome c levels ratio of the DC+Ins mice was significantly decreased (16.57%; P<0.05) compared to the DC group (Table 19; Figures 46-48).

Table 19. Effect of diabetes and insulin treatment on hippocampus cytochrome c levels ratio.

	Cytochrome c ratio levels (cytoplasm/mitochondria)		
	EC *(n=3)*	**DC** *(n=3)*	**DC+Ins** *(n=3)*
Hippocampus	1.00±0.074	1.37±0.042 (↑36.76%) **	1.14±0.050 [↓16.57%] *

Values are expressed as mean ± estimated SEM. The rate in the parenthesis ( ) is the % change compared to the levels of the EC. The rate on the hook [ ] is the % change compared to the levels of DC. * P<0.05 and **P<0.01 denote the significant differences.

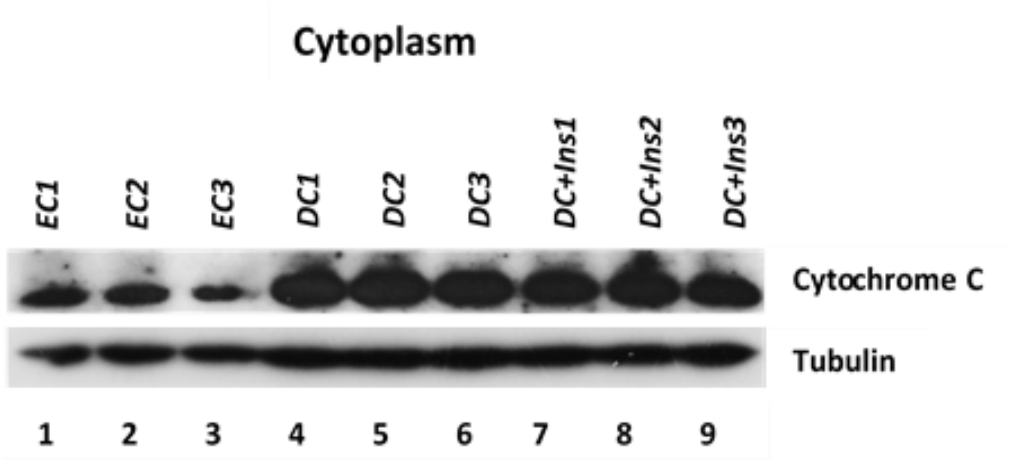

Figure 46.Hippocampus-Western blot analysis for cytoplasmic cytochrome c levels with its cytoplasmic internal control Tubulin. Data were produced from the same blot probed with the indicated antibodies.

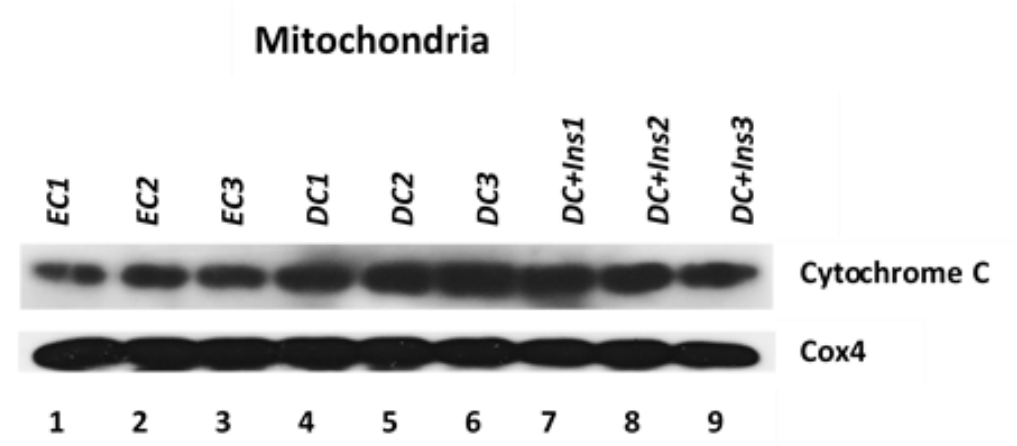

Figure 47. Hippocampus-Western blot analysis for mitochondrial cytochrome c levels with its mitochondrial internal control Cox4. Data were produced from the same blot probed with the indicated antibodies.

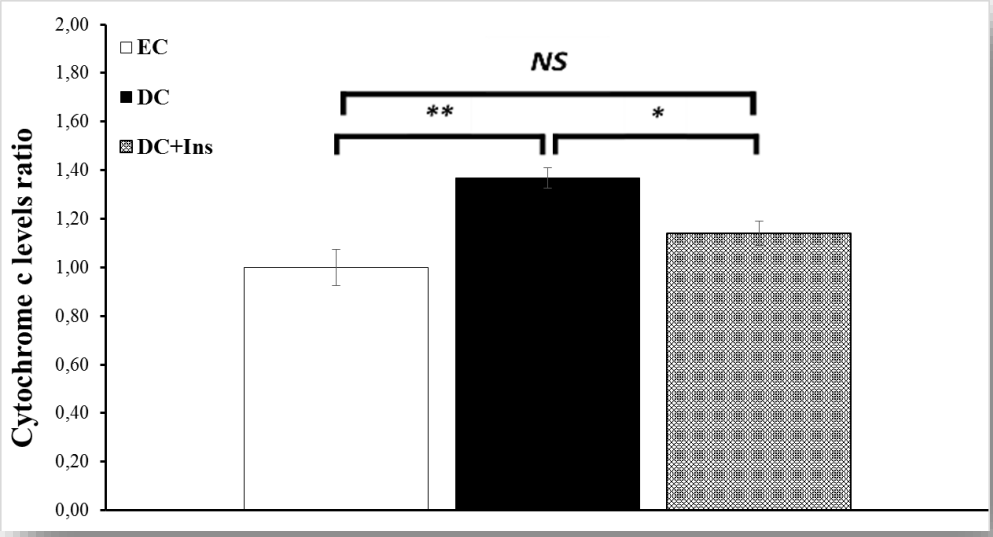

*Figure 48. Hippocampus-Cytochrome c levels ratio. Columns represent the mean and error bars represent estimated SEM (n=3 mice/group). ** indicates P < 0.01 between the compared groups. * indicates P < 0.05 between the compared groups.*

3.10.4. Effect of diabetes and insulin treatment on striatum cytochrome c levels ratio

Western blot analysis on mitochondrial lysates and cytoplasmic samples of striatum, determined the ratio of the cytoplasmic cytochrome c content to the mitochondrial cytochrome c content. More specifically the cytochrome c levels ratio of the DC mice was significantly increased (292.92%; P<0.01) compared to the EC group. On the other hand, the cytochrome c levels ratio of the DC+Ins mice was significantly decreased (45.13%; P<0.01) compared to the DC group while at the same time it was observed having significant difference compared to the EC group (115.59%; P<0.05) indicating the incomplete recovery of this region (Table 20; Figures 49-51).

Table 20. Effect of diabetes and insulin treatment on striatum cytochrome c levels ratio.

	Cytochrome c ratio levels (cytoplasm/mitochondria)		
	EC *(n=3)*	**DC** *(n=3)*	**DC+Ins** *(n=3)*
Striatum	0.18±0.059	0.69±0.042 (↑292.92%) **	0.38±0.034 [↓45.13%] ** (↑115.59%) *

Values are expressed as mean ± estimated SEM. The rate in the parenthesis ( ) is the % change compared to the levels of the EC. The rate on the hook [ ] is the % change compared to the levels of DC. * P<0.05 and **P<0.01 denote the significant differences.

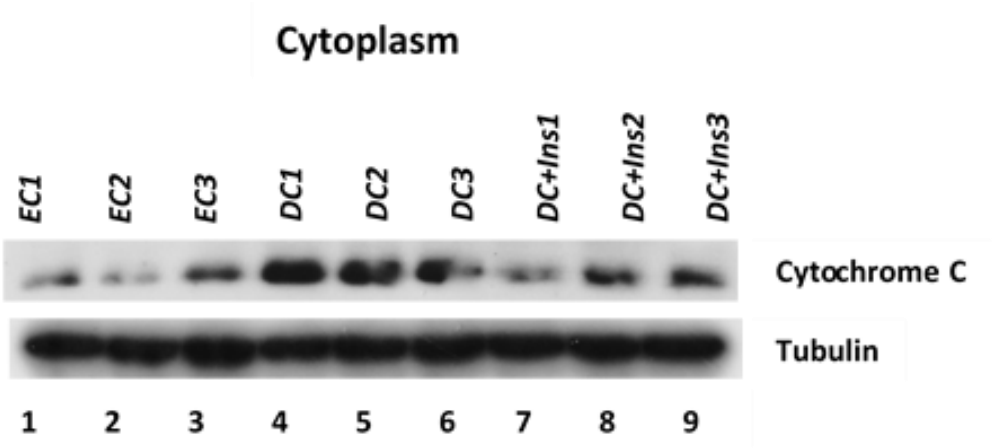

Figure 49. Striatum-Western blot analysis for cytoplasmic cytochrome c levels with its cytoplasmic internal control Tubulin. Data were produced from the same blot probed with the indicated antibodies.

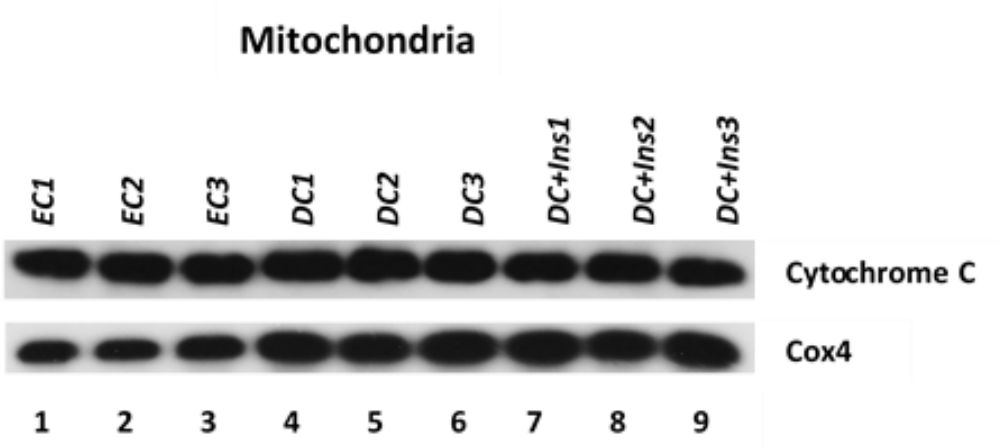

Figure 50. Striatum-Western blot analysis for mitochondrial cytochrome c levels with its mitochondrial internal control Cox4. Data were produced from the same blot probed with the indicated antibodies.

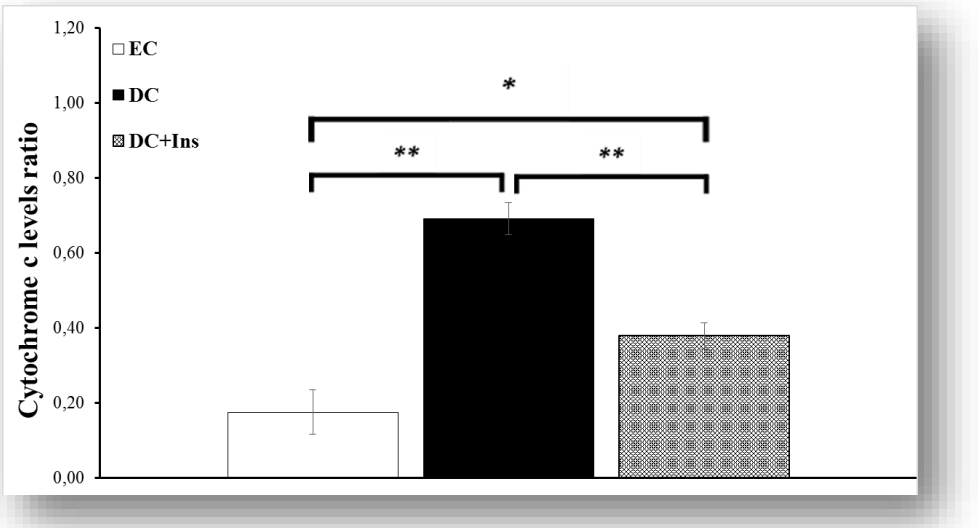

*Figure 51. Striatum-Cytochrome c levels ratio. Columns represent the mean and error bars represent estimated SEM (n=3 mice/group). ** indicates P < 0.01 between the compared groups. * indicates P < 0.05 between the compared groups.*

3.10.5. Effect of diabetes and insulin treatment on diencephalon cytochrome c levels ratio

Western blot analysis on mitochondrial lysates and cytoplasmic samples of diencephalon, determined the ratio of the cytoplasmic cytochrome c content to the mitochondrial cytochrome c content. More specifically the cytochrome c levels ratio of the DC mice was significantly increased (58.64%; P<0.05) compared to the EC group. On the other hand, the cytochrome c levels ratio of the DC+Ins mice was significantly decreased (35.77%; P<0.05) compared to the DC group (Table 21; Figures 52-54).

Table 21. Effect of diabetes and insulin treatment on diencephalon cytochrome c levels ratio.

	Cytochrome c ratio levels (cytoplasm/mitochondria)		
	EC *(n=3)*	**DC** *(n=3)*	**DC+Ins** *(n=3)*
Diencephalon	0.35±0.042	0.56±0.046 (↑58.64%) *	0.36±0.042 [↓35.77%] *

Values are expressed as mean ± estimated SEM. The rate in the parenthesis ( ) is the % change compared to the levels of the EC. The rate on the hook [ ] is the % change compared to the levels of DC. * P<0.05 denotes the significant differences.

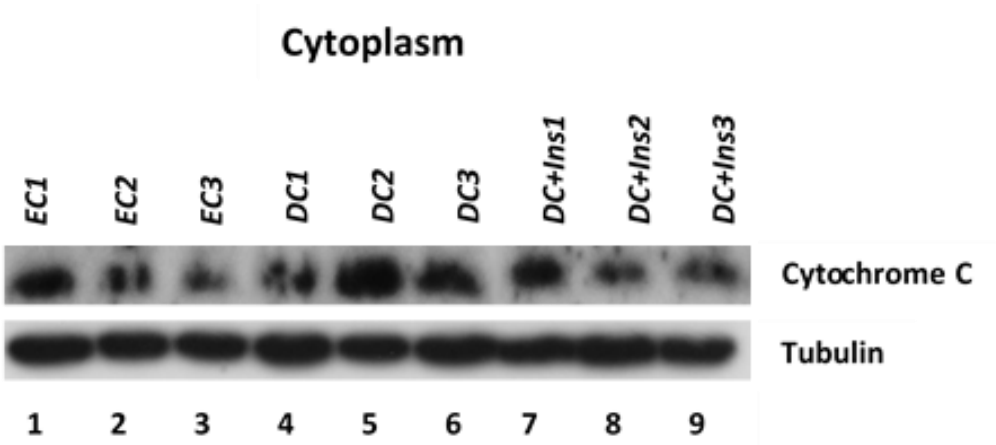

Figure 52. Diencephalon-Western blot analysis for cytoplasmic cytochrome c levels with its cytoplasmic internal control Tubulin. Data were produced from the same blot probed with the indicated antibodies.

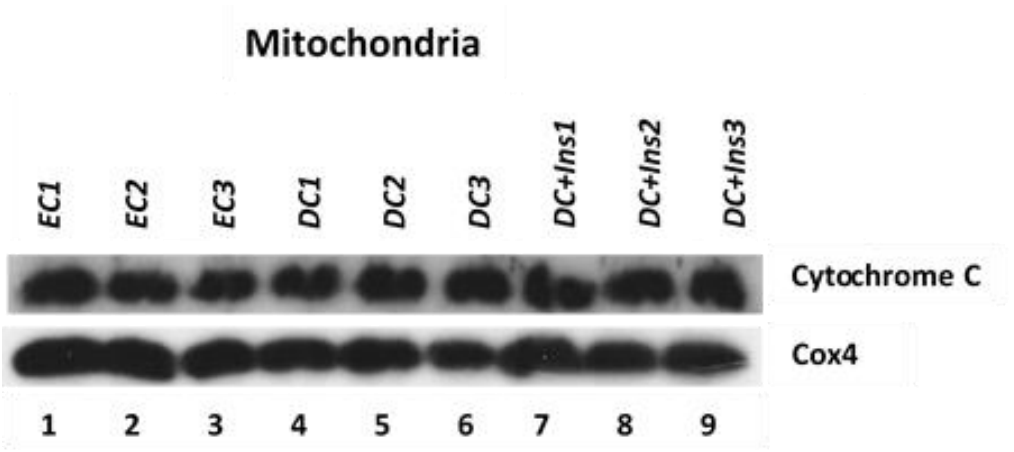

Figure 53. Diencephalon-Western blot analysis for mitochondrial cytochrome c levels with its mitochondrial internal control Cox4. Data were produced from the same blot probed with the indicated antibodies.

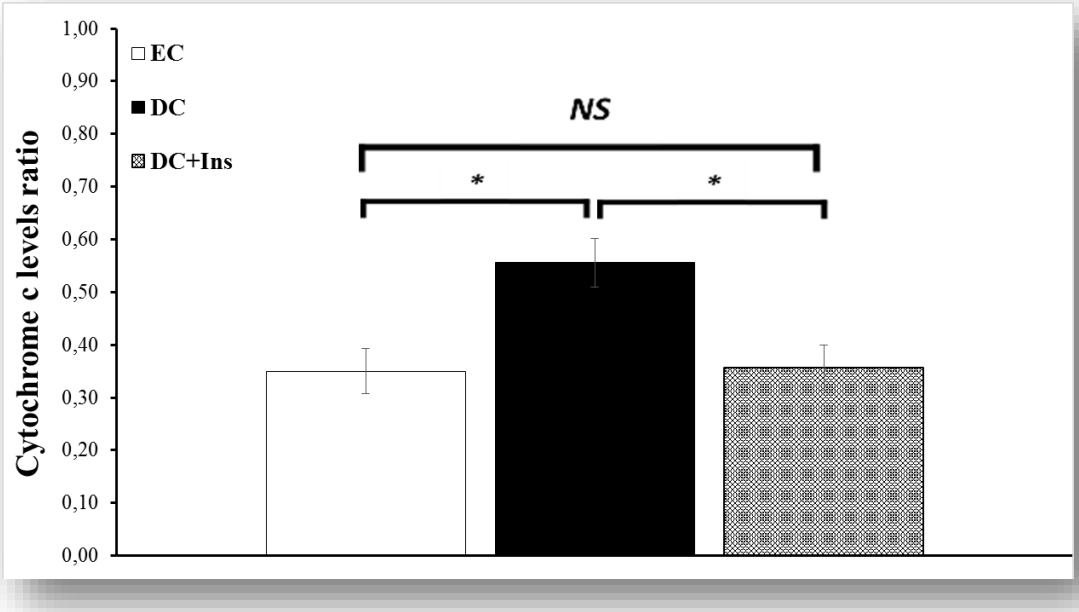

*Figure 54. Diencephalon-Cytochrome c levels ratio. Columns represent the mean and error bars represent estimated SEM (n=3 mice/group). * indicates P < 0.05 between the compared groups.*

IV. DISCUSSION

As previously described in the proposed sequential mechanisms underlying T1DM encephalopathy (Figure 4), insulin and C-peptide deficiency result in impaired insulin signaling, affecting inflammation, oxidative stress, apoptosis and cognitive deficits. These lead to suppressed expression of neurotrophic factors and their receptors, impacting on neuronal integrity with neurite degeneration as well as increased apoptotic activity with neuronal loss and gray matter atrophy. Apoptotic cell loss of white matter oligodendroglial cells results in white matter atrophy. On the other hand, hyperglycemia and activation of the polyol pathway lead to increased AGE's formation that contributes to increased RAGE expression, inflammation, apoptosis and cognitive deficits (42).

In our study, we sought to investigate the effects of streptozotocin-induced Type I diabetes and its short-term insulin treatment (6 days) on mice. The study was focused on cognitive dysfunction, cholinergic system aberrations, induction of oxidative stress and mitochondrial signals of neuronal apoptosis. The variety of the brain regions examined, had the purpose of unveiling the response each one of them had, after the induction of diabetes and its treatment with insulin.

4.1. Insulin regulated the increased glucose levels and attenuated the symptoms of polyphagia, polydipsia and weight loss from the diabetic mice

It has been shown that high blood glucose levels (> 200 mg/dL) lead to marked polydipsia and polyuria and weight loss (123). In our study the fasted plasma glucose levels of the diabetic groups presented over a 300% increase, before the treatment with insulin. After the insulin treatment the glucose levels of the DC+Ins group were reduced significantly (70%) regulating their glucose levels, while the DC group further increased its food intake (470%).

The classic symptoms of diabetes, as it was mentioned before, are polyphagia, polydipsia, polyuria and weight loss (149). The diabetic mice in our study followed the above pattern and revealed dramatic changes regarding the daily food and water intake per mouse (Table 2 and Figures 18, 19). The food consumption of the diabetic groups presented an 87% increase, before the treatment with insulin. After the insulin treatment the food consumption of the DC+Ins group was reduced significantly (41%) approaching the levels of the EC group, while the DC group further increased its food intake (110.81%) compared to the EC.

If glucose utilization were the predominant influence on hunger, diabetic hyperphagia would begin soon after treatment with drugs which cause insulin deficient diabetes. However, diabetic hyperphagia develops slowly, reaching a maximum many days after treatment with STZ on rats (150). It has even been reported that the initial effect of experimental diabetes in rats (single dose of 120 mg/kg STZ) is several days of reduced food intake followed by recovery and hyperphagia (151). Booth (150) suggested that the utilization of body fat may suppress hunger after STZ treatment. Consistent with this idea, Storlein (152) found that rats which are first made to lose body fat by food restriction show diabetic hyperphagia much sooner than rats of normal body weight.

Regarding the water consumption, the diabetic groups presented an over 530% increase, before the treatment with insulin. After the insulin treatment the water consumption of the DC+Ins group was reduced significantly (64%) approaching the levels of the EC group, while the DC group further increased its water intake (640%) compared to the EC (Table 3 and Figures 20, 21).

It has been shown that when glucose concentration in the blood rises above approximately 180 mg/dL (10.0 mmol/L), glucosuria occurs, leading to an osmotic diuresis that causes polyuria. The polyuria stimulates polydipsia to maintain euvolemia. With further insulin deficiency, there is an increase in lipolysis from fat cells as well as protein breakdown, an exaggeration of the normal fasting state designed to provide alternative sources of fuel. These mechanisms, along with the caloric loss from glucosuria, result in the hyperphagia and weight loss typical of the undiagnosed diabetic state. With profound insulin deficiency, the process devolves into ketoacidosis, with marked hyperglycemia, dehydration driven by the glucosuric osmotic diuresis, and accumulation of ketoacids from the hepatic metabolism of the liberated fatty acids (149).

Regarding the body weight, the diabetic groups presented an over 24% decrease, before the treatment with insulin. After the insulin treatment the body weight of the DC+Ins group was increased significantly (11%) approaching the normal weight of the EC group, while the DC group further decreased its body weight (28%).

Conclusively, the treatment with insulin of the diabetic mice regulated the increased glucose levels and attenuated the symptoms of polyphagia, polydipsia and weight loss, which is consistent with studies that have shown that CNS insulin implicated in the control of glucose levels and body weight (153).

4.2. Insulin attenuated the increased triglycerides and total cholesterol levels in the diabetic mice

Hypertriglyceridemia of chronic diabetes was associated with a statistically significant decrease in TG entry rate in alloxan-diabetic rats (154). This result indicate that the elevated basal levels of plasma TG in rats with chronic diabetes must be due to a decrease in TG removal from plasma. Since base-line TG levels were increased in rats eating a fat-free diet, the defect in lipoprotein removal involves endogenous lipoproteins (154). Bierman, Bagdade, and Porte have earlier provided evidence that this mechanism is responsible for hypertriglyceridemia in insulin-deficient diabetic patients (155).

Hypercholesterolemia may be attributed to increased dietary cholesterol absorption from the small intestine following the intake of fat in a diabetic condition (156). One striking finding was the synergistic effects of dietary fat and cholesterol on plasma TG and TC levels in T1DM developing severe hypertriglyceridemia and hypercholesterolemia (157).

The results in the present study showed that the DC mice had significantly higher triglycerides (207%) and total cholesterol levels (77%) compared to the EC group, while the treatment of the DC mice with insulin reduced significantly both of them (56% and 37% respectively) (Table 4 and Figures 22, 23). The control levels of the EC mice as well as the effects caused by diabetes upon triglycerides and total cholesterol levels, are in agreement with previous studies showing that at the end of a 4-week period after the induction of diabetes (single streptozotocin dose of 60 mg/kg), both triglycerides and cholesterol levels were significantly increased on the diabetic group (158). However, the % increase observed in our study regarding the total cholesterol levels was much greater possibly because of the higher streptozotocin dosage we administered. On the other hand, based upon the stimulatory effect insulin has on the uptake of monosaccharides, fatty acids, and their conversions to the forms of glycogen and triglycerides (55), we observed regulation of both triglycerides and total cholesterol levels on the DC+Ins group.

4.3. Insulin exerts anxiolytic effects on the diabetes-induced anxiety

Our findings suggest that diabetes caused anxiety-like behavior in the diabetic mice as evidenced in all the parameters of both open-field and elevated plus-maze tests (Table 5-6 and Figures 24-27). Experimental type 1 diabetes (T1DM) in rodents has been correlated

with increased expression of hypothalamic hormones (159, 160) which is intimately linked to a marked hyperactivity of the hypothalamopituitary-adrenal axis (161) and a higher susceptibility to stress (162, 163). Also, epidemiological cross-sectional reports have shown that patients with T1DM present impaired cognitive function, associating diabetes with anxiety (14).

In our study, regarding the Open-field test we noticed a significant increase (67%) of thigmotaxis time (index of anxiety) while at the same time the number of entries to the center (index of anxiolysis) were significantly decreased (56%). However, some studies have revealed inconsistent results, showing no significant differences, which may be due to smaller doses of STZ used (single dose of 50-60 mg/kg) and duration of diabetes condition employed on rats (164, 165). The treatment with insulin of the DC mice reversed the pattern by attenuating significantly (36%) the thigmotaxis time, while increasing twofold (96%) the number of entries to the center, giving to the DC+Ins group a much more exploratory and anxiolytic behavior.

Furthermore, regarding the elevated plus-maze test we noticed a significant decrease (70%) of the % ratio of open/total time spent on open and closed arms (low ratio is index of anxiogenesis) while at the same time the number of entries to the open arms (index of anxiolysis) were significantly decreased (58%). The treatment with insulin of the DC mice reversed the pattern by enhancing more than twofold (169%) the ratio of open/total time spent on open and closed arms, while increasing twofold (86%) the number of entries to the open arms, giving to the DC+Ins group a much more exploratory and anxiolytic behavior. This is in accordance with a previous report showing that 2 months after the induction of diabetes (with a single dose of STZ 200 mg/kg) it was presented a lower increase of anxiogenesis than our DC presented, and a complete reverse of the anxiety-like behavior after a lower dose of insulin treatment (2 U/kg) in diabetic mice (166). While, previous reports have shown that diabetic complications are associated with HPA-axis hyperactivity, the high corticosterone levels (as a marker of HPA-axis activity) are correlated with anxiety-like behavioral effects (167). Moreover, it has been found that some of these effects can be reversed by insulin treatment (161). Therefore, it may be related that dysregulated HPA-axis as a consequence of diabetes may develop behavioral deficits such as anxiety, which may be prevented by insulin therapy.

The purpose of using two different behavioral tests was the different manner with which they approach the behavioral indice of fear-anxiety. According to Ramos et al. (168), there are several test-specific anxiety factors in the general behavioral term of anxiety. Some

of these significant factors are the locomotion-related factor, the openness-related factor, the height-related factor and the open/closed arm-related factor. The first two are more thoroughly examined at the OF test, while the last two at the EPM test. In our study the % ratio of open/total time (EPM test) of the DC group was decreased reaching the one third of the EC group ratio (0.14 to 0.48 respectively), while at the OFT the DC group had a less than two fold increase,2 in its thigmotaxis time compared to the EC group (505 sec to 303 sec respectively). The specific factors that the EPM test examined (height and arm preference) compared to the OFT factors (locomotion and openness), was the cause of the observed differences at the anxiogenesis of the DC mice, showing that the factors of the EPM test had a stronger effect upon them. Hence, the detection and evaluation of these sub-behavioral indices was necessary for a more representative examination of the multifaceted behavior of anxiety.

4.4. Insulin has an enhancing effect on diabetes-induced memory impairment

Systematic reviews of population-based studies brings together the evidence that the risk of dementia is, in general, increased in patients with diabetes mellitus (16, 169). Overall, the incidence of dementia in patients with diabetes was increased by 50–100%, relative to non-diabetic individuals. This increased risk involved both Alzheimer's disease and vascular dementia (seven of 11 studies, six of seven studies, respectively), with a ~50–100% increased risk of Alzheimer's disease, and a ~100% increased risk of vascular dementia. Using voxel-based morphometry, patients with type 1 diabetes showed lower gray matter densities (GMD) in posterior temporal, hippocampus, and parahippocampal gyri, which contribute to memory, compared to healthy controls (24). Moreover, the accumulation of AGEs can damage brain by eliciting oxidative stress which have been implicated in the damage of the structure and function of the brain's neurons and hippocampus, which is directly associated with the memory (170).

Memory impairment is the most studied and correlated with diabetes behavioral index. Several papers sought to correlate both diabetes type 1 and 2 with dementia and memory loss. The vast majority of these studies are focused upon the domain of working memory and short-term memory, which is why, Morris water maze (MWM) test (158, 164, 171-175), and complex visual task (174), are mainly used. They observed memory deficiency, regarding the

short-term memory with small aberrations of the impaired levels of working memory at the experimental model of STZ. However in our study we focused on the indice of learning-memory and memory consolidation. Thus, our findings suggest that diabetes caused significant learning and memory deficits in the diabetic mice as evidenced in the step-through passive avoidance test (Table 7 and Figure 28). Specifically, it was noticed a dramatic decrease (78%) in the step-through latency time compared to the EC mice, indicating memory impairment upon the DC mice.

On the other hand, the treatment of the DC mice with insulin, proved the previous theory since it significantly increased fivefold (288%) the STL, confronting the memory loss effects caused by diabetes. Memory enhancement effects of a smaller dose of insulin treatment (2-4 U/kg/day) were indicated on STZ-induced diabetic rats (single dose 40 mg/kg) (171), while LTP was restored only partially (28).

4.5. Insulin alleviates diabetes-induced depressive-like effects

Clinical neuropsychology studies have shown that patients with T1DM present impaired cognitive function and depression-like effects (15). While incapable of fully encapsulating the wide-ranging sequelae of chronic stress in humans, animal models have been useful in elucidating many of the underlying links between psychological stress, memory, and depressive-like behavior (176, 177). Also in rodents, it has been shown that many of the stress-induced pathological behaviors are accompanied by morphological and neurochemical changes in the limbic system (177, 178). For instance, chronic stress induces reversible dendritic atrophy in CA3 pyramidal cells (177, 179). Because these limbic regions and PFC are heavily implicated in emotional regulation and depression (180), the normalization of their function is a fundamental goal to improve mood in individuals subjected to chronic stress owing to type 1 diabetes.

Our findings suggest that diabetes caused significant depressive-like effects upon the diabetic mice as evidenced in the forced swimming test, which is the most widely used model for depressant activity. (Table 8 and Figure 29). In particular, diabetic mice exhibited significant increase (63%) in the duration of immobility time compared to the EC mice, indicating depressive-like episodes as a consequence of diabetes. This is in accordance with the depression-like effects observed in STZ-induced diabetic mice and rats (single dose 50 and 200 mg/kg respectively) (153, 165). However, the depression-like effect in our study was

higher which may be due to differences to the higher doses of STZ we used, or possibly because the vehicle group in both studies presents an already increased, above the normal (~100 sec), immobility time.

On the other hand, insulin treatment reversed completely (31%) the diabetes-induced immobility time, indicating antidepressant activity. The antidepressant effects were also observed in diabetic mice, after a lower two-week dose of insulin treatment (2 U/kg) (153).It is known that insulin increases reward behavior in STZ diabetic mice subjected to an intracranial self-stimulation testing paradigm (181). While insulin deficiency leads to depression like symptoms in STZ-diabetic rats (182).

4.6. Diabetes correlates with behavioral indices independently body weight

As it was mentioned before the behavioral tests are conducted under careful and insulated conditions, since a plethora of factors can alter the behavior of the animals. In our study, diabetes type I caused a great loss of body weight (over 24% decrease) on both the DC and DC+Ins mice. However, a sudden and excess loss body weight may lead to fatigue, weakness and muscle atrophy (183), and all these factors may exert effects upon behavioral factors (locomotion, exploration, fatigue and helplessness). For this reason, we performed ANCOVA analysis to elucidate further the relationship between the glucose levels/body weight and the behavioral indices (Figures 30-A-L). ANCOVA analysis showed that glucose levels had stronger effect size and power upon the behavioral indices, than the body weight had. Also, the linear regressions of the glucose levels were more closely clustered around the regression line than the covariate of body weight, supporting our ANCOVA analysis.

Clinical reports and previous research have only investigated the diabetes-induced behavioral indices, regardless whether hyperglycemia or body loss is the direct modulator. It is an important issue show that the behavioral changes observed on the DC and DC+Ins mice, during the behavioral tasks, are solely an effect of diabetes and its treatment with insulin.

Although body weight did not have any strong effect upon the behavioral indices, it was possible to have mediation effects upon the relationship between the glucose levels and each behavioral indice. Consequently we performed the mediation process by Hayes (Table 9 and Figure 17), which ensured that the body weight had very low and insignificant indirect

effect upon the direct relationship of the glucose levels and the behavioral indices. On the contrary, the direct effects glucose levels had, were a lot higher and significant upon the behavioral indices. The above indicate that the behavioral changes observed on the DC and DC+Ins mice, during the behavioral tasks, were solely an effect of diabetes and its treatment with insulin.

4.7. Insulin reverses the diabetes-induced cholinergic impairment

One of the earliest studies that dealt with the impact of diabetes upon the cholinergic system (184), showed that acetylcholine release and synthesis in the striatum and hippocampus of streptozotocin-induced diabetic rats is decreased 7 weeks after the administration of STZ (albeit at a lower dose), although the steady-state concentration of acetylcholine is unaltered (185), which cannot be attributed to the amount of choline available. Also this altered acetylcholine metabolism may contribute to the cognitive deficits exhibited in diabetes.

There is evidence that the effect glucose on cognition and the ACh release in euglycemic mice, follows an inverted-U dose curve. On the one hand, acetylcholine (ACh) output increases in the hippocampus of rats performing a spatial alternation task and peripheral and hippocampal injections of glucose enhance that release along with increasing scores on the behavioral task (93, 94). However, there appears to be an inverted-U dose effect curve for glucose effect on memory (95) and ACh release (93), indicating the negative effects that high glucose levels have, even if it is a single quickly absorbable injection of glucose.

In our study, the effect of STZ-induced diabetes and insulin treatment on acetylcholine (ACh) levels in several brain region of DC and DC+Ins mice are presented in Table 11 and Figure 34. As expected, the % changes upon the ACh levels are inversely proportional to the % changes of AChE activity. In particular, the hierarchy of the changes in ACh levels, is exactly the same hierarchy that the DS fraction's activity presents, since the G4 isoform is the most abundant AChE isoform (132). Moreover, we observed that the ACh levels of the striatum were the largest between all regions.

More specifically the ACh levels were significantly decreased in all brain regions of the DC mice examined, compared to the EC group, at a brain-specific manner. The largest declines of ACh levels were observed in striatum and hippocampus, both are rich cholinergic

synapse regions (186), and these changes are the direct consequence of the respective largest enhancements that were observed in both the SS and DS activity of hippocampus and striatum. Midbrain and diencephalon follow with lower declines, while the smallest declines were observed in cerebellum and cerebral cortex, with the same hierarchy the changes were observed in the AChE activity. On the other hand, the DC+Ins group presented a significant increase at ACh levels, in most of the brain regions examined compared to the DC group and as it was expected they follow the same hierarchy the DS AChE activity had. More particularly, the largest augmentations were observed in striatum and hippocampus. Midbrain and diencephalon, follow with lower augmentations. Characteristically, the only regions that had no significant increase of ACh levels were cerebellum and cerebral cortex, with the last one having a significant difference compared to the EC group indicating the incomplete recovery of this region regarding the ACh levels (Table 11 and Figure 34).

Peripheral administration of insulin (1 U) in euglycemic mice, also it has been shown to act and increase the ACh levels in the amygdala (96) while intracerebroventricular administration (100 μU) increases ACh levels in the midbrain, caudate nucleus and pons medulla in alloxan-induced diabetic rats (97).

There are several mechanisms that could be responsible for the observed decrease in ACh synthesis and release. Emerging evidences indicated that apoptosis was one of the underlying mechanism on the impairment of cognitive functions and the abnormalities of neurochemistry and structure (187). Also, it has been indicated marked neuronal loss in hippocampus and frontal cortex and white matter atrophy of frontal and temporal regions (36).

Moreover, alterations in the supply of either acetyl CoA or choline could directly affect the ability of these neurons to synthesize ACh. It is unlikely that a decreased supply of acetyl CoA is responsible for the deficit in ACh synthesis because it has been reported that brains from STZ-diabetic rats contain at least twice the control amount of acetyl CoA (188). It is possible, however, that this acetyl CoA is unavailable for ACh synthesis.

A decreased availability of choline as a result of decreased circulating levels of choline decreased transport of choline into the brain, as well as decreased high affinity uptake of choline into cholinergic neurons would also lead to a deficit in ACh synthesis. Although it has been reported that the transport of choline across the blood brain barrier in rats is decreased 9 weeks after the intraperitoneal injection of STZ (189), the steady-state concentration of free choline is unaltered in striatum from rats 7 weeks after the in intravenous administration of STZ, suggesting that the amount of choline available to the cholinergic neuron is unaltered. Hence, it is possible that esterified sources of choline used to support neurotransmitter

synthesis are affected. Since evidence has indicated that choline used for ACh synthesis may be derived, in part, from phosphatidylcholine synthesized by transmethylation (190), and that the concentration of S-adenosylmethionine in brain is significantly decreased in brain of diabetic rats (191), this source of precursor may be limited and could impair ACh synthesis. However, a recent study (164) has presented a reduction of the choline esterase on cerebral cortex and hippocampus, indicating possible deficiency of choline levels.

A change in the synthetic or hydrolytic activity of cholinergic enzymes in vivo would also have an impact on the ability of neurons to synthesize ACh. A decrease in ChAT activity may directly impair ACh synthesis, however no changes in the activity of either enzyme were demonstrable in striatal tissue from 7-week diabetic rats (185). Hence the examination of the AChE activity was crucial in order to further elucidate the mechanism that diabetes acts upon the cholinergic system.

The effect of STZ-induced diabetes and insulin treatment on acetylcholinesterase (AChE) SS and DS fraction (G1 and G4 isoforms respectively) activities in mice are presented in Table 10 and Figures 32-33. As expected, the activity of the enzyme in the DS fraction (G4) was much higher than that of the SS fraction (G1) in all brain tissues tested. As was expected, we observed that the DS fraction of the striatum displayed the greatest AChE activity of all tissues (192)

Specifically, we observed that Diabetes induced significant increase of SS fractions' activity although in different brain-region patterns (Table 10; Figure 32). The largest, statistically significant, AChE G1 enhancements were observed in hippocampus, cerebral cortex and striatum. The cerebellum follows, while midbrain and diencephalon had the smallest enhancements compared to the rest brain regions. Moreover, the DC+Ins group presented significant decrease at the SS fraction activity, in most of the brain regions examined compared to the DC group. More particularly, the largest AChE G1 inhibitions were observed in hippocampus, striatum and cerebellum. Midbrain and diencephalon follow with lower inhibitions. The only region that had no significant recovery was cerebral cortex.

Respectively, we observed that Diabetes induced significant increase of DS fractions' activity although in different brain-region patterns (Table 10; Figure 33). The largest AChE G4 enhancements were observed in hippocampus and striatum. Midbrain and diencephalon were very close, while the smallest enhancements were observed in cerebral cortex and cerebellum. On the other hand, the DC+Ins group presented significant decrease at the DS fraction activity, in most of the brain regions examined compared to the DC group. More particularly, the largest AChE G4 inhibitions were observed in hippocampus and striatum.

Cerebellum, midbrain and diencephalon, follow with lower inhibitions. Characteristically, as observed in the SS fraction's activity, the only region that had no significant recovery was cerebral cortex. These results are consistent with other studies showing that induction of T1DM with intraperitoneal administration of STZ (single dose 40 and 60 mg/kg respectively) increases AChE levels in rats (cerebral cortex & hippocampus). However, these studies have been conducted either on hippocampus and cerebral cortex regions and do not examine AChE activity on an isoform-specific manner (164, 175).

4.8. Insulin stimulates antioxidant effect in diabetes-induced oxidative stress

The persistent hyperglycemia appears to have a major role in the onset of cognitive and affective disorders associated with diabetes (109). It is commonly thought that oxidative stress is the critical pathologic process in a number of diabetes-related complications including nerve degeneration (107, 108). It has been suggested that hyperglycemia causes tissue damage through several mechanisms, such as an increase in glucose flux and other sugars through the polyol pathway, increase of advanced glycation end-products (AGEs) synthesis, increase of AGEs receptor expression, activation of protein kinase C isoforms and overactivity of the hexosamine pathway (110). Furthermore, evidence indicate that these

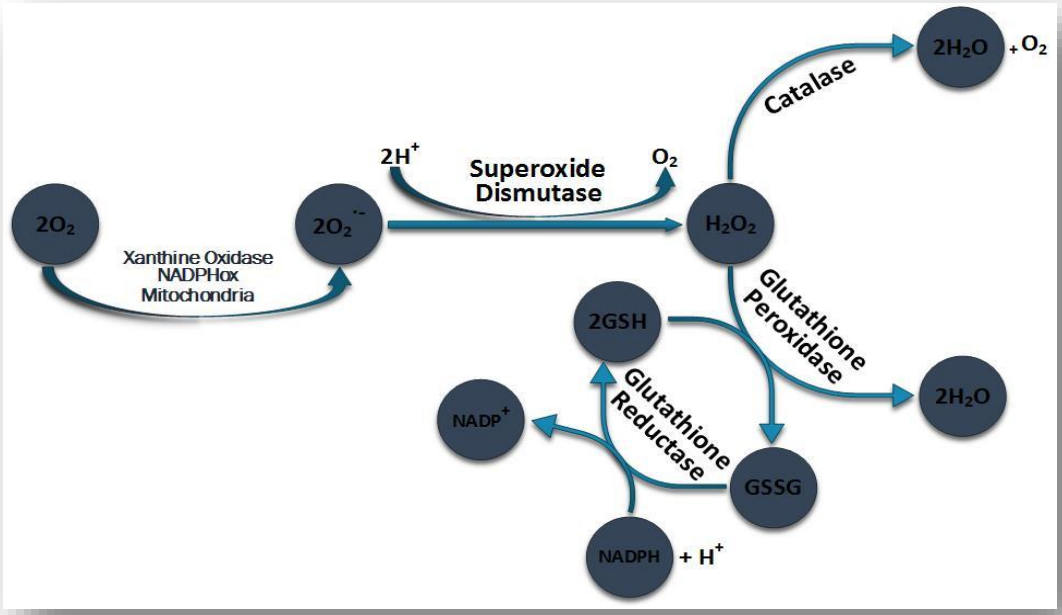

Figure 55. Schematic representation of the main antioxidant activity. $O_2^{\bullet-}$, superoxide; CAT, catalase; Cu-SOD, copper SOD; Mn-SOD, manganese SOD; GPx, glutathione peroxidase; GSH, glutathione; GSSG, glutathione disulfide; H_2O_2, hydrogen peroxide; NAD(P)H, nicotinamide adenine dinucleotide phosphate.

mechanisms are activated by increased oxidative stress (111), which results from increasing of reactive species of oxygen or nitrogen (ROS/RNS) production and/or impairment of antioxidant defenses (112) (Figure 55).

4.8.1. Insulin stimulates an antioxidant enzymatic activity in diabetes-induced oxidative stress

Studies associated with the impact of diabetes upon the antioxidant enzymatic activity are in controversy. The first study reported a significant decrease (after a single i.p. dose 60mg/kg of STZ) on SOD and CAT activity in hippocampus (three-week protocol) (158), while the second reported a significant increase on SOD and CAT activity (after a single i.p. dose 60mg/kg of STZ) in hippocampus and prefrontal cortex (five-week protocol) (165). Moreover, the second study has also reported that treatment with insulin (6 U/day, for 28 days) of the DC mice has presented significant decrease of the activity of both SOD and CAT enzymes on these two brain regions.

Hence, in an effort to elucidate the antioxidant pattern followed in type 1 diabetes we tried to determine whether we had any effect of STZ-induced diabetes and insulin treatment on antioxidant defense we measured the activity of three major antioxidant enzymes: superoxide dismutase, catalase and glutathione peroxidase.

More specifically the SOD activity was significantly increased in all brain regions of the DC mice compared to the EC group. The largest increase of SOD activity was observed in hippocampus and striatum. Diencephalon and midbrain follow, while the smallest augmentations were observed in cerebral cortex and cerebellum (Table 12 and Figure 35). On the other hand, the DC+Ins group presented significant decrease of SOD activity, in most of the brain regions examined compared to the DC group. More particularly, the largest decrease was observed in hippocampus and striatum. Diencephalon, midbrain and cerebellum follow with lower decrease. Characteristically, the only region that had no significant decrease of SOD activity was cerebral cortex. The regions that were observed having significant differences compared to the EC group, were cerebral cortex, midbrain and diencephalon, indicating the incomplete recovery of these regions regarding the SOD activity (Table 12 and Figure 35).

Furthermore, CAT activity was significantly increased in all brain regions of the DC mice compared to the EC group (Table 13 and Figure 36). The largest increase of CAT activity was observed in cerebral cortex and striatum. Midbrain and hippocampus follow,

while the smallest augmentations were observed in diencephalon and cerebellum. On the other hand, the DC+Ins group presented significant decrease of CAT activity, in all the brain regions examined compared to the DC group. More particularly, the largest decrease was observed in striatum and hippocampus. Midbrain and diencephalon follow with lower decrease, while the smallest decrease was observed in cerebellum and cerebral cortex. Cerebral cortex was observed having significant difference compared to the EC group indicating the incomplete recovery of this region regarding the CAT activity (Table 13 and Figure 36).

Moreover, GPx activity was significantly increased in all brain regions of the DC mice compared to the EC group (Table 14 and Figure 37). The largest increase of GPx activity was observed in cerebral cortex and diencephalon. Midbrain and cerebellum follow, while the smallest augmentations were observed in hippocampus and striatum. On the other hand, the DC+Ins group presented significant decrease of GPx activity, in all the brain regions examined compared to the DC group. More particularly, the largest decrease was observed in cerebellum and diencephalon. Hippocampus and midbrain follow with lower decrease, while the smallest decline was observed in striatum and cerebral cortex. Cerebral cortex and midbrain were observed having significant difference compared to the EC group indicating the incomplete recovery of these regions regarding the GPx activity (Table 14 and Figure 37).

Our results demonstrate an enhancement of the antioxidant enzymatic activity which is a possible outcome of the diabetes-induced oxidative stress. The results are consistent with the second pre-mentioned study (165) as concern as both the increase on the DC group and the respective decrease on the DC+Ins group after its treatment with insulin (same dose with our study: 6 UI/day but for 28 days) for both the SOD and CAT activity. However our study used a short-term insulin treatment in order to clarify the primary and immediate responses that observed on several brain regions, after the regulation of diabetes type 1 with insulin treatment. Characteristically, there were observed brain region-specific changes on each enzymatic activity, however the only region that had incomplete recovery effect in all three antioxidant enzymes was cerebral cortex. If we take into consideration that the same dose of insulin on the previously mentioned study had shown significant recovery effect of prefrontal cortex on SOD and CAT activity, we must assume that the prolonged period (28 days) of insulin treatment, was the main reason for this result.

4.8.2. Insulin stimulates free radical scavenging in diabetes-induced oxidative stress

Glutathione is the major endogenous antioxidant produced by the cells, participating directly in the neutralization of free radicals and reactive oxygen compounds, as well as maintaining exogenous antioxidants such as vitamins C and E in their reduced (active) forms (193). It is also used in metabolic and biochemical reactions such as DNA synthesis and repair, protein synthesis, prostaglandin synthesis, amino acid transport, and enzyme activation. Thus, every system in the body can be affected by the state of the glutathione system, especially the immune system and the nervous system.

In continuation of the previous results, we wanted to evaluate this crucial factor that maintains the cellular redox homeostasis. In several studies, it has been proved that the ratio GSSG/GSH ratio is considered a representative measure of antioxidant status (194, 195), since the evaluation of only one of the two glutathione forms does not reflect the glutathione cycle that occurs inside the cell. Several studies upon diabetes type 1 demonstrate a significant decrease of reduced glutathione levels in hippocampus and cerebral hemispheres (158, 164, 165), indicating enhancement of the oxidative stress occurred by the induction (single STZ i.p. dose 60mg/kg) of type 1 diabetes in rats.

More specifically the GSSG/GSH ratio was significantly increased in all brain regions of the DC mice compared to the EC group (Table 15 and Figure 38). The largest increase of GSSG/GSH ratio was observed in hippocampus and striatum. Cerebral cortex and cerebellum follow, while the smallest augmentations were observed in diencephalon and midbrain. Our data are in agreement with the increased GSSG/GSH ratio that was observed after a 21-day protocol, in the cerebral hemispheres of diabetic rats after the STZ-induced diabetes (single i.p. dose 50mg/kg) (195).

On the other hand, the DC+Ins group presented significant decrease of GSSG/GSH ratio, in all the brain regions examined compared to the DC group. More particularly, the largest decrease was observed in hippocampus and striatum. Cerebellum and cerebral cortex follow with lower decrease, while the smallest decline was observed in midbrain and diencephalon. Cerebral cortex, diencephalon and midbrain were observed having significant difference compared to the EC group indicating the incomplete recovery of these regions regarding the GSSG/GSH ratio (Table 15 and Figure 38), which is agreement with the pattern of the results observed in the antioxidant activity of GPx, SOD and CAT.

4.8.3. Insulin inhibits diabetes-induced lipid peroxidation

As mentioned before, lipids are particularly vulnerable to oxidation because membranes of some cells are rich in polyunsaturated fatty acids and because of the presence of oxygen at millimolar levels in the lipid bilayer. Unsaturated phospholipids, glycolipids, and cholesterol in cell membranes and other organized systems are prominent targets of oxidant attack. This can result in lipid peroxidation, a degenerative process that disturbs structure/ function of the target system (107, 116, 117).

More specifically the MDA levels were significantly increased in all brain regions of the DC mice compared to the EC group (Table 16 and Figure 39). The largest increase of MDA levels was observed in hippocampus and diencephalon. Midbrain and striatum follow, while the smallest augmentations were observed in cerebral cortex and cerebellum.

On the other hand, the DC+Ins group presented significant decrease of MDA levels, in most of the brain regions examined compared to the DC group. More particularly, the largest decrease was observed in striatum and hippocampus. Diencephalon and cerebellum follow with lower decrease, while the smallest decline was observed in midbrain. Characteristically, the only region that had no significant decrease of MDA levels compared to the DC group was cerebral cortex, while at the same time it was observed having significant difference compared to the EC group indicating the incomplete recovery of this region regarding the MDA levels (Table 16 and Figure 39).

Our data are in accordance with previous studies upon the lipid peroxidation of STZ-induced diabetes (single i.p. dose 60mg/kg) on cerebral cortex, hippocampus (164) and prefrontal cortex (165) of rats, however the MDA levels of the EC and DC rats on the second study were a lot higher than in our study, which are the normal levels that are usually observed. As expected the cerebral cortex follows the pattern of the rest oxidative markers indicating that its recovery is slower than the other regions' recovery and consequently a longer period of insulin treatment.

4.9. Insulin stimulates neuroprotective effect in diabetes-induced neuronal apoptosis

The loss of Cytc function is a contributing factor to mitochondrial dysfunction or secondary energy failure, and Cytc release from mitochondria is an initiating event in mitochondrial apoptosis and cell death (195, 196).

Western blot analysis on mitochondrial lysates and cytoplasmic samples of brain regions: cerebral cortex, midbrain, hippocampus, striatum and diencephalon, determined the ratio of the cytoplasmic cytochrome c content to the mitochondrial cytochrome c content. Regarding the cerebral cortex, the cytochrome c levels ratio of both the DC mice and DC+Ins groups showed small but no significant increase changed compared to the EC group. (Table 17; Figures 40-42). On the other hand, the cytochrome c levels ratio of the DC mice on the rest regions were significantly increased: midbrain (59.79%; $P<0.01$), hippocampus (36.76%; $P<0.01$), striatum (292.92%; $P<0.01$) and diencephalon (58.64%; $P<0.05$) (Tables 18-21; Figures 43-54). On the other hand, the cytochrome c levels ratio of the DC+Ins mice showed a brain specific pattern of changes. Regarding the midbrain, no significant decrease compared to the DC group was observed, while at the same time it was significantly increased (42.38%; $P<0.05$) compared to the EC group indicating the incomplete recovery of this region (Table 18; Figures 43-45).

Regarding the hippocampal region, the cytochrome c levels ratio of the DC+Ins mice was significantly decreased (16.57%; $P<0.05$) compared to the DC group (Table 19; Figures 46-48). Regarding the region of striatum, the cytochrome c levels ratio of the DC+Ins mice was significantly decreased (45.13%; $P<0.01$) compared to the DC group while at the same time it was observed having significant difference compared to the EC group (115.59%; $P<0.05$) indicating the incomplete recovery of this region (Table 20; Figures 49-51).

Regarding the region of diencephalon, the cytochrome c levels ratio of the DC+Ins mice was significantly decreased (35.77%; $P<0.05$) compared to the DC group (Table 21; Figures 52-54). In support of the neuronal apoptosis observed on the DC mice, is a study which demonstrated cytochrome c release (measured spectrophotometrically) in the cytosol fraction of cerebral hemispheres after the induction of STZ-induced diabetes (single i.p. dose 50mg/kg) (195).

The previously observed GSH loss might be partially dependent on the opening of the mitochondrial permeability transition pore (197), as suggested by the observation of a higher

release of cytochrome c in mitochondria isolated from STZ rats. The mitochondrial pool of GSH is considered vital for cell survival: after severe mitochondrial GSH depletion, cell death occurs; this, however, is delayed by antioxidant treatment (198, 199).

Moreover, the brain mitochondria of diabetic rats show consistently reduced ATP levels, as a result of the prominent changes in activity of the mitochondrial respiratory chain enzymes in such rats. ATP content is closely related to maintenance of membrane potential; thus, a reduction in ATP would produce an irreversible drop in membrane potential, opening the permeability transition pore and triggering mechanisms of cell death. Indeed, we also observed increased cytochrome c release into the cytosol. Cytochrome c is a marker of mitochondrial dysfunction (200) and a cell-death trigger activator that operates through activation of specific caspases and consequent induction of apoptosis.

V. CONCLUSIONS

Conclusively, our study demonstrated that Type I diabetes caused:

- Polyphagia and polydipsia
- Hyperglycemia and weight loss
- Hypertriglyceridemia, Hypercholesterolemia
- Behavioral deficits: Anxiogenesis, Memory loss, Depressive-like behavior
- Cholinergic dysfunction: Brain region-specific reduction of ACh levels and respective brain region-specific increase of SS and DS AChE activity.
- Increase of oxidative stress:
  - Increase of antioxidant defense markers: Brain region-specific increased activities of SOD, CAT and GPx, in response to the increased oxidative stress.
  - Increase of the GSSG/GSH ratio, on a brain region-specific manner.
  - Increase of lipid peroxidation marker: Increase of MDA levels on a brain region-specific manner.
- Neuronal apoptosis: Increased ratio of the cytoplasmic cytochrome c content to the mitochondrial cytochrome c content, on mitochondrial lysates and cytoplasmic samples on a brain region-specific manner, with the exception of cerebral cortex.

The short term insulin treatment of Type I diabetes significantly attenuated:

- Polyphagia and polydipsia
- Hyperglycemia and weight loss
- Hypertriglyceridemia, Hypercholesterolemia
- Behavioral deficits: Anxiolysis, Memory enhancement, Anti-depressant effect
- Cholinergic dysfunction: Brain region-specific increase of ACh levels, except for cerebral cortex and cerebellum. Respective brain region-specific decrease of SS and DS AChE activity except for cerebral cortex
- Oxidative stress:
  - Decrease of antioxidant defense markers: Brain region-specific decreased activities of SOD (except for cerebral cortex), CAT and GPx.
  - Decrease of the GSSG/GSH ratio, on a brain region- specific manner.
  - Decrease of lipid peroxidation marker: Decrease of MDA levels on a brain region-specific manner, except for cerebral cortex.
- Neuronal apoptosis: Decreased ratio of the cytoplasmic cytochrome c content to the mitochondrial cytochrome c content, on mitochondrial lysates and cytoplasmic samples on a brain region-specific manner, with the exception of cerebral cortex.

References

1. Jahromi MM, and Eisenbarth GS. Cellular and molecular pathogenesis of type 1A diabetes. *Cellular and molecular life sciences : CMLS.* 2007;64(7-8):865-72.
2. Castano L, and Eisenbarth GS. Type-I diabetes: a chronic autoimmune disease of human, mouse, and rat. *Annual review of immunology.* 1990;8(647-79.
3. Winter WE, and Schatz DA. Autoimmune markers in diabetes. *Clinical chemistry.* 2011;57(2):168-75.
4. Abiru N, Kawasaki E, and Eguch K. Current knowledge of Japanese type 1 diabetic syndrome. *Diabetes/metabolism research and reviews.* 2002;18(5):357-66.
5. Kostas K, Alexandra S, Feneli K, and Kyriaki K. Associated autoimmunity in children and adolescents with type 1 diabetes mellitus (T1DM). *Autoimmunity reviews.* 2015.
6. Awdeh ZL, Yunis EJ, Audeh MJ, Fici D, Pugliese A, Larsen CE, and Alper CA. A genetic explanation for the rising incidence of type 1 diabetes, a polygenic disease. *Journal of autoimmunity.* 2006;27(3):174-81.
7. Borchers AT, Uibo R, and Gershwin ME. The geoepidemiology of type 1 diabetes. *Autoimmunity reviews.* 2010;9(5):A355-65.
8. Bach JF. Infections and autoimmune diseases. *Journal of autoimmunity.* 2005;25 Suppl(74-80.
9. Karvonen M, Viik-Kajander M, Moltchanova E, Libman I, LaPorte R, and Tuomilehto J. Incidence of childhood type 1 diabetes worldwide. Diabetes Mondiale (DiaMond) Project Group. *Diabetes care.* 2000;23(10):1516-26.
10. Desrocher M, and Rovet J. Neurocognitive correlates of type 1 diabetes mellitus in childhood. *Child neuropsychology : a journal on normal and abnormal development in childhood and adolescence.* 2004;10(1):36-52.
11. Hannonen R, Komulainen J, Riikonen R, Ahonen T, Eklund K, Tolvanen A, Keskinen P, and Nuuja A. Academic skills in children with early-onset type 1 diabetes: the effects of diabetes-related risk factors. *Developmental medicine and child neurology.* 2012;54(5):457-63.
12. Collins MM, Corcoran P, and Perry IJ. Anxiety and depression symptoms in patients with diabetes. *Diabetic medicine : a journal of the British Diabetic Association.* 2009;26(2):153-61.
13. Li C, Barker L, Ford ES, Zhang X, Strine TW, and Mokdad AH. Diabetes and anxiety in US adults: findings from the 2006 Behavioral Risk Factor Surveillance System. *Diabetic medicine : a journal of the British Diabetic Association.* 2008;25(7):878-81.
14. Dantzer C, Swendsen J, Maurice-Tison S, and Salamon R. Anxiety and depression in juvenile diabetes: a critical review. *Clinical psychology review.* 2003;23(6):787-800.
15. Grey M, Whittemore R, and Tamborlane W. Depression in type 1 diabetes in children: natural history and correlates. *Journal of psychosomatic research.* 2002;53(4):907-11.
16. Weinger K, Jacobson AM, Musen G, Lyoo IK, Ryan CM, Jimerson DC, and Renshaw PF. The effects of type 1 diabetes on cerebral white matter. *Diabetologia.* 2008;51(3):417-25.
17. Hershey T, Bhargava N, Sadler M, White NH, and Craft S. Conventional versus intensive diabetes therapy in children with type 1 diabetes: effects on memory and motor speed. *Diabetes care.* 1999;22(8):1318-24.
18. Northam EA, Anderson PJ, Werther GA, Warne GL, Adler RG, and Andrewes D. Neuropsychological complications of IDDM in children 2 years after disease onset. *Diabetes care.* 1998;21(3):379-84.
19. Northam EA, Rankins D, Lin A, Wellard RM, Pell GS, Finch SJ, Werther GA, and Cameron FJ. Central nervous system function in youth with type 1 diabetes 12 years after disease onset. *Diabetes care.* 2009;32(3):445-50.
20. Ryan CM. Why is cognitive dysfunction associated with the development of diabetes early in life? The diathesis hypothesis. *Pediatric diabetes.* 2006;7(5):289-97.

21. Fox MA, Chen RS, and Holmes CS. Gender differences in memory and learning in children with insulin-dependent diabetes mellitus (IDDM) over a 4-year follow-up interval. *Journal of pediatric psychology.* 2003;28(8):569-78.
22. de Leeuw FE, de Groot JC, Achten E, Oudkerk M, Ramos LM, Heijboer R, Hofman A, Jolles J, van Gijn J, and Breteler MM. Prevalence of cerebral white matter lesions in elderly people: a population based magnetic resonance imaging study. The Rotterdam Scan Study. *Journal of neurology, neurosurgery, and psychiatry.* 2001;70(1):9-14.
23. Vermeer SE, Den Heijer T, Koudstaal PJ, Oudkerk M, Hofman A, and Breteler MM. Incidence and risk factors of silent brain infarcts in the population-based Rotterdam Scan Study. *Stroke; a journal of cerebral circulation.* 2003;34(2):392-6.
24. Musen G, Lyoo IK, Sparks CR, Weinger K, Hwang J, Ryan CM, Jimerson DC, Hennen J, Renshaw PF, and Jacobson AM. Effects of type 1 diabetes on gray matter density as measured by voxel-based morphometry. *Diabetes.* 2006;55(2):326-33.
25. Wessels AM, Simsek S, Remijnse PL, Veltman DJ, Biessels GJ, Barkhof F, Scheltens P, Snoek FJ, Heine RJ, and Rombouts SA. Voxel-based morphometry demonstrates reduced grey matter density on brain MRI in patients with diabetic retinopathy. *Diabetologia.* 2006;49(10):2474-80.
26. Gispen WH, and Biessels GJ. Cognition and synaptic plasticity in diabetes mellitus. *Trends in neurosciences.* 2000;23(11):542-9.
27. Biessels GJ, and Gispen WH. The impact of diabetes on cognition: what can be learned from rodent models? *Neurobiology of aging.* 2005;26 Suppl 1(36-41.
28. Biessels GJ, Kamal A, Urban IJ, Spruijt BM, Erkelens DW, and Gispen WH. Water maze learning and hippocampal synaptic plasticity in streptozotocin-diabetic rats: effects of insulin treatment. *Brain research.* 1998;800(1):125-35.
29. Bliss TV, and Collingridge GL. A synaptic model of memory: long-term potentiation in the hippocampus. *Nature.* 1993;361(6407):31-9.
30. Lynch MA. Long-term potentiation and memory. *Physiological reviews.* 2004;84(1):87-136.
31. Massey PV, and Bashir ZI. Long-term depression: multiple forms and implications for brain function. *Trends in neurosciences.* 2007;30(4):176-84.
32. Artola A. Diabetes-, stress- and ageing-related changes in synaptic plasticity in hippocampus and neocortex--the same metaplastic process? *European journal of pharmacology.* 2008;585(1):153-62.
33. Chabot C, Massicotte G, Milot M, Trudeau F, and Gagne J. Impaired modulation of AMPA receptors by calcium-dependent processes in streptozotocin-induced diabetic rats. *Brain research.* 1997;768(1-2):249-56.
34. Kamal A, Biessels GJ, Urban IJ, and Gispen WH. Hippocampal synaptic plasticity in streptozotocin-diabetic rats: impairment of long-term potentiation and facilitation of long-term depression. *Neuroscience.* 1999;90(3):737-45.
35. Artola A, Kamal A, Ramakers GM, Biessels GJ, and Gispen WH. Diabetes mellitus concomitantly facilitates the induction of long-term depression and inhibits that of long-term potentiation in hippocampus. *The European journal of neuroscience.* 2005;22(1):169-78.
36. Hoffman WH, Artlett CM, Zhang W, Kreipke CW, Passmore GG, Rafols JA, and Sima AA. Receptor for advanced glycation end products and neuronal deficit in the fatal brain edema of diabetic ketoacidosis. *Brain research.* 2008;1238(154-62.
37. van Duinkerken E, Klein M, Schoonenboom NS, Hoogma RP, Moll AC, Snoek FJ, Stam CJ, and Diamant M. Functional brain connectivity and neurocognitive functioning in patients with long-standing type 1 diabetes with and without microvascular complications: a magnetoencephalography study. *Diabetes.* 2009;58(10):2335-43.
38. Albers JW, and Pop-Busui R. Diabetic neuropathy: mechanisms, emerging treatments, and subtypes. *Current neurology and neuroscience reports.* 2014;14(8):473.
39. Biessels GJ, Kamal A, Ramakers GM, Urban IJ, Spruijt BM, Erkelens DW, and Gispen WH. Place learning and hippocampal synaptic plasticity in streptozotocin-induced diabetic rats. *Diabetes.* 1996;45(9):1259-66.

40. Kong WX, Chen SW, Li YL, Zhang YJ, Wang R, Min L, and Mi X. Effects of taurine on rat behaviors in three anxiety models. *Pharmacology, biochemistry, and behavior.* 2006;83(2):271-6.
41. Brownlee M. Biochemistry and molecular cell biology of diabetic complications. *Nature.* 2001;414(6865):813-20.
42. Yasuda H, Terada M, Maeda K, Kogawa S, Sanada M, Haneda M, Kashiwagi A, and Kikkawa R. Diabetic neuropathy and nerve regeneration. *Progress in neurobiology.* 2003;69(4):229-85.
43. Nakamura J, Kato K, Hamada Y, Nakayama M, Chaya S, Nakashima E, Naruse K, Kasuya Y, Mizubayashi R, Miwa K, et al. A protein kinase C-beta-selective inhibitor ameliorates neural dysfunction in streptozotocin-induced diabetic rats. *Diabetes.* 1999;48(10):2090-5.
44. Roberts RE, and McLean WG. Protein kinase C isozyme expression in sciatic nerves and spinal cords of experimentally diabetic rats. *Brain research.* 1997;754(1-2):147-56.
45. Liao MH, Xiang YC, Huang JY, Tao RR, Tian Y, Ye WF, Zhang GS, Lu YM, Ahmed MM, Liu ZR, et al. The disturbance of hippocampal CaMKII/PKA/PKC phosphorylation in early experimental diabetes mellitus. *CNS neuroscience & therapeutics.* 2013;19(5):329-36.
46. Vetri F, Chavez R, Xu HL, Paisansathan C, and Pelligrino DA. Complex modulation of the expression of PKC isoforms in the rat brain during chronic type 1 diabetes mellitus. *Brain research.* 2013;1490(202-9.
47. Salem MA, Matta LF, Tantawy AA, Hussein M, and Gad GI. Single photon emission tomography (SPECT) study of regional cerebral blood flow in normoalbuminuric children and adolescents with type 1 diabetes. *Pediatric diabetes.* 2002;3(3):155-62.
48. Haneda M, Araki S, Togawa M, Sugimoto T, Isono M, and Kikkawa R. Mitogen-activated protein kinase cascade is activated in glomeruli of diabetic rats and glomerular mesangial cells cultured under high glucose conditions. *Diabetes.* 1997;46(5):847-53.
49. Tomlinson DR. Mitogen-activated protein kinases as glucose transducers for diabetic complications. *Diabetologia.* 1999;42(11):1271-81.
50. Sima AA, Zhang W, Muzik O, Kreipke CW, Rafols JA, and Hoffman WH. Sequential abnormalities in type 1 diabetic encephalopathy and the effects of C-Peptide. *The review of diabetic studies : RDS.* 2009;6(3):211-22.
51. Sima AA, and Li ZG. The effect of C-peptide on cognitive dysfunction and hippocampal apoptosis in type 1 diabetic rats. *Diabetes.* 2005;54(5):1497-505.
52. Balakrishnan S, Mathew J, and Paulose CS. Cholinergic and glutamergic receptor functional regulation in long-term, low dose somatotropin and insulin treatment to ageing rats: rejuvenation of brain function. *Molecular and cellular endocrinology.* 2010;314(1):23-30.
53. Conner JM, Franks KM, Titterness AK, Russell K, Merrill DA, Christie BR, Sejnowski TJ, and Tuszynski MH. NGF is essential for hippocampal plasticity and learning. *The Journal of neuroscience : the official journal of the Society for Neuroscience.* 2009;29(35):10883-9.
54. La Fleur SE, Fliers E, and Kalsbeek A. Neuroscience of glucose homeostasis. *Handbook of clinical neurology.* 2014;126(341-51.
55. Kahn CR. The molecular mechanism of insulin action. *Annual review of medicine.* 1985;36(429-51.
56. Simpson IA, and Cushman SW. Hormonal regulation of mammalian glucose transport. *Annual review of biochemistry.* 1986;55(1059-89.
57. Hoyer S, Henneberg N, Knapp S, Lannert H, and Martin E. Brain glucose metabolism is controlled by amplification and desensitization of the neuronal insulin receptor. *Annals of the New York Academy of Sciences.* 1996;777(374-9.
58. Woods SC, Figlewicz Lattemann DP, Schwartz MW, and Porte D, Jr. A re-assessment of the regulation of adiposity and appetite by the brain insulin system. *International journal of obesity.* 1990;14 Suppl 3(69-73; discussion 4-6.
59. Chavez M, Kaiyala K, Madden LJ, Schwartz MW, and Woods SC. Intraventricular insulin and the level of maintained body weight in rats. *Behavioral neuroscience.* 1995;109(3):528-31.
60. Schwartz MW, Figlewicz DP, Baskin DG, Woods SC, and Porte D, Jr. Insulin in the brain: a hormonal regulator of energy balance. *Endocrine reviews.* 1992;13(3):387-414.

61. Menendez JA, and Atrens DM. Insulin increases energy expenditure and respiratory quotient in the rat. *Pharmacology, biochemistry, and behavior.* 1989;34(4):765-8.
62. Oomura Y, Aou S, Matsumoto I, and Sakata T. Physiological significance of 2-buten-4-olide (2-B4O), an endogenous satiety substance increased in the fasted state. *Experimental biology and medicine (Maywood, NJ).* 2003;228(10):1146-55.
63. Shibata S, Liou SY, Ueki S, and Oomura Y. Inhibitory action of insulin on suprachiasmatic nucleus neurons in rat hypothalamic slice preparations. *Physiology & behavior.* 1986;36(1):79-81.
64. Palovcik RA, Phillips MI, Kappy MS, and Raizada MK. Insulin inhibits pyramidal neurons in hippocampal slices. *Brain research.* 1984;309(1):187-91.
65. Phillips MI, and Palovcik RA. Dose-response testing of peptides by hippocampal brain slice recording. *Methods in enzymology.* 1989;168(129-44.
66. Park CR. Cognitive effects of insulin in the central nervous system. *Neuroscience and biobehavioral reviews.* 2001;25(4):311-23.
67. Steffens AB, Scheurink AJ, Porte D, Jr., and Woods SC. Penetration of peripheral glucose and insulin into cerebrospinal fluid in rats. *The American journal of physiology.* 1988;255(2 Pt 2):R200-4.
68. Schwartz MW, Bergman RN, Kahn SE, Taborsky GJ, Jr., Fisher LD, Sipols AJ, Woods SC, Steil GM, and Porte D, Jr. Evidence for entry of plasma insulin into cerebrospinal fluid through an intermediate compartment in dogs. Quantitative aspects and implications for transport. *The Journal of clinical investigation.* 1991;88(4):1272-81.
69. Banks WA, Jaspan JB, and Kastin AJ. Selective, physiological transport of insulin across the blood-brain barrier: novel demonstration by species-specific radioimmunoassays. *Peptides.* 1997;18(8):1257-62.
70. Banks WA, and Kastin AJ. Differential permeability of the blood-brain barrier to two pancreatic peptides: insulin and amylin. *Peptides.* 1998;19(5):883-9.
71. Banks WA, Jaspan JB, Huang W, and Kastin AJ. Transport of insulin across the blood-brain barrier: saturability at euglycemic doses of insulin. *Peptides.* 1997;18(9):1423-9.
72. Kaiyala KJ, Prigeon RL, Kahn SE, Woods SC, and Schwartz MW. Obesity induced by a high-fat diet is associated with reduced brain insulin transport in dogs. *Diabetes.* 2000;49(9):1525-33.
73. Baura GD, Foster DM, Kaiyala K, Porte D, Jr., Kahn SE, and Schwartz MW. Insulin transport from plasma into the central nervous system is inhibited by dexamethasone in dogs. *Diabetes.* 1996;45(1):86-90.
74. Duarte AI, Moreira PI, and Oliveira CR. Insulin in central nervous system: more than just a peripheral hormone. *Journal of aging research.* 2012;2012(384017.
75. Havrankova J, Roth J, and Brownstein M. Insulin receptors are widely distributed in the central nervous system of the rat. *Nature.* 1978;272(5656):827-9.
76. Schechter R, Beju D, Gaffney T, Schaefer F, and Whetsell L. Preproinsulin I and II mRNAs and insulin electron microscopic immunoreaction are present within the rat fetal nervous system. *Brain research.* 1996;736(1-2):16-27.
77. Freude S, Plum L, Schnitker J, Leeser U, Udelhoven M, Krone W, Bruning JC, and Schubert M. Peripheral hyperinsulinemia promotes tau phosphorylation in vivo. *Diabetes.* 2005;54(12):3343-8.
78. Clarke DW, Mudd L, Boyd FT, Jr., Fields M, and Raizada MK. Insulin is released from rat brain neuronal cells in culture. *Journal of neurochemistry.* 1986;47(3):831-6.
79. Hoyer S. Memory function and brain glucose metabolism. *Pharmacopsychiatry.* 2003;36 Suppl 1(S62-7.
80. Olefsky JM. The insulin receptor. A multifunctional protein. *Diabetes.* 1990;39(9):1009-16.
81. Myers MG, Jr., and White MF. The new elements of insulin signaling. Insulin receptor substrate-1 and proteins with SH2 domains. *Diabetes.* 1993;42(5):643-50.
82. Adamo M, Raizada MK, and LeRoith D. Insulin and insulin-like growth factor receptors in the nervous system. *Molecular neurobiology.* 1989;3(1-2):71-100.
83. Unger J, McNeill TH, Moxley RT, 3rd, White M, Moss A, and Livingston JN. Distribution of insulin receptor-like immunoreactivity in the rat forebrain. *Neuroscience.* 1989;31(1):143-57.
84. Unger JW, Livingston JN, and Moss AM. Insulin receptors in the central nervous system: localization, signalling mechanisms and functional aspects. *Progress in neurobiology.* 1991;36(5):343-62.

85. Baskin DG, Porte D, Jr., Guest K, and Dorsa DM. Regional concentrations of insulin in the rat brain. *Endocrinology.* 1983;112(3):898-903.
86. Baskin DG, Sipols AJ, Schwartz MW, and White MF. Immunocytochemical detection of insulin receptor substrate-1 (IRS-1) in rat brain: colocalization with phosphotyrosine. *Regulatory peptides.* 1993;48(1-2):257-66.
87. Corp ES, Woods SC, Porte D, Jr., Dorsa DM, Figlewicz DP, and Baskin DG. Localization of 125I-insulin binding sites in the rat hypothalamus by quantitative autoradiography. *Neuroscience letters.* 1986;70(1):17-22.
88. Taylor JL, Mayer RT, and Himel CM. Conformers of acetylcholinesterase: a mechanism of allosteric control. *Molecular pharmacology.* 1994;45(1):74-83.
89. Massoulie J. The origin of the molecular diversity and functional anchoring of cholinesterases. *Neuro-Signals.* 2002;11(3):130-43.
90. Li Y, Camp S, Rachinsky TL, Getman D, and Taylor P. Gene structure of mammalian acetylcholinesterase. Alternative exons dictate tissue-specific expression. *The Journal of biological chemistry.* 1991;266(34):23083-90.
91. Kaufer D, Friedman A, Seidman S, and Soreq H. Acute stress facilitates long-lasting changes in cholinergic gene expression. *Nature.* 1998;393(6683):373-7.
92. Zimmerman G, and Soreq H. Termination and beyond: acetylcholinesterase as a modulator of synaptic transmission. *Cell and tissue research.* 2006;326(2):655-69.
93. Ragozzino ME, Unick KE, and Gold PE. Hippocampal acetylcholine release during memory testing in rats: augmentation by glucose. *Proceedings of the National Academy of Sciences of the United States of America.* 1996;93(10):4693-8.
94. Ragozzino ME, Pal SN, Unick K, Stefani MR, and Gold PE. Modulation of hippocampal acetylcholine release and spontaneous alternation scores by intrahippocampal glucose injections. *The Journal of neuroscience : the official journal of the Society for Neuroscience.* 1998;18(4):1595-601.
95. Gold PE. Role of glucose in regulating the brain and cognition. *The American journal of clinical nutrition.* 1995;61(4 Suppl):987s-95s.
96. Hajnal A, Pothos EN, Lenard L, and Hoebel BG. Effects of feeding and insulin on extracellular acetylcholine in the amygdala of freely moving rats. *Brain research.* 1998;785(1):41-8.
97. Bhattacharya SK, and Saraswati M. Effect of intracerebroventricularly administered insulin on brain monoamines and acetylcholine in euglycaemic and alloxan-induced hyperglycaemic rats. *Indian journal of experimental biology.* 1991;29(12):1095-100.
98. Messier C, Durkin T, Mrabet O, and Destrade C. Memory-improving action of glucose: indirect evidence for a facilitation of hippocampal acetylcholine synthesis. *Behavioural brain research.* 1990;39(2):135-43.
99. Halliwell B, and Gutteridge JM. The definition and measurement of antioxidants in biological systems. *Free radical biology & medicine.* 1995;18(1):125-6.
100. Vergely C, Maupoil V, Clermont G, Bril A, and Rochette L. Identification and quantification of free radicals during myocardial ischemia and reperfusion using electron paramagnetic resonance spectroscopy. *Archives of biochemistry and biophysics.* 2003;420(2):209-16.
101. Rochette L, Zeller M, Cottin Y, and Vergely C. Diabetes, oxidative stress and therapeutic strategies. *Biochimica et biophysica acta.* 2014;1840(9):2709-29.
102. Melo A, Monteiro L, Lima RM, Oliveira DM, Cerqueira MD, and El-Bacha RS. Oxidative stress in neurodegenerative diseases: mechanisms and therapeutic perspectives. *Oxidative medicine and cellular longevity.* 2011;2011(467180.
103. Jones DP. Redefining oxidative stress. *Antioxidants & redox signaling.* 2006;8(9-10):1865-79.
104. Jones DP, and Go YM. Redox compartmentalization and cellular stress. *Diabetes, obesity & metabolism.* 2010;12 Suppl 2(116-25.
105. Roede JR, Go YM, and Jones DP. Redox equivalents and mitochondrial bioenergetics. *Methods in molecular biology (Clifton, NJ).* 2012;810(249-80.

106. Poli G, Schaur RJ, Siems WG, and Leonarduzzi G. 4-hydroxynonenal: a membrane lipid oxidation product of medicinal interest. *Medicinal research reviews.* 2008;28(4):569-631.
107. Obrosova IG. How does glucose generate oxidative stress in peripheral nerve? *International review of neurobiology.* 2002;50(3-35.
108. Vincent AM, Russell JW, Low P, and Feldman EL. Oxidative stress in the pathogenesis of diabetic neuropathy. *Endocrine reviews.* 2004;25(4):612-28.
109. Bahrmann A, Bahrmann P, Kubiak T, Kopf D, Oster P, Sieber CC, and Daniel WG. [Diabetes and dementia]. *Zeitschrift fur Gerontologie und Geriatrie.* 2012;45(1):17-22.
110. Giacco F, and Brownlee M. Oxidative stress and diabetic complications. *Circulation research.* 2010;107(9):1058-70.
111. Naudi A, Jove M, Ayala V, Cassanye A, Serrano J, Gonzalo H, Boada J, Prat J, Portero-Otin M, and Pamplona R. Cellular dysfunction in diabetes as maladaptive response to mitochondrial oxidative stress. *Experimental diabetes research.* 2012;2012(696215.
112. Ceriello A. New insights on oxidative stress and diabetic complications may lead to a "causal" antioxidant therapy. *Diabetes care.* 2003;26(5):1589-96.
113. Valko M, Leibfritz D, Moncol J, Cronin MT, Mazur M, and Telser J. Free radicals and antioxidants in normal physiological functions and human disease. *The international journal of biochemistry & cell biology.* 2007;39(1):44-84.
114. Young IS, and Woodside JV. Antioxidants in health and disease. *Journal of clinical pathology.* 2001;54(3):176-86.
115. Beckman KB, and Ames BN. The free radical theory of aging matures. *Physiological reviews.* 1998;78(2):547-81.
116. Nishikawa T, Edelstein D, Du XL, Yamagishi S, Matsumura T, Kaneda Y, Yorek MA, Beebe D, Oates PJ, Hammes HP, et al. Normalizing mitochondrial superoxide production blocks three pathways of hyperglycaemic damage. *Nature.* 2000;404(6779):787-90.
117. Russell JW, Golovoy D, Vincent AM, Mahendru P, Olzmann JA, Mentzer A, and Feldman EL. High glucose-induced oxidative stress and mitochondrial dysfunction in neurons. *FASEB journal : official publication of the Federation of American Societies for Experimental Biology.* 2002;16(13):1738-48.
118. Obrosova IG, Pacher P, Szabo C, Zsengeller Z, Hirooka H, Stevens MJ, and Yorek MA. Aldose reductase inhibition counteracts oxidative-nitrosative stress and poly(ADP-ribose) polymerase activation in tissue sites for diabetes complications. *Diabetes.* 2005;54(1):234-42.
119. Nishikawa T, Edelstein D, and Brownlee M. The missing link: a single unifying mechanism for diabetic complications. *Kidney international Supplement.* 2000;77(S26-30.
120. Schnedl WJ, Ferber S, Johnson JH, and Newgard CB. STZ transport and cytotoxicity. Specific enhancement in GLUT2-expressing cells. *Diabetes.* 1994;43(11):1326-33.
121. Szkudelski T. The mechanism of alloxan and streptozotocin action in B cells of the rat pancreas. *Physiological research / Academia Scientiarum Bohemoslovaca.* 2001;50(6):537-46.
122. Kumagai AK. Glucose transport in brain and retina: implications in the management and complications of diabetes. *Diabetes/metabolism research and reviews.* 1999;15(4):261-73.
123. Biessels GJ. Sweet memories: 20 years of progress in research on cognitive functioning in diabetes. *European journal of pharmacology.* 2013;719(1-3):153-60.
124. Simon P, Dupuis R, and Costentin J. Thigmotaxis as an index of anxiety in mice. Influence of dopaminergic transmissions. *Behavioural brain research.* 1994;61(1):59-64.
125. Ferlemi AV, Avgoustatos D, Kokkosis AG, Protonotarios V, Constantinou C, and Margarity M. Lead-induced effects on learning/memory and fear/anxiety are correlated with disturbances in specific cholinesterase isoform activity and redox imbalance in adult brain. *Physiology & behavior.* 2014;131(115-22.
126. Pellow S, Chopin P, File SE, and Briley M. Validation of open:closed arm entries in an elevated plus-maze as a measure of anxiety in the rat. *Journal of neuroscience methods.* 1985;14(3):149-67.
127. Fernandez Espejo E. Structure of the mouse behaviour on the elevated plus-maze test of anxiety. *Behavioural brain research.* 1997;86(1):105-12.

128. Kaneto H. Learning/memory processes under stress conditions. *Behavioural brain research.* 1997;83(1-2):71-4.
129. Papandreou MA, Tsachaki M, Efthimiopoulos S, Cordopatis P, Lamari FN, and Margarity M. Memory enhancing effects of saffron in aged mice are correlated with antioxidant protection. *Behavioural brain research.* 2011;219(2):197-204.
130. Castagne V, Moser P, Roux S, and Porsolt RD. Rodent models of depression: forced swim and tail suspension behavioral despair tests in rats and mice. *Current protocols in pharmacology / editorial board, SJ Enna (editor-in-chief) [et al].* 2010;Chapter 5(Unit 5.8.
131. Porsolt RD, Le Pichon M, and Jalfre M. Depression: a new animal model sensitive to antidepressant treatments. *Nature.* 1977;266(5604):730-2.
132. Das A, Dikshit M, and Nath C. Profile of acetylcholinesterase in brain areas of male and female rats of adult and old age. *Life sciences.* 2001;68(13):1545-55.
133. Bradford MM. A rapid and sensitive method for the quantitation of microgram quantities of protein utilizing the principle of protein-dye binding. *Analytical biochemistry.* 1976;72(248-54.
134. Ellman GL, Courtney KD, Andres V, Jr., and Feather-Stone RM. A new and rapid colorimetric determination of acetylcholinesterase activity. *Biochemical pharmacology.* 1961;7(88-95.
135. Lassiter TL, Barone S, Jr., and Padilla S. Ontogenetic differences in the regional and cellular acetylcholinesterase and butyrylcholinesterase activity in the rat brain. *Brain research Developmental brain research.* 1998;105(1):109-23.
136. Linardaki ZI, Orkoula MG, Kokkosis AG, Lamari FN, and Margarity M. Investigation of the neuroprotective action of saffron (Crocus sativus L.) in aluminum-exposed adult mice through behavioral and neurobiochemical assessment. *Food and chemical toxicology : an international journal published for the British Industrial Biological Research Association.* 2013;52(163-70.
137. Hestrin S. The reaction of acetylcholine and other carboxylic acid derivatives with hydroxylamine, and its analytical application. *The Journal of biological chemistry.* 1949;180(1):249-61.
138. Sinha AK. Colorimetric assay of catalase. *Analytical biochemistry.* 1972;47(2):389-94.
139. Rotruck JT, Pope AL, Ganther HE, Swanson AB, Hafeman DG, and Hoekstra WG. Selenium: biochemical role as a component of glutathione peroxidase. *Science (New York, NY).* 1973;179(4073):588-90.
140. Hissin PJ, and Hilf R. A fluorometric method for determination of oxidized and reduced glutathione in tissues. *Analytical biochemistry.* 1976;74(1):214-26.
141. Grotto D, Santa Maria LD, Boeira S, Valentini J, Charao MF, Moro AM, Nascimento PC, Pomblum VJ, and Garcia SC. Rapid quantification of malondialdehyde in plasma by high performance liquid chromatography-visible detection. *Journal of pharmaceutical and biomedical analysis.* 2007;43(2):619-24.
142. Jentzsch AM, Bachmann H, Furst P, and Biesalski HK. Improved analysis of malondialdehyde in human body fluids. *Free radical biology & medicine.* 1996;20(2):251-6.
143. Fernandez-Vizarra E, Lopez-Perez MJ, and Enriquez JA. Isolation of biogenetically competent mitochondria from mammalian tissues and cultured cells. *Methods (San Diego, Calif).* 2002;26(4):292-7.
144. Constantinou C, Mpatsoulis D, Natsos A, Petropoulou PI, Zvintzou E, Traish AM, Voshol PJ, Karagiannides I, and Kypreos KE. The low density lipoprotein receptor modulates the effects of hypogonadism on diet-induced obesity and related metabolic perturbations. *Journal of lipid research.* 2014;55(7):1434-47.
145. Shapiro SS, and Wilk MB. An analysis of variance test for normality (complete samples). *Biometrika.* 1965;52(3-4):591-611.
146. *The SAGE Dictionary of Statistics. The SAGE Dictionary of Statistics. SAGE Publications, Ltd.* London, England: SAGE Publications, Ltd.
147. E DPDaL. Measuring Skewness: A Forgotten Statistic? *Journal of Statistics Education.* 2011;19(2):1-18.
148. Hayes AF. An Index and Test of Linear Moderated Mediation. *Multivariate Behavioral Research.* 2015;50(1):1-22.

149. Cooke DW, and Plotnick L. Type 1 diabetes mellitus in pediatrics. *Pediatrics in review / American Academy of Pediatrics.* 2008;29(11):374-84; quiz 85.
150. Booth DA. Some characteristics of feeding during streptoxotocin-induced diabetes in the rat. *Journal of comparative and physiological psychology.* 1972;80(2):238-49.
151. Carpenter RG, and Grossman SP. Early streptozotocin diabetes and hunger. *Physiology & behavior.* 1983;31(2):175-8.
152. Storlein LH. The role of the ventromedial hypothalamus in glucoregulation. *Australian National University.* 1977Doctoral Dissertation).
153. Gupta D, Kurhe Y, and Radhakrishnan M. Antidepressant effects of insulin in streptozotocin induced diabetic mice: Modulation of brain serotonin system. *Physiology & behavior.* 2014;129(73-8.
154. Reaven EP, and Reaven GM. Mechanisms for development of diabetic hypertriglyceridemia in streptozotocin-treated rats. Effect of diet and duration of insulin deficiency. *The Journal of clinical investigation.* 1974;54(5):1167-78.
155. Bierman EL, Bagdade JD, and Porte D, Jr. A concept of the pathogenesis of diabetic lipemia. *Transactions of the Association of American Physicians.* 1966;79(348-60.
156. Colca JR, Dailey CF, Palazuk BJ, Hillman RM, Dinh DM, Melchior GW, and Spilman CH. Pioglitazone hydrochloride inhibits cholesterol absorption and lowers plasma cholesterol concentrations in cholesterol-fed rats. *Diabetes.* 1991;40(12):1669-74.
157. He L, Hao L, Fu X, Huang M, and Li R. Severe hypertriglyceridemia and hypercholesterolemia accelerating renal injury: a novel model of type 1 diabetic hamsters induced by short-term high-fat / high-cholesterol diet and low-dose streptozotocin. *BMC nephrology.* 2015;16(1):51.
158. Samarghandian S, Azimi-Nezhad M, and Samini F. Ameliorative effect of saffron aqueous extract on hyperglycemia, hyperlipidemia, and oxidative stress on diabetic encephalopathy in streptozotocin induced experimental diabetes mellitus. *BioMed research international.* 2014;2014(920857.
159. Dheen ST, Tay SS, and Wong WC. Arginine vasopressin- and oxytocin-like immunoreactive neurons in the hypothalamic paraventricular and supraoptic nuclei of streptozotocin-induced diabetic rats. *Archives of histology and cytology.* 1994;57(5):461-72.
160. Saravia FE, Gonzalez SL, Roig P, Alves V, Homo-Delarche F, and De Nicola AF. Diabetes increases the expression of hypothalamic neuropeptides in a spontaneous model of type I diabetes, the nonobese diabetic (NOD) mouse. *Cellular and molecular neurobiology.* 2001;21(1):15-27.
161. Chan O, Inouye K, Riddell MC, Vranic M, and Matthews SG. Diabetes and the hypothalamo-pituitary-adrenal (HPA) axis. *Minerva endocrinologica.* 2003;28(2):87-102.
162. Bluth, Jafarian-Tehrani M, Michaud B, Haour F, Dantzer R, and Homo-Delarche F. Increased sensitivity of prediabetic nonobese diabetic mouse to the behavioral effects of IL-1. *Brain, behavior, and immunity.* 1999;13(4):303-14.
163. Magarinos AM, and McEwen BS. Experimental diabetes in rats causes hippocampal dendritic and synaptic reorganization and increased glucocorticoid reactivity to stress. *Proceedings of the National Academy of Sciences of the United States of America.* 2000;97(20):11056-61.
164. Bhutada P, Mundhada Y, Bansod K, Tawari S, Patil S, Dixit P, Umathe S, and Mundhada D. Protection of cholinergic and antioxidant system contributes to the effect of berberine ameliorating memory dysfunction in rat model of streptozotocin-induced diabetes. *Behavioural brain research.* 2011;220(1):30-41.
165. de Morais H, de Souza CP, da Silva LM, Ferreira DM, Werner MF, Andreatini R, da Cunha JM, and Zanoveli JM. Increased oxidative stress in prefrontal cortex and hippocampus is related to depressive-like behavior in streptozotocin-diabetic rats. *Behavioural brain research.* 2014;258(52-64.
166. Gupta D, Radhakrishnan M, and Kurhe Y. Insulin reverses anxiety-like behavior evoked by streptozotocin-induced diabetes in mice. *Metabolic brain disease.* 2014;29(3):737-46.
167. Tsigos C, and Chrousos GP. Hypothalamic-pituitary-adrenal axis, neuroendocrine factors and stress. *Journal of psychosomatic research.* 2002;53(4):865-71.

168. Ramos A, Pereira E, Martins GC, Wehrmeister TD, and Izidio GS. Integrating the open field, elevated plus maze and light/dark box to assess different types of emotional behaviors in one single trial. *Behavioural brain research.* 2008;193(2):277-88.
169. Biessels GJ, Staekenborg S, Brunner E, Brayne C, and Scheltens P. Risk of dementia in diabetes mellitus: a systematic review. *The Lancet Neurology.* 2006;5(1):64-74.
170. Timaru-Kast R, Luh C, Gotthardt P, Huang C, Schafer MK, Engelhard K, and Thal SC. Influence of age on brain edema formation, secondary brain damage and inflammatory response after brain trauma in mice. *PloS one.* 2012;7(8):e43829.
171. Shingo AS, Kanabayashi T, Kito S, and Murase T. Intracerebroventricular administration of an insulin analogue recovers STZ-induced cognitive decline in rats. *Behavioural brain research.* 2013;241(105-11.
172. Du LL, Chai DM, Zhao LN, Li XH, Zhang FC, Zhang HB, Liu LB, Wu K, Liu R, Wang JZ, et al. AMPK activation ameliorates Alzheimer's disease-like pathology and spatial memory impairment in a streptozotocin-induced Alzheimer's disease model in rats. *Journal of Alzheimer's disease : JAD.* 2015;43(3):775-84.
173. Santos TO, Mazucanti CH, Xavier GF, and Torrao AS. Early and late neurodegeneration and memory disruption after intracerebroventricular streptozotocin. *Physiology & behavior.* 2012;107(3):401-13.
174. Popovic M, Biessels GJ, Isaacson RL, and Gispen WH. Learning and memory in streptozotocin-induced diabetic rats in a novel spatial/object discrimination task. *Behavioural brain research.* 2001;122(2):201-7.
175. Liu J, Feng L, Ma D, Zhang M, Gu J, Wang S, Fu Q, Song Y, Lan Z, Qu R, et al. Neuroprotective effect of paeonol on cognition deficits of diabetic encephalopathy in streptozotocin-induced diabetic rat. *Neuroscience letters.* 2013;549(63-8.
176. Buynitsky T, and Mostofsky DI. Restraint stress in biobehavioral research: Recent developments. *Neuroscience and biobehavioral reviews.* 2009;33(7):1089-98.
177. McEwen BS, Albeck D, Cameron H, Chao HM, Gould E, Hastings N, Kuroda Y, Luine V, Magarinos AM, McKittrick CR, et al. Stress and the brain: a paradoxical role for adrenal steroids. *Vitamins and hormones.* 1995;51(371-402.
178. Sapolsky RM, Krey LC, and McEwen BS. Prolonged glucocorticoid exposure reduces hippocampal neuron number: implications for aging. *The Journal of neuroscience : the official journal of the Society for Neuroscience.* 1985;5(5):1222-7.
179. Watanabe Y, Gould E, and McEwen BS. Stress induces atrophy of apical dendrites of hippocampal CA3 pyramidal neurons. *Brain research.* 1992;588(2):341-5.
180. Naert G, Ixart G, Maurice T, Tapia-Arancibia L, and Givalois L. Brain-derived neurotrophic factor and hypothalamic-pituitary-adrenal axis adaptation processes in a depressive-like state induced by chronic restraint stress. *Molecular and cellular neurosciences.* 2011;46(1):55-66.
181. Ho N, Balu DT, Hilario MR, Blendy JA, and Lucki I. Depressive phenotypes evoked by experimental diabetes are reversed by insulin. *Physiology & behavior.* 2012;105(3):702-8.
182. Haider S, Ahmed S, Tabassum S, Memon Z, Ikram M, and Haleem DJ. Streptozotocin-induced insulin deficiency leads to development of behavioral deficits in rats. *Acta neurologica Belgica.* 2013;113(1):35-41.
183. Payne C, Wiffen PJ, and Martin S. Interventions for fatigue and weight loss in adults with advanced progressive illness. *The Cochrane database of systematic reviews.* 2012;1(Cd008427.
184. Biessels GJ, Kappelle AC, Bravenboer B, Erkelens DW, and Gispen WH. Cerebral function in diabetes mellitus. *Diabetologia.* 1994;37(7):643-50.
185. Welsh B, and Wecker L. Effects of streptozotocin-induced diabetes on acetylcholine metabolism in rat brain. *Neurochemical research.* 1991;16(4):453-60.
186. Fan QI, and Hanin I. Effects of AF64A on gene expression of choline acetyltransferase (ChAT) in the septo-hippocampal pathway and striatum in vivo. *Neurochemical research.* 1999;24(1):15-24.
187. Kim DS, Kim JY, and Han Y. Curcuminoids in neurodegenerative diseases. *Recent patents on CNS drug discovery.* 2012;7(3):184-204.

188. Ruderman NB, Ross PS, Berger M, and Goodman MN. Regulation of glucose and ketone-body metabolism in brain of anaesthetized rats. *The Biochemical journal.* 1974;138(1):1-10.
189. Mooradian AD. Blood-brain barrier choline transport is reduced in diabetic rats. *Diabetes.* 1987;36(10):1094-7.
190. Blusztajn JK, Liscovitch M, and Richardson UI. Synthesis of acetylcholine from choline derived from phosphatidylcholine in a human neuronal cell line. *Proceedings of the National Academy of Sciences of the United States of America.* 1987;84(15):5474-7.
191. Dyer JR, and Greenwood CE. Evidence for altered methionine methyl-group utilization in the diabetic rat's brain. *Neurochemical research.* 1988;13(6):517-23.
192. Das A, Dikshit M, and Nath C. Role of molecular isoforms of acetylcholinesterase in learning and memory functions. *Pharmacology, biochemistry, and behavior.* 2005;81(1):89-99.
193. Ursini F, and Bindoli A. The role of selenium peroxidases in the protection against oxidative damage of membranes. *Chemistry and physics of lipids.* 1987;44(2-4):255-76.
194. Zhang C, Rodriguez C, Spaulding J, Aw TY, and Feng J. Age-dependent and tissue-related glutathione redox status in a mouse model of Alzheimer's disease. *Journal of Alzheimer's disease : JAD.* 2012;28(3):655-66.
195. Mastrocola R, Restivo F, Vercellinatto I, Danni O, Brignardello E, Aragno M, and Boccuzzi G. Oxidative and nitrosative stress in brain mitochondria of diabetic rats. *The Journal of endocrinology.* 2005;187(1):37-44.
196. Huttemann M, Helling S, Sanderson TH, Sinkler C, Samavati L, Mahapatra G, Varughese A, Lu G, Liu J, Ramzan R, et al. Regulation of mitochondrial respiration and apoptosis through cell signaling: cytochrome c oxidase and cytochrome c in ischemia/reperfusion injury and inflammation. *Biochimica et biophysica acta.* 2012;1817(4):598-609.
197. Moreira PI, Custodio JB, Oliveira CR, and Santos MS. Brain mitochondrial injury induced by oxidative stress-related events is prevented by tamoxifen. *Neuropharmacology.* 2005;48(3):435-47.
198. Han D, Sen CK, Roy S, Kobayashi MS, Tritschler HJ, and Packer L. Protection against glutamate-induced cytotoxicity in C6 glial cells by thiol antioxidants. *The American journal of physiology.* 1997;273(5 Pt 2):R1771-8.
199. Han D, Canali R, Rettori D, and Kaplowitz N. Effect of glutathione depletion on sites and topology of superoxide and hydrogen peroxide production in mitochondria. *Molecular pharmacology.* 2003;64(5):1136-44.
200. Yang J, Liu X, Bhalla K, Kim CN, Ibrado AM, Cai J, Peng TI, Jones DP, and Wang X. Prevention of apoptosis by Bcl-2: release of cytochrome c from mitochondria blocked. *Science (New York, NY).* 1997;275(5303):1129-32.